2013

THE ROLE OF MACROPHAGES IN EXERCISE AND INSULIN RESISTANCE IN HUMAN SKELETAL MUSCLE

Jason S. Groshong
University of Kentucky, Magna1970@hotmail.com

STUDENT AGREEMENT:

I represent that my thesis or dissertation and abstract are my original work. Proper attribution has been given to all outside sources. I understand that I am solely responsible for obtaining any needed copyright permissions. I have obtained and attached hereto needed written permission statements(s) from the owner(s) of each third-party copyrighted matter to be included in my work, allowing electronic distribution (if such use is not permitted by the fair use doctrine).

I hereby grant to The University of Kentucky and its agents the non-exclusive license to archive and make accessible my work in whole or in part in all forms of media, now or hereafter known. I agree that the document mentioned above may be made available immediately for worldwide access unless a preapproved embargo applies.

I retain all other ownership rights to the copyright of my work. I also retain the right to use in future works (such as articles or books) all or part of my work. I understand that I am free to register the copyright to my work.

REVIEW, APPROVAL AND ACCEPTANCE

The document mentioned above has been reviewed and accepted by the student's advisor, on behalf of the advisory committee, and by the Director of Graduate Studies (DGS), on behalf of the program; we verify that this is the final, approved version of the student's dissertation including all changes required by the advisory committee. The undersigned agree to abide by the statements above.

Jason S. Groshong, Student

Dr. Charlotte A. Peterson, Major Professor

Dr. Bret N. Smith, Director of Graduate Studies

THE ROLE OF MACROPHAGES IN EXERCISE AND INSULIN RESISTANCE IN HUMAN SKELETAL MUSCLE

DISSERTATION

A dissertation submitted in partial fulfillment of the
requirements for the degree of Doctor of Philosophy in the
College of Medicine
at the University of Kentucky

By
Jason Sean Groshong

Lexington, Kentucky

Director: Dr. Charlotte A. Peterson,
Professor,
Associate Dean for Research
College of Health Sciences

Co-Director: Dr. Michael B. Reid, Professor of Physiology

Lexington, Kentucky

2013

ABSTRACT OF DISSERTATION

Muscle biopsies were taken at baseline, post eccentric exercise, post aerobic training, and after training followed by eccentric exercise from adults with different health status. In Cell Western analysis of pAkt/Akt ratio suggests that muscle cells isolated from baseline biopsies respond to insulin in a dose dependent manner that tracks with sensitivity to insulin of the host; however, this is uncoupled from glucose disposal *in vitro*. Nitrotyrosine (NY), a marker of free radical damage, was employed to assess the efficacy of the exercise paradigm. NY immunohistochemistry on muscle cross-sections revealed that eccentric exercise significantly increased damage in older (>55 years of age), but not middle aged (<55 years of age) subjects, and that training reversed the post eccentric damage significantly in the younger, but not the older group, suggesting distinct adaptation to eccentric exercise. Assessment of total macrophage content by CD68 immunohistochemistry showed that macrophage abundance increased in response to training in the >55 years age group, but not in the <55 years of age group. Following training, macrophages increased in response to eccentric exercise in middle aged and decreased in older subjects, showing a disconnect from NY damage. Macrophage phenotypes were assessed in these groups via the M1 marker CD11b, and the M2 marker, CD206. Two dominant populations of macrophages were identified, one of which co-expressed CD11b and CD206, and another which only expressed CD11b. These two populations of macrophages showed the same trends in expression in response to exercise observed with CD68, but did not achieve statistical significance. Bivariate analysis revealed that CD11b/CD206 macrophage densities were correlated with gene activities associated with fibrosis and angiogenesis, whereas CD11b macrophages correlated with gene activities associated with proteostasis and cellular turnover. Lastly, an *in vitro* model of skeletal muscle cell and macrophage integration was developed to study how macrophage phenotype influences insulin responsiveness. Data suggest that M1 macrophages inhibit insulin stimulated glucose disposal, whereas M2 macrophages enhance this response. Taken together these results suggest a functional distinction between inflammatory (M1) and alternative macrophages (M2) in exercise and insulin resistance that is altered with age.

KEYWORDS: Skeletal Muscle, Exercise, Insulin Resistance, Aging, In Cell Western

Jason Sean Groshong
Student's Signature

November 26, 2013
Date

THE ROLE OF MACROPHAGES IN EXERCISE AND INSULIN RESISTANCE IN HUMAN SKELETAL MUSCLE

By

Jason Sean Groshong

Charlotte A. Peterson, Ph.D.
Director of Dissertation

Michael B. Reid, Ph.D.
Co-Director of Dissertation

Bret N. Smith, Ph.D.
Director of Graduate Studies

November 26, 2013
Date

Dedicated to:

My Grandpa: Clyde Calvin Groshong
September 15, 1925 - September 12, 2012

ACKNOWLEDGEMENTS

Graduate school required enormous patience of two people, my wife Dr. Ansam Naoum Groshong and my mentor Dr. Charlotte Peterson. I am indebted for their understanding when health or studies required an unbalanced devotion. I want to thank my committee, Dr. Karyn Esser, Dr. Mike Reid, Dr. Phil Kern, for advice on these projects, and Dr. Daniel Noonan for volunteering his time as outside examiner.

I knew I wanted to be a scientist since I was a little boy, having a ravenous curiosity, and love for nature. I spent my boyhood wandering the woods and wetlands of Ham Lake, Minnesota. Early inspirations were nature show hosts Marlon Perkins, David Attenborough, and Jacques Custeau. My reading of those days was natural history.

I am here today because of the support of many. I give thanks: My wife's parents Dr. Adil Naoum and Nedhal Abdallahad, for the financial assistance that made this all possible. My family who tried to understand this "someday when I go to graduate school" obsession. My Grandparents were especially important and taught me how to love and to live. My Mom, Olivia Groshong, whom enrolled me in summer school "mini-scientists" courses. My Dad, Larry Groshong, who shared a love for nature. To my excellent biology teachers and friends, Jim Barnett and Warren Rumsch. To my biology professors, Dr. John C. Cronn, and Dr. David K. DeGroote, for being great mentors and friends. To Dr. Christopher Gomez, whom recognized I had creativity, and allowed me to flourish independently in his lab. To my old crew mates, Steve "Tiny" McGuire, Dale Everson, Robert "Bubba" Paul, Conrad Groshong, James "Jim-Bob" Blood and the late Lloyd Murphy, I learned so much from you. My friends Kevin Cole and Family, and Richard Pontius, for help in hard times. There were times when my life got off track, but I would always somehow end up back on this course, because of the God's Grace. After all I have been through, this is another miracle. My whole life is a testimony to Christ.

TABLE OF CONTENTS

List of Tables

List of Figures

Chapter 1: An Introduction to Integrated Macrophage and Skeletal Muscle Biology.

OVERVIEW

The overall goal of this study was to learn how macrophages and skeletal muscle interact together as an integrated organ. We are specifically interested in this relationship because macrophages have been implicated in muscle in the context of exercise, insulin resistance, obesity and aging. There are three studies included. The first focuses on insulin signaling and insulin stimulated glucose uptake in primary muscle cell cultures derived from donors that are clinically insulin sensitive or resistant (Chapter 2). The second focuses on the role of macrophages in the exercise response in skeletal muscle *in vivo*, in human subjects with a range of insulin sensitivity, obesity or age (Chapter 3). The third study focuses on the influence of macrophage subtypes on primary muscle cell cultures derived from donors that are clinically insulin sensitive or resistant on glucose uptake *in vitro* (Chapter 4). Chapter 5 summarizes the findings of the study overall, concludes with some speculations and suggests further studies. The rationale for embarking on these studies is described below.

Rationale for Chapter 2

The need for an *in vitro* model system to study insulin resistance in human skeletal muscle is great, not only because of the human health factor, but also because mechanistic studies in humans are not possible. Human skeletal muscle can be studied *in vitro* by primary cell culture of myotubes (see below, Muscle Cell Culture). The consumption of dietary fatty acids, has been studied extensively as a determinant of insulin resistance(2, 14, 64, 71, 139, 193). Our laboratory's previous work on macrophages and myotubes in co-culture with palmitic acid to mimic the obese environment(184), showed that macrophages and palmitic acid synergize to blunt Akt phosphorylation and induce myotubes to express a more inflammatory profile. In another study of myotubes from Type 2 Diabetes Mellitus (T2DM) donors, the investigators found blunting of phosphorylation distinctly on all three Akt isoforms, due to an upregulation in protein phosphatase PH domain rich in leucine repeat protein phosphatase 1(PHLPP1)(39). Chapter 2 was designed to extend these studies to quantify effects on glucose uptake, a more functionally relevant measure of insulin action.

Only two published studies attempt to biologically validate human primary muscle cell culture for the retention of intrinsic properties of the donors in terms of insulin stimulated glucose uptake. Henry and colleagues (30, 73) reported nearly two decades ago that the insulin sensitivity status of the donor was passed on to the culture, and insulin signaling was retained; however, this was only demonstrated in acutely cultured muscle cells and has not been replicated

our knowledge. There are several probable reasons for this. First, the cells must be cultured directly from the muscle biopsy. Second, it is difficult to recruit enough human patients and biopsy them at once to do a statistically valid experiment. Third, human subjects have enormous genetic variability. These problems can be circumvented if one is able to store the cells over time, gathering more patients for the study, and expanding the cells over several passages, so many experiments can be done at the same time. One of the major findings in the 1995 publications by Henry et al. was the retention of the insulin response of the donor, providing evidence for a genetic basis for T2DM, but experiments needed to be repeated at later passages to confirm that finding. Our work presented in Chapter 2 is performed in cells of later passages. We also developed the use of In-Cell-Western to measure Akt phosphorylation in cultured human muscle cells from insulin resistant and sensitive donors. The experiments are performed in 96 well microplates, and are especially suited for applying drugs as interventions. We predicted that Akt phosphorylation and insulin stimulated glucose uptake would be preserved *in vitro,* congruent with the insulin sensitivity of the host.

Rationale for Chapter 3

Chapter 3 focuses on the role of macrophages in exercised muscle in adult humans in the context of obesity, aging and insulin resistance, which was conceived for two obvious reasons. First, a sedentary lifestyle has known morbidity, where exercise has been prescribed as an intervention medically known to improve overall health; however, cellular and molecular mechanisms in muscle responsible for this improvement are not well understood(8, 121). Second, although exercise is generally beneficial, the response to exercise is highly variable between individuals, which we hypothesize is influenced by the inflammatory state of the muscle prior to exercise and to the inflammatory response of the muscle to the exercise stimulus. In sedentary individuals, muscle macrophage abundance is associated with obesity and insulin resistance(184). Macrophages also infiltrate muscle in response to damage that occurs in certain types of exercise, such as downhill running and weight lifting, that emphasize eccentric contractions(89, 104-106, 123, 169). Our laboratory and others are exploring the role of macrophages in skeletal muscle in the context of exercise, insulin resistance, obesity and aging(23, 44, 80, 126). Our study includes human subjects of variable health status, examining the types of macrophages that populate the muscles, how the gene messages in muscle tissue change with exercise, and whether or not the measures correlate with health status. We predicted that aerobic exercise training would produce beneficial adaptations, reflected in macrophage content in the muscle, which would alter the response of the muscle to a subsequent acute bout of eccentric exercise, potentially

minimizing inflammation and damage. With damage, it is known that inflammatory macrophages increase; we predicted that anti-inflammatory macrophage content would dominate following aerobic exercise training, and an eccentric bout of exercise after aerobic training, would yield a diminished level of inflammatory macrophage infiltration. The last portion of our hypothesis was that adverse health status, such as obesity or insulin resistance would impair these adaptations.

Rationale for Chapter 4

The third and last study was designed to determine the effects of secretory products from different macrophage subtypes on the ability of human skeletal muscle cells to clear glucose. Studies in adipose and muscle have determined that low grade inflammation is linked to obesity and insulin resistance(48, 178). Our laboratory has reported that macrophage densities increase in muscle with insulin resistance and obesity *in vivo*(184), but the phenotype, or polarization state, of those macrophages is currently unknown. Chapter 3 will fill that knowledge gap. We previously showed that inflammatory macrophages inhibit Akt phosphorylation in cocultured myotubes (184). The Klip laboratory activated a mouse macrophage cell line with palmitate, the palmitate conditioned media was applied to rat myoblasts, which inhibited Akt phosphorylation, Glut4 translocation and glucose uptake(139). In this chapter, our intent was to dissect the molecular events of insulin resistance and glucose

uptake on muscle cell cultures exposed to conditioned media from macrophages polarized into different phenotypes. We quantified both the cytokine secretions from macrophages, as well as cytokines that were induced by macrophage products from the muscle cells. We measured glucose uptake at baseline and with insulin stimulation after exposure to macrophage conditioned media. We hypothesized that secretory products from the different macrophage subtypes would influence glucose uptake in muscle cells *in vitro* consistent with insulin sensitivities and macrophage profiles *in vivo*. We have touched upon aspects of macrophages, insulin signaling, muscle *in vivo* and *in vitro* and exercise. Next we provide a brief summary of the basic biology of these processes pertinent to the study.

MUSCLE CELL CULTURE

Adult skeletal muscle harbors stem cells, termed satellite cells(47), identified by expression of the transcription factor Pax7, that give rise to mononuclear progenitor cells or myoblasts, characterized by the expression of the transcription factor MyoD(11, 172). Myoblasts are capable of regenerating multinucleate post-mitotic skeletal muscle myofibers (37, 38, 131). Through a skeletal muscle biopsy, myoblasts can be isolated by enzymatic dissociation and expanded in cell culture. Myoblast proliferation is governed by MyoD, which suppresses the differentiation program. *In vitro*, myoblasts can be differentiated into multinucleated myotubes, mimicking myofiber formation *in vivo*, through serum restriction(43). Myoblast differentiation is governed by a drop in MyoD

expression and induction of myogenin, which signals for fusion of myoblasts into syncitial myotubes. Henry's group found a preservation of insulin signal and glucose uptake in human myotube cultures(30, 73).

INSULIN AND SKELETAL MUSCLE

Insulin is a peptide hormone of energy utilization, storage and growth. Figure 1.1 is a schematic of insulin dependent energy homeostasis in muscle during the absorptive phase. About 75% of the plasma glucose disposal is handled by skeletal muscle, consequently, 75% of the glucose derived energy expenditure occurs in muscle(138), Impaired glucose uptake in response to insulin is one of the hallmarks of T2DM(17, 86). Skeletal muscle is also the major depot of glycogen storage in mammals; glycogen synthesis is also an insulin dependent process

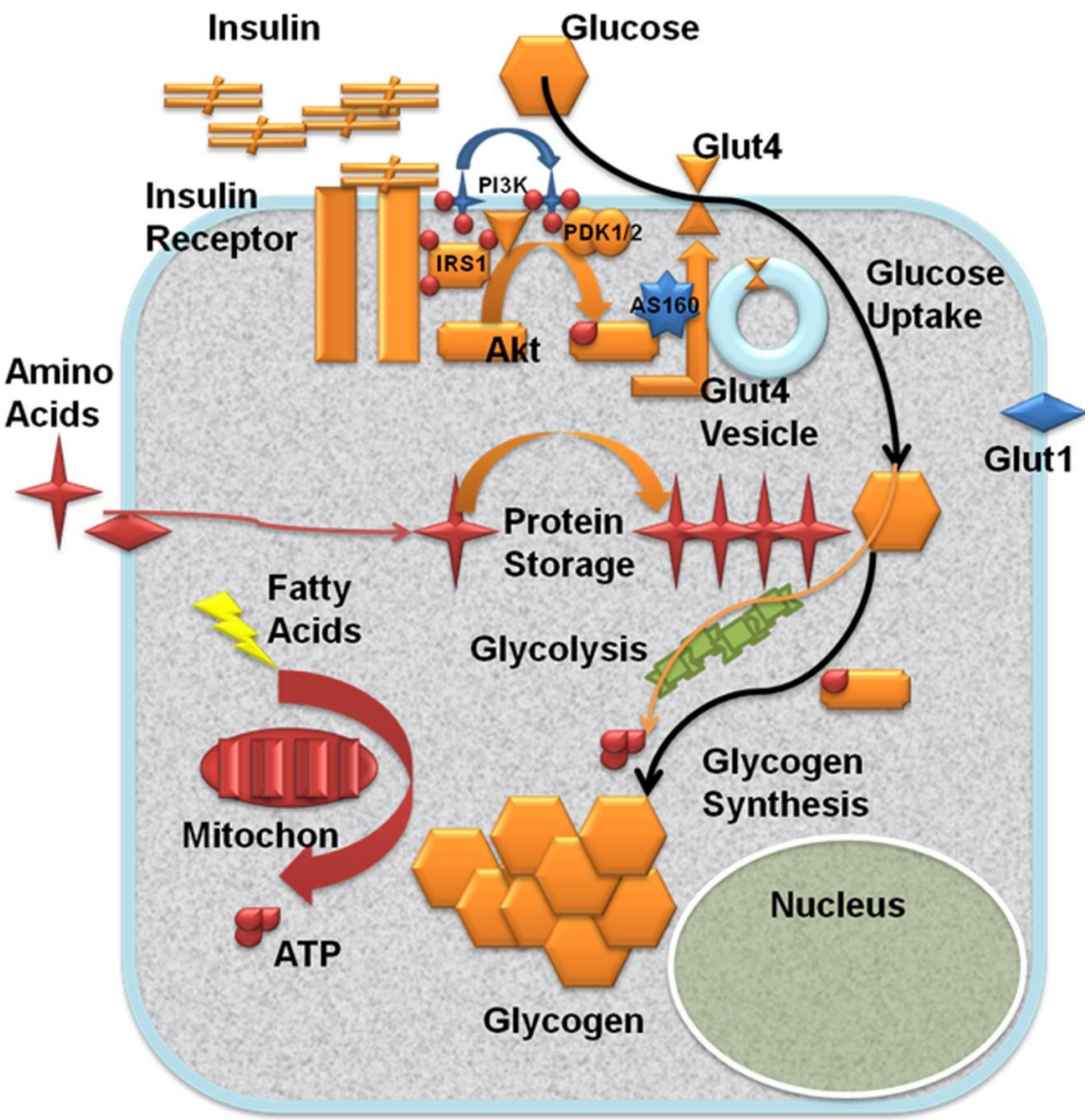

Figure 1.1 Insulin and homeostasis in skeletal muscle.

(196). Insulin signaling also promotes protein synthesis(95), cell growth and survival(107),but inhibits protein degradation(168, 187).

Glut4 vesicles translocate (blue vesicle) and coalesce with the cellular membrane, thereby inserting Glut4, for glucose uptake (black line). Glucose uptake in muscle can occur through multiple mechanisms which impinge upon independent activation of AS160(137). For example, exercise depletes muscle cells of energy stores, which activates AMPK, thereby inducing glucose uptake(175, 197). On the other hand, insulin stimulated glucose uptake depends upon the activation of Akt, and subsequent activation of AS160 for Glut4 translocation to the cell membrane, which is why we chose to measure phospho-Akt, in addition to glucose uptake, as our insulin signaling endpoints in Chapter 2.

BASIC MACROPHAGE BIOLOGY

Macrophages are cells of the immune system, specifically myeloid in origin, and are resident in the peripheral tissues of most higher organisms. Macrophages distinctively originate from CD68-bearing monocytes, which are recruited into peripheral tissue, where they differentiate into tissue resident macrophages (Figure 1.2, green cells). Macrophages were once thought to only

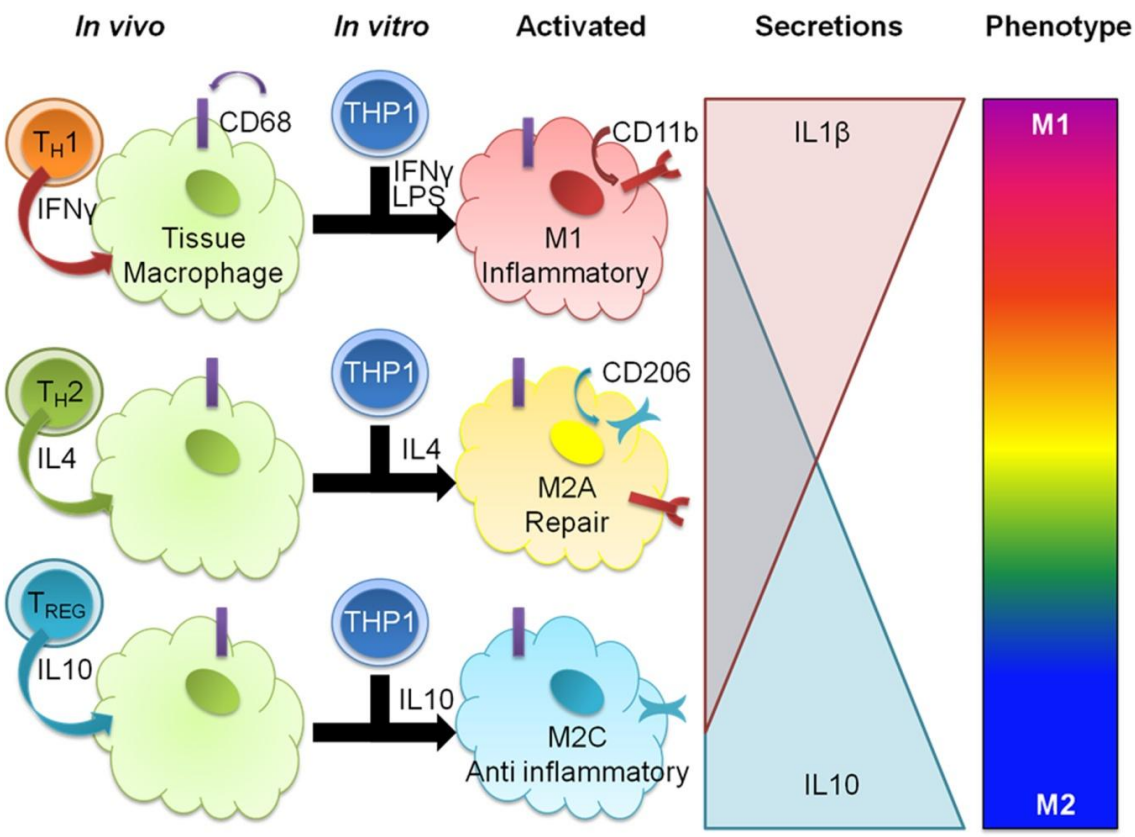

Figure 1.2 Basic macrophage biology

function as custodians, and present antigens to the T-cells, of which some have**.** cytotoxic effects (the classical view). We now know that macrophages are heterogeneous, exhibiting different activation states. Basic nomenclature of macrophages is based upon the type of integrated T-cell response (Th1 or Th2)(155), related to the activation state known as polarization (M1 or M2, respectively). One of the types of M2 macrophages, M2C integrates its response with T-regulatory cells (T_{REG}) which are thought to be inhibitory to Th1 responses, and whose activities with macrophages are mediated through the anti-inflammatory Th2 cytokine IL10(15, 67, 155). Activated by IFNγ and LPS, M1 classically activated macrophages (Figure. 1.2, red cell) can be identified by the cellular marker CD11b, and secrete inflammatory cytokines (IL-1β, IL-6,TNFα), which induce inflammatory pathways(JNK1, NFκB, SOCS). Alternatively activated via IL4 or IL10, M2A and M2C macrophages (Figure. 1.2, yellow and blue cells, respectively) can be identified by surface expression of mannose receptor, CD206, and secrete anti-inflammatory cytokines such as IL-4, IL-10, IL-13. Polarized macrophages can be produced in the laboratory, using the same cytokines which mediate their polarization *in vivo;* we treat THP1 (a human monocyte cell line) cells *in vitro* with these cytokines to specifically polarize macrophages (IFNγ/LPS for M1, IL-4 for M2A, and IL-10 for M2C)(179); we confirm the phenotype by measuring levels of cytokines they secrete. M1 macrophages are IL1β ^{hi}, IL10^{lo}; conversely M2 macrophages are IL1β^{lo} and IL10^{hi}. However, macrophage functional variation is clearly a continuum(108, 113). Some harbor both M1 and M2 "mixed" characteristics, such as M2A

macrophages (yellow cell) which function in allergic response, isolation and killing of parasites, but secret IL-1β, as well as anti-inflammatory IL-10. M2C macrophages serve similarly, but they also serve in matrix deposition and tissue remodeling, secreting IL-10 and TGFβ. How anti-inflammatory cytokines work is still not completely understood; however, they mostly function through the suppression of inflammatory pathways. For example, IL-10 is known to inhibit the expression of the inflammatory TLR4/MyD88 signaling pathway(108).

INSULIN RESISTANCE AND INFLAMMATION

There is a significant body of evidence suggesting that inflammation in adipose tissue contributes to the pathogenesis of insulin resistance (Figure 1.3, purple and red pathways) (5, 118, 138, 143-145, 198). As we have pointed out in the previous section on macrophage biology, macrophages are a significant source of inflammatory cytokines. Macrophage content in adipose is elevated in obese and insulin resistant individuals compared to that of healthy patients(190, 192)

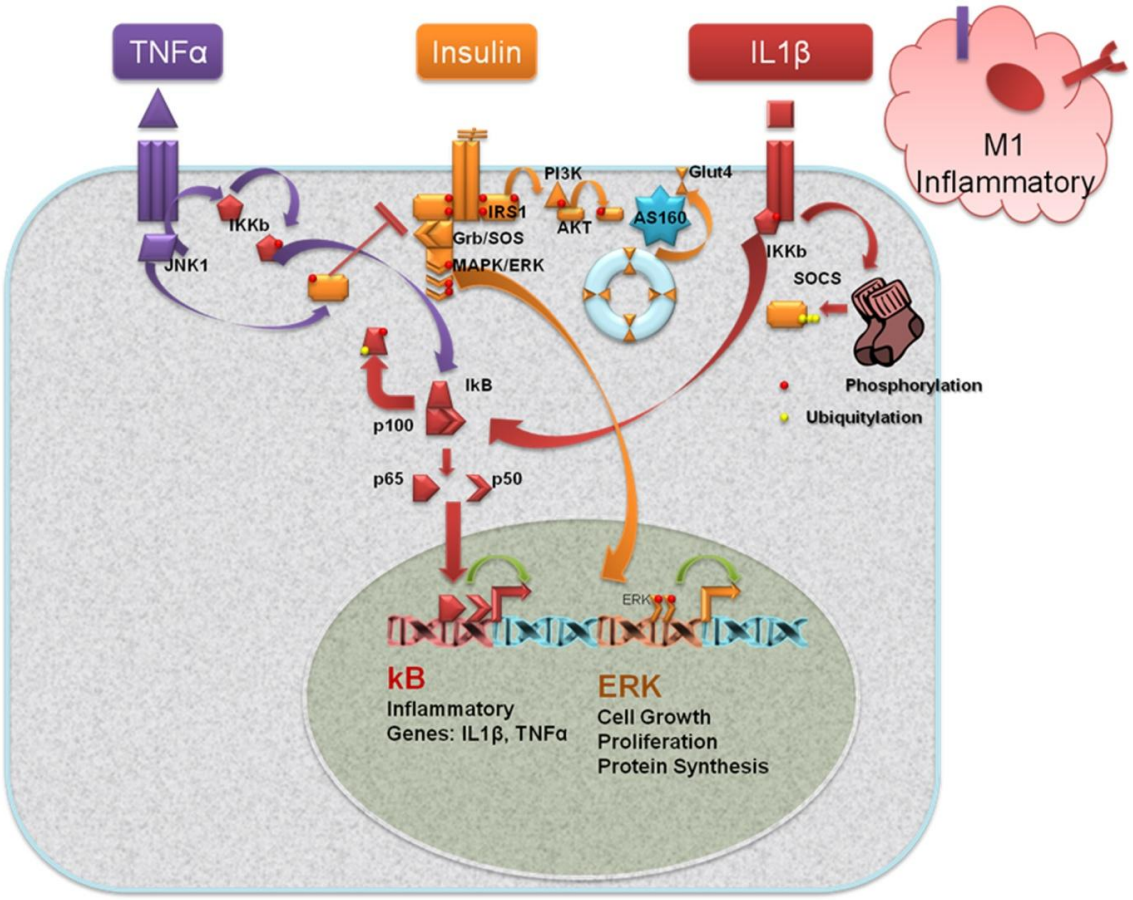

Figure 1.3 Insulin resistance and inflammation

When insulin signaling is impaired by inflammatory cytokines, energy containing molecules are unavailable to insulin sensitive tissues for metabolism, leading to global hyperglycemia and hyperlipidemia. Hyperlipidemia and insulin resistance can lead to ectopic deposition of fat in peripheral tissues. Macrophages clear this lipid, and are of the inflammatory M1 type(68, 192). M1 macrophages are known to secrete TNFα (Figure 1.3, purple pathway); when bound to its receptor, TNFα induces JNK1 dependent phosphorylation of serine 307 of the insulin receptor substrate 1 (IRS1) that inhibits recruitment to the insulin receptor (IR)(5, 76, 118). M1 macrophages also secrete IL1β and IL6. Insulin signal transduction may also be impaired when IRS1 is degraded via ubiquitin mediated pathways after IL6/SOCS activation (189) (Figure 1.3, red pathway). Activation of either of these inflammatory pathways (Figure 1.3, purple and red) concomitantly activates the NF-κB, signaling which induces secretion of inflammatory cytokines in the target tissue, amplifying the initial inflammatory signal through a feed forward mechanism.

Most of the data regarding macrophage infiltration of adipose and the effects of obesity have been derived from rodent studies(13, 138, 190). In mice, as diabetes progresses, adipose resident macrophages undergo what is known as the M2 to M1 transition (102). In diet induced obesity, the M1 to M2 ratio was skewed towards an M1 phenotype in the epididymal fat of mice, and pioglitizone treatment reduced the M1 content of epididymal fat(62). In impaired glucose tolerance humans, our group determined that pioglitazone decreased the macrophage content in adipose tissue through apoptosis(16). Further study by

our group indicated, insulin sensitivity (S_I) was inversely correlated with CD68 mRNA in subcutaneous adipose. CD68 mRNA was also directly correlated to plasma IL6 levels and to TNFα secreted from the adipose biopsies incubated for 2 hours in culture medium. Ten weeks of pioglitazone treatment in these subjects improved insulin sensitivity and reduced both CD68 and MCP1 mRNAs. Thus, the reduction in macrophages improved the inflammatory profile and S_I(48). However, these studies did not discriminate between macrophages types, and what the interaction may be with adipocytes. One of the hallmarks of obesity in mouse adipose are crown like structures (CLS), which are conglomerations of multinucleate M1 macrophages and dying or dead adipocytes. However, CLS in human subcutaneous adipose during obesity are also primarily composed of M1 macrophages; however, these are much less abundant in human adipose than mouse. Further, our group has shown that obesity and insulin resistance in humans is associated with fibrosis in adipose, largely comprised of Collagen VI, which is inversely correlated with insulin sensitivity, and directly correlated to macrophage number. Macrophages that accumulate in fibrotic areas are primarily M2 anti-inflammatory macrophages; only a fraction of the macrophages in obese adipose tissue were of the M1 type, the majority of macrophages were of the M2 anti-inflammatory type. Overall, In healthy subject adipose, more M1/M2 mixed macrophages were counted, which was reduced in obese subjects Thus, this study suggested for the first time that in humans, M2, and M1/M2 mixed macrophages may play a significant role in insulin resistance and obesity(162). Further studies from our group indicated decreased elastin and

increased Collagen V was correlated with decreased in the capillarization in adipose tissue of obese human subjects. Coculture experiments with M2 macrophages and adipocytes resulted in reduced elastin and collagen V mRNA in the macrophages, and the addition of Collagen V to endothelial cultured cells inhibited endothelial budding. Thus, with obesity in humans, M2 macrophages may contribute to defects in ECM and angiogenesis in adipose tissue(161).

Compared to adipose, very little is known regarding the influence of muscle macrophage content on insulin responsiveness. Our laboratory was the first to describe a greater accumulation of macrophages in the muscle of obese and insulin resistant humans(184). The Klip laboratory used a chemokine ligand knockout mouse (CCL2) and wild type litter mates to study macrophage infiltration in muscle in response to a high fat diet. The wild type mice showed increased accumulation of CD11C inflammatory macrophages, and glucose intolerance compared to CCL2KO littermates. In this same study they found in human skeletal muscle, CD68 and CD11C were associated with poor glucose disposal and adiposity(57). Furthermore, Klip found in the skeletal muscles of diabetic human subjects, that CD11C were correlated with clinical measures of diabetes and obesity, an observation which was ameliorated after correction for age. In exercised obese subjects, they found transcripts of anti-inflammatory macrophage markers CD206 and CD163 correlated with a high glucose disposal rate(58). The present study endeavors to examine how both classically (M1) and alternatively activated (M2) macrophages change in response to different types of exercise *in vivo* (Chapter 3), and how their secretory products modulate

glucose uptake in human skeletal muscle-derived myotubes (Chapter 4). The characterization of skeletal muscle/ macrophage interactions may lead to novel approaches of preventing and/or treating the insulin impairment manifested by T2DM.

MACROPHAGES IN MUSCLE RESPONSE TO EXERCISE

Studies in mice reveal that experimentally-induced damage to skeletal muscle increases macrophage content(49, 176, 177). M1 macrophages participate in an inflammatory response to damage and phagocytize degenerating myofibers. Subsequently, M2 macrophages are recruited that secrete anti-inflammatory cytokines and growth factors, aiding in repair and regeneration. Many labs have demonstrated the absolute requirement for macrophages for muscle regeneration to proceed(6, 28, 29). For example, MCP1 (macrophage chemokine protein 1) knockout and chemokine receptor knockout mice subjected to muscle damage are unable to regenerate or repair their muscles(109, 152, 153). These are genetic strategies which cannot be used on humans. However, we do know that certain types of exercise induce muscle damage, which can be studied in humans.

Some activities, such as downhill running and resistance exercise, are prone to injure skeletal muscle. In general, resistance exercise (weight lifting) is composed of two motions (Figure 1.4). Lifting the weight requires a contraction

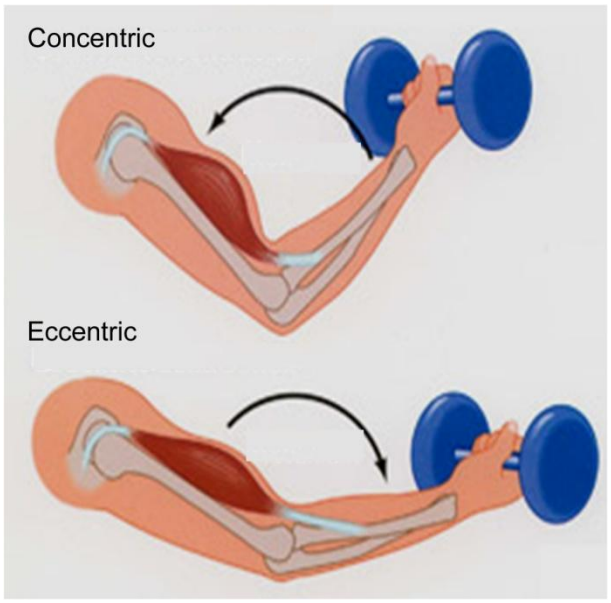

Figure 1.4 Concentric and eccentric contractions.

of the muscle; muscle fibers contracting and shortening at the same time is known as concentric contraction. Conversely, extending the limb to lower the weight, requires simultaneous lengthening of the fibers while contracting to maintain the load, referred to as an eccentric contraction. Eccentric contractions cause muscle damage, allowing study of muscle repair in humans, a process which is mediated by macrophages.

Aerobic exercise, in general, does not cause damage to muscle. Indeed, aerobic exercise, such as cycling, is beneficial to the muscle by increasing blood flow, conditioning the muscle for endurance, improving insulin sensitivity and decreasing obesity. Through extended aerobic exercise, the increased demands for energy by the muscle induces increased vascularization (65, 66). Another adaptation is that the oxidative capacity of the muscle is increased, through upregulating genes within the oxidative phosphorylation pathway(77), and/or by increasing mitochondrial content(63, 119, 195). More efficient oxidative phosphorylation consumes more fatty acids and produces less reactive oxygen species(21, 55). In response to aerobic exercise, muscle is also known to increase the content of its buffers to free radical stress(129).

Resistance and aerobic exercise induce different programs of remodeling of the muscle tissue and interstitium, and Chapter 3 was designed to determine if different subtypes of macrophages mediate these processes. Alternatively activated, tissue resident M2 macrophages are involved in angiogenesis, tissue remodeling, and wound repair in mice and humans(108). The concerted infiltration of M1 and M2 macrophages into skeletal muscle is associated with the

proliferation and differentiation of myoblasts in the repair of damaged myofibers(177). *In vitro*, macrophage products can promote the differentiation of satellite cells(36). Studies in rodents suggests that there is phenotypic shifting from an M1 inflammatory to an M2 anti-inflammatory mode which promotes repair programs(6), protects against muscle atrophy(52), and supports muscle recovery *in vivo* and *in vitro*(23, 27, 52). Mechanistically, secretory products from M2 macrophages directly aid in growth and repair by stimulating the activity of muscle satellite cells(135). The different macrophage phenotypes we have described have distinct effects on myoblasts. Work by the Chazaud group suggests that inflammatory M1 macrophages promote myogenic cell proliferation, and that anti-inflammatory M2 macrophages promote differentiation(6). Further studies by Chazaud suggest that coinjected bone marrow derived macrophages and myogenic precursor cells improve survival in myogenic precursor cells after implantation in mdx mouse skeletal muscle(98), but they did not identify the phenotype of the macrophages. Results reported in Chapter 3 suggest coincident changes in macrophage populations congruent with changes in genes involved with fibrosis and angiogenesis, emphasizing that macrophages are important in interstitial tissue remodeling in muscle response to exercise. Although we have described distinct macrophage phenotypes in this review, investigators have probably not identified all the cellular markers and macrophage types involved skeletal muscle repair. With the available tools

we can only conclude that M1s and mixed M1/M2 macrophages are important elements of the muscle repair program.

Chapter 2: Human skeletal muscle cell cultures from obese subjects retain insulin signaling through Akt, but are disconnected from insulin stimulated glucose transport.

SUMMARY

We determined the insulin stimulated Akt protein phosphorylation at serine 473 and glucose disposal *in vitro* in differentiated myotubes derived from muscle biopsies from several human subjects with a spectrum of clinical insulin sensitivities (S_I, 1.3 - 5.41 x 10^{-4} $min^{-1}\cdot(\mu U\cdot ml)^{-1}$ by FSIGT). Using In-Cell-Western, we found a dose response in insulin signaling through Akt phosphorylation that was, for the most part, congruent with the S_I of the donor; those with the highest S_I demonstrated the highest dose response. Further, myotubes derived from more insulin sensitive individuals had a higher pAkt/Akt ratio at 5 nM insulin. However, glucose uptake in myotubes was minimal and not correlated to Akt phosphorylation. Individual comparisons of glucose uptake revealed that the myotubes from the most insulin resistant donor had a significant increase in 5 nM insulin stimulated glucose uptake compared to myotubes from more insulin sensitive individuals. We conclude that late passage myotubes activate insulin signaling pathways consistent with the clinical insulin sensitivity of the donor but have lost the ability to respond to insulin at the level of glucose disposal.

INTRODUCTION

Type 2 Diabetes Mellitus (T2DM) is a devastating and lethal disease if untreated, characterized chiefly by a person's inability to respond to insulin, thereby restricting access and storage of available nutrients. The dominating feature is impaired insulin response (138, 198), in the beginning, known as insulin resistance, then later through pancreatic β cell exhaustion as a result of compensatory hyperinsulinemia, where insulin is no longer secreted. Insulin is a peptide hormone of energy utilization, storage and growth. When insulin signaling is impaired, energy containing molecules are unavailable to insulin sensitive tissues for metabolism, leading to global hyperglycemia and hyperlipidemia. T2DM is an important disease in developed societies leading to many billions of dollars in medical costs per annum (79). T2DM leads to a whole host of secondary diseases including diabetic neuropathy, nephropathy, retinopathy, obesity, stroke and cardiac disease, such that T2DM is among the highest ranking disease related to mortality beyond middle age (79). Treatment involves oral therapies including insulin sensitizers (ie.metformin), insulin secretion agonists (secretogogues, ie. glipizide), or by injection with recombinant insulins. The mechanisms of insulin sensitizers are not well characterized in skeletal muscle, and have primarily been studied in liver and white adipose.

The crosstalk of other tissues and skeletal muscle related to T2DM is not well understood, therefore, skeletal muscle is a novel therapeutic target for insulin sensitizers. Dysfunctional insulin response is thought to be the cause of

this disease, but the molecular pathogenesis is not fully delineated. Impaired glucose uptake in skeletal muscle is one of the hallmarks of T2DM; about 75% of the plasma glucose disposal is handled by skeletal muscle. Consequently, 75% of the glucose derived energy expenditure occurs in muscle (138). It has been reported that muscle cells from diabetic subjects retain their phenotype *in vitro*, suggesting stable intrinsic alterations to cellular metabolism (30, 73). On the other hand, in white adipose, the development of inflammation is thought to be a major determinant in the etiology of insulin resistance (138, 198). Through hyperlipidemia and response to adipose derived inflammatory cytokines, the deposition of ectopic fat and impaired insulin signaling in skeletal muscle are also thought to be a player in the insulin impairment under diabetic conditions(128, 160-162, 184).

Skeletal muscle harbors stem cells, termed satellite cells that give rise to daughter cells or myoblasts, that are capable of regenerating and replacing damaged post-mitotic skeletal muscle myofibers. Through a tissue biopsy, myoblasts can be isolated by cell culture, and grown *in vitro*. Skeletal muscle fibers can be emulated in the laboratory by growing myoblasts on special medium, inducing fusion and differentiation into multinucleate tube like syncitia, so-called myotubes. We use insulin-treated cultured myotubes to explore underlying, intrinsic mechanisms of insulin resistance in skeletal muscle. We have collected quantitative data and observations related to insulin signaling fluxes by infrared detection. We rely principally on a technique termed, In-Cell-Western (ICW), which eliminates the need for manipulations such as cellular

disruption. ICW utilizes a 96-well plate setup, coupled with the 10,000 fold detection range of infrared labeling technology, providing a novel system for studying insulin signaling *in vitro*.

We hypothesized that insulin response of the donor would be preserved in cultured myotubes. We determined the insulin stimulated Akt protein phosphorylation and glucose disposal *in vitro* on differentiated myotubes of several donors with a spectrum of clinical insulin sensitivities. We found that insulin signaling through Akt phosphorylation was, for the most part, congruent with the clinical sensitivity, but glucose disposal, a further downstream result of insulin signaling, was disconnected from both the degree of Akt phosphorylation and clinical sensitivity. Thus, we conclude that although skeletal muscle cells *in vitro* activate signaling pathways in response to insulin, this is disconnected from glucose disposal.

MATERIALS AND METHODS

Subjects and Tissue Collection

Human non-diabetic subjects were recruited through local advertising. All subjects included in the study were recruited by informed consent approved by the institutional review board at the University of Arkansas for Medical Sciences

or the University of Kentucky. Muscle biopsies from six subjects were included in this study. Muscle biopsies were collected from vastus lateralis muscle under local anesthesia. Standard fasting blood lipids were measured at the time of biopsy. The clinical insulin sensitivity (S_I) was measured by frequently sampled IV glucose tolerance test (FSIGT) with minimal model calculation (191). Subjects were considered insulin sensitive at $S_I > 2.5$ and resistant at $S_I < 2.5 \times 10^{-4}$ $min^{-1} \cdot (\mu U \cdot ml)^{-1}$. See Table 2.1 for details.

Cell Culture

Myoblasts were isolated as previously described (184). Passage 4 myoblasts were propagated on Primaria p100 plates (BD Biosciences, 353803, Franklin Lakes, NJ), in growth medium composed of Hams/F10 medium (Cellgro/Mediatech, 10-070-CV, Manassas, VA) supplemented with 20% fetal bovine serum (FBS, Atlanta Biologicals, S12450, Lawrenceville, GA), 5 mg/ml basic Fibroblast Growth Factor (bFGF,Millipore, GF003) and 1% Penicillin/Streptomycin (Gibco/Life Technologies, 15140, Grand Island, NY), and maintained with 5% CO_2 at 37°C. Cells were split at 50% confluence. At passage 6 or 7 the myoblasts were released with 1% trypsin (Gibco/Life Technologies, 15400-054) and seeded at 150 cells/mm^2 onto 96-well Primaria plates (BD Biosciences,353872 San Jose, CA) pre-coated with collagen I at 0.3 mg/ml (Gibco/Life Technologies, A1048301) in PBS overnight. All liquid handling at

Table 2.1 Clinical subject characteristics.

SI	Gender	Age	BMI	cholesterol	triglycerides	LDL	HDL	glucose 0 hr	glucose 2 hr
1.30	F	51	36	205	205	111	53	82	155
1.51	F	56	45	229	111	151	56	87	86
1.53	F	42	40	207	126	143	39	114	197
3.09	F	38	27	249	164	176	40	104	190
4.17	F	44	38	160	59	84	64	85	44
5.41	F	53	35	205	126	106	74	89	121

Units for S_I (insulin sensitivity): value x 10^{-4} $min^{-1}\cdot(\mu U\cdot ml)^{-1}$, BMI (body mass index): kg/m^2. Fasting lipids, cholesterol, triglycerides, LDL (low density lipoprotein), HDL (high density lipoprotein), and glucose 0 hour (oral glucose tolerance test baseline), glucose 2 hour (oral glucose tolerance test 2 hour time point): mg/dl.

this point was performed with a 12-well multi-channel Research Pro© electronic pipette (Ependorf, Hauppauge, NY) set on the slowest speeds for both aspiration and application of media/washes to 96-well plates. The medium was changed to differentiation medium, αMEM (Gibco/Invitrogen, 12561-049) supplemented with 2% FBS and 1% Pen/Strep, the next morning. The cells were observed and the medium changed every 48-72 hours. Differentiated myotubes were studied following 12 days in differentiation medium.

In-Cell-Western (ICW)

Differentiated myotubes were treated with increasing concentrations of insulin, 2.5, 5, 10, 20, 40 nM, (Novolin human recombinant insulin, Lilly, Indianapolis, IN) for 30 minutes with 3 replicates per concentration. Cells were fixed with 4% methanol-free formalin (Electron Microscopy Sciences, Hatfield, PA), washed with Cell Signaling Technologies (CST, Danvers, MA) immuno formulation PBS (CSTPBS) and levels of the insulin signal transduction pathway (pAkt/Akt) quantified by ICW. Cells were permeabilized in 5 washes of PBS with 0.1 % Triton-X100 (PBSX), at room temperature and blocked with Odyssey Blocking Reagent (LI-COR, 927-40000, Lincoln, NE) for 1 hour at room temperature. Primary antibody incubation solutions were prepared in 1:100 Odyssey Block and CSTPBS and allowed to incubate overnight at 4°C.

Following incubation with mouse α phospho serine 473 Akt (MsαpAkt, CST 4051) and rabbit α total Akt (RbαAkt, CST 9272), cells were washed five times in CSTPBS containing 0.1 % Tween-20 (PBST) at room temperature. Secondary antibodies, conjugated to different infrared (IR) tags were applied at 1:500 dilution; donkey α rabbit IR700 (DkαRb700) and goat α mouse IR 800(GtαMs800), LI-COR, 926-32223, 926-32210) for 1 hour at room temperature, followed by five washes in PBST at room temperature, and three final washes in CSTPBS containing no detergent. ICW signals from all wells were scanned at once, detected and quantified as raw integrated counts, in both the pseudocolored red 680 and the green 800 infrared detection channels via the LI-COR Odyssey infrared imaging system using the default ICW settings. The integrated values of the 800 nm pAkt channel divided by the 680 nm Akt channel x 100 are the values reported, mean % ±SE.

Glucose Transport Assay

Glucose transport assays were performed on differentiated myotubes in 6-well Primaria plates as follows. Myotubes were washed in 37°C Hank's balanced salt solution with phenol red (HBSS, Gibco/Life Technologies, 24020-117), then serum starved by incubation in fresh HBSS for 30 minutes. Fresh warm HBSS or 5 nM insulin in HBSS was then added for an additional 30 minutes. Cell plates were placed on a heated working surface composed of a top layer of 1 blue

chuck, then fiber glass dinner tray as the middle layer, then on a sunbeam heating pad as the bottom layer, prewarmed on the lowest setting. Cells were then washed three times in warm 37°C, PBS supplemented with 100 μM Ca^{2+} and Mg^{2+} (PBSCaMg). Wells were carefully aspirated, then 1ml of 0.33 μCi 2-deoxy-d[1,2-^{3}H]glucose (NEN Life Science Products, NEC495250UC, Waltham, MA) in HBSS was applied/well, and incubated for 30 minutes. Cells were washed three times in 37°C HBSS. The cytoplasmic fraction was liberated with 550 μl of 1% Triton X-100 in PBS by incubating for at least 5 minutes. Four hundred microliters was transferred to scintillation vials, 4.5 ml of Scintiverse cocktail (ThermoFisher, SX18-4, Waltham, MA) added and vials counted for 10 minutes each in a Beckman Coulter liquid scintillation counter. Counts per minute of the insulin treated samples were normalized to the baseline samples, and reported as relative units.

Statistical Considerations

Repeated measures ANOVA was used to determine statistical significance within subjects among the curves generated in ICW in response to different insulin concentrations. Pair wise comparisons between subjects were analyzed for statistical significance by one way ANOVA followed by two tailed Student's t-test. JMP software (SAS Institute Inc. Cary, NC) or Excel (Microsoft Corporation, Seattle, WA), was used for all analyses. There was one outlier

excluded from the measurements summarized in Table 2, which was 2 standard deviations outside of the mean, for the isolate 4.17 at 20 nM insulin, so only 2 measurements were used to calculate the mean.

RESULTS

We collected cells from muscle biopsies from individuals with a range of S_I's to quantify pAkt/Akt ratio compared to glucose transport in response to insulin in vitro. Table 2.1 shows clinical measures of body mass index (BMI), fasting blood lipids, and the fasting glucose at baseline and 2 hour postprandial, and insulin sensitivity (S_I) determined by frequently sampled IV glucose tolerance test (FSIGT) (191). The amount of variability is commonly observed in clinical data. We found a disconnect in the subjects between S_I and BMI. These measures appear to be counter intuitive when compared with fasting baseline and the 2 hour postprandial glucose. For example, the patient with an S_I of 1.51 x 10^{-4} $min^{-1}\cdot(\mu U\cdot ml)^{-1}$, considered insulin resistant, had both a fasting and a 2 hour glucose disposal that were quite effective at 87 and 86 mg/dl, respectively. On the other hand, the patient with an S_I of 3.09, considered insulin sensitive clinically, had baseline/postprandial values of 104 and 190, respectively, suggesting a less effective integrated glucose transport response. This indicates that in the clinical setting there is a disconnect between glucose disposal and S_I;

therefore, the integrated response is more complex. Our study of molecular events in vitro was designed to examine the relationship between insulin signaling and glucose uptake.

We utilized differentiated myotubes from six different individuals in 96-well plates (Figure 2.1A) to accurately measure the level of Akt phosphorylation via In-Cell-Western (ICW). The ICW analysis showed an insulin dose response in phosphorylation of Akt (Figure 2.1B), relative to total Akt (Figure2.1C; pAkt/Akt overlayed in Figure 2.1D). The ratio of pAkt/Akt with increasing doses of insulin, expressed as a percentage, is quantified in Figure 2.2. Results indicate that the insulin induced phospho-Akt response in the cultured myotubes was related to S_I of the cell donor. This observation suggests that heritable, intrinsic alterations in insulin sensitivity have been retained in myotubes through passage 7 in culture; even after our culture manipulations, the cells preserve an insulin-induced Akt response in vitro congruent with clinical insulin sensitivity measures. The numerical means and standard errors of each myotube culture are reported in Table 2.2. The main goal of this experiment was to determine if myotubes from different donors differed in Akt phosphorylation consistent with clinical insulin sensitivities, therefore, we compared subject-to-subject within each insulin concentration. In Table 2.3, the significant pairs of myotube cultures as indicated by S_I are listed for each insulin concentration. The dose response shows that most of the myotubes approached a mid-range in Akt phosphorylation at 5 nM insulin. The response approached an asymptote at 10, 20 and 40 nM. For this reason, 5 nM insulin was chosen for further experiments.

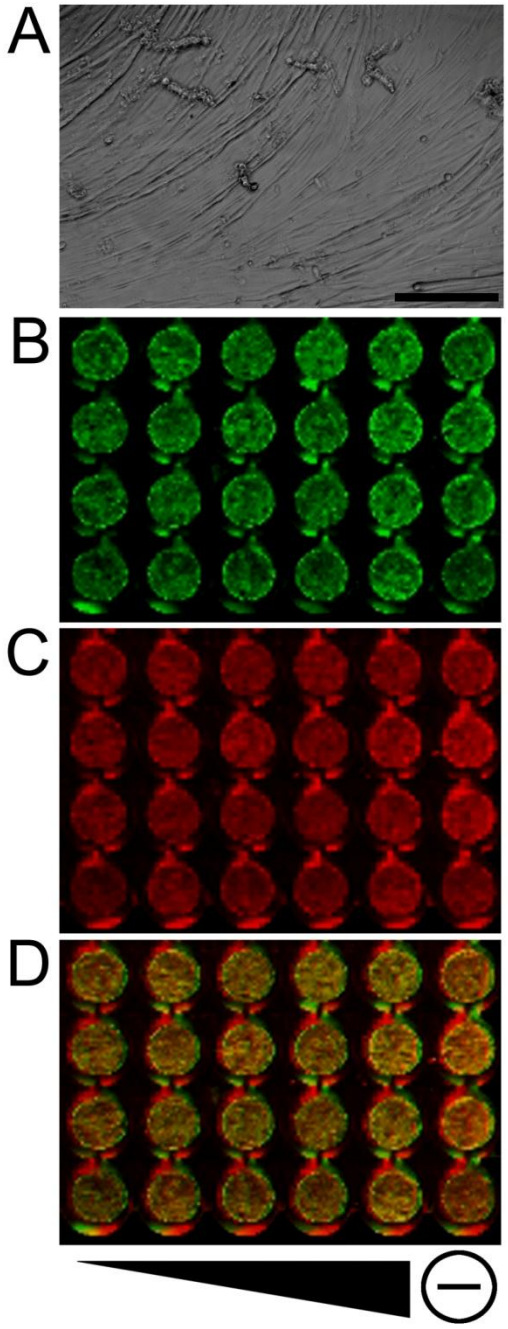

Figure 2.1 Representative images derived from a donor having a clinical insulin sensitivity of 3.09 x 10^{-4} min^{-1}·(μU·ml)$^{-1}$. (*A*) The grayscale panel is the visible light image of myotubes from the 96 well plate after 15 days of differentiation. Scale bar = 200 μM. (*B*) The green wells represent the ICW phospho-Akt signal. (*C*) The red wells represent the total Akt signal from these cells. (*D*) The orange to yellow wells are the overlay of the Akt and pAkt signals, in response to

increasing doses of insulin (2.5nM to 40nM). Far right column indicates cells with no insulin for baseline.

The pAkt/Akt percentage at 5nM insulin (Figure 2.3A) generally correlated with the S_I of the donor. There is some overlap between the donors of S_I 1.52 and 3.09 x 10^{-4} $min^{-1}\cdot(\mu U\cdot ml)^{-1}$, indicating that perhaps at mid range, our assay does not resolve the differences found by FSIGT. The asterisks in Figure 2.3A indicate that myotubes from an insulin resistant donor with S_I of 1.3 have a pAkt/Akt ratio expressed as a percentage (47.8±0.66), which was significantly different from myotubes from insulin sensitive donors, with S_I's 3.09(59.0±1.62), 4.17(63.7±1.69) and 5.41(67.5±2.04), and that myotubes from an insulin resistant donor with an S_I of 1.51 (51.7±1.98) were also significantly different from these insulin sensitive donors. However, myotubes from one insulin resistant donor (S_I 1.52) were not significantly different than the insulin sensitive donors. The pound sign indicates that cells from insulin resistant subjects with S_I 1.3 and 1.51 were significantly different from myotubes from a subject with an S_I of 1.52 (61.1±1.50, $p<0.05$, all ratios were measured in triplicate).

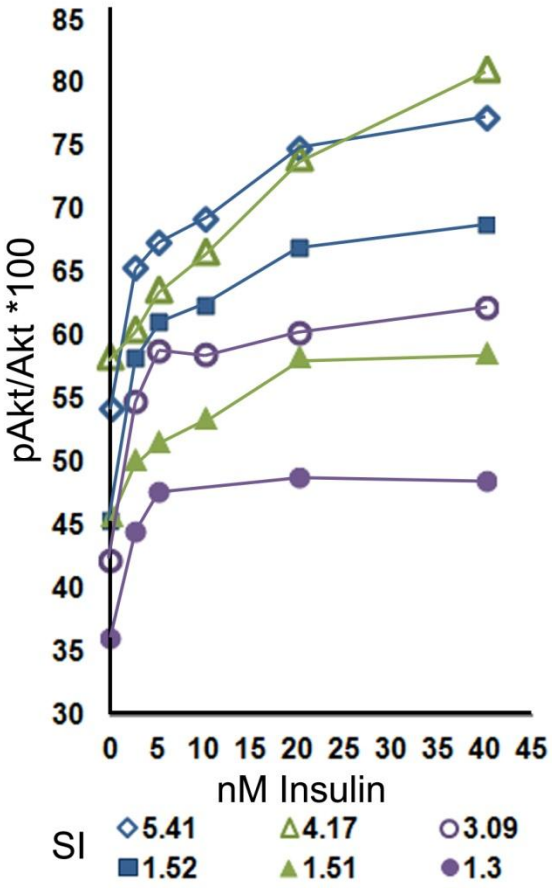

Figure 2.2. The quantified ratios of pAkt/Akt determined by In-Cell-Western (ICW) shows that insulin signaling through Akt is retained in human myotubes. The phospho-Akt to Akt ratio of each isolate expressed as mean percentage. Open symbols, cells from insulin sensitive subjects; closed symbols, cells from insulin resistant subjects. Insulin sensitivity of each subject (S_I) is shown.

The phosphorylation of Akt triggers a signaling cascade leading to Glut4 vesicle translocation to the plasma membrane, promoting accelerated glucose transport (199). Classically, this has been measured by [H^3]-2-deoxyglucose (2-DG) uptake at baseline and following insulin stimulation. We quantified 2-DG uptake at 5nM insulin, which is in the linear range of the pAkt/Akt ratios (see Figure 2.2).

Figure 2.3B depicts insulin stimulated glucose uptake, normalized to basal glucose uptake, for each myotube culture. Our observations indicate in general, that insulin stimulated glucose uptake is unchanged from basal, and that glucose uptake does not follow the pattern of Akt activation observed in Figure 2.3A or clinical S_I shown in Table 2.1. Of note, myotubes from the subject with the lowest BMI had the highest insulin stimulated glucose uptake. Individual comparisons reveal that cells from a subject with an S_I of 1.3 (in RU: 1.25 ± 0.02 n=3) had a significant increase in insulin stimulated glucose uptake when compared with those with S_I of 1.51, 1.52, 4.17 and 5.41 (0.97 ±0.10 n=2, 0. 97 ± 0.07 n=4, 1.02 ± 0.06 n=6, 0.97 ± 0.08 n=5, respectively, $p<0.05$), but was not different from S_I 3.09 (1.61 ± 0.39 n=6). An additional insulin dose response study on myotubes from the subject with S_I 3.09 revealed peak glucose uptake at 5nM and that higher concentrations were inhibitory (data not shown). Thus, our study finds that in vitro, glucose disposal is disconnected from phosphorylation of Akt.

Table 2.2 Insulin dose response in myotubes from donors of different S_I's.

SI	1.3		1.51		1.52		3.09		4.17		5.41	
BMI	36		45		40		27		38		35	
nM Ins	Mean	±SE	Mean	±SE	Mean	±SE	Mean	±SE	Mean	±SE	Mean	±SE
0.0	36.2	0.82	45.9	2.05	45.4	2.29	42.3	1.40	58.4	0.48	54.2	0.44
2.5	44.7	1.01	50.3	1.51	58.4	1.50	55.0	1.69	60.6	2.08	65.5	3.02
5.0	47.8	0.66	51.7	1.98	61.1	1.50	59.0	1.62	63.7	1.69	67.5	2.04
10.0	44.8	1.87	53.7	1.33	62.5	1.19	58.6	3.81	66.8	1.68	69.3	1.96
20.0	48.9	1.02	58.5	0.32	67.0	1.34	60.3	3.19	74.2	2.77	74.9	2.11
40.0	48.6	1.67	58.8	2.04	68.8	2.28	62.3	3.42	81.1	0.32	77.3	3.98

The numerical pAkt/Akt *100 values of the myotubes at different insulin doses as shown in Figure 2.2, mean ± SEM.

Table 2.3 Statistically significant pairs of donors by S_I, for each insulin dose.

0		2.5		5		10		20		40	
4.17	1.3	5.41	1.3	5.41	1.3	5.41	1.3	4.17	1.3	4.17	1.3
5.41	1.3	4.17	1.3	4.17	1.3	4.17	1.3	5.41	1.3	5.41	1.3
4.17	3.09	5.41	1.51	5.41	1.51	1.52	1.3	1.52	1.3	4.17	1.51
4.17	1.52	1.52	1.3	1.52	1.3	5.41	1.51	4.17	1.51	1.52	1.3
4.17	1.51	5.41	3.09	4.17	1.51	3.09	1.3	5.41	1.51	4.17	3.09
5.41	3.09	4.17	1.51	3.09	1.3	4.17	1.51	4.17	3.09	5.41	1.51
1.51	1.3	3.09	1.3	1.52	1.51	5.41	3.09	5.41	3.09	5.41	3.09
1.52	1.3	1.52	1.51	5.41	3.09	1.51	1.3	3.09	1.3	3.09	1.3
5.41	1.52	5.41	1.52	3.09	1.51	1.52	1.51	1.51	1.3	4.17	1.52
5.41	1.51			5.41	1.52	4.17	3.09	4.17	1.52	1.51	1.3
3.09	1.3					5.41	1.52	1.52	1.51	1.52	1.51
								5.41	1.52	5.41	1.52
								1.52	3.09		

Pairs are listed in ascending order by p value. Pairs with lowest p values are at the top of each column, at the bottom of each column are pairs with p values approaching 0.05.

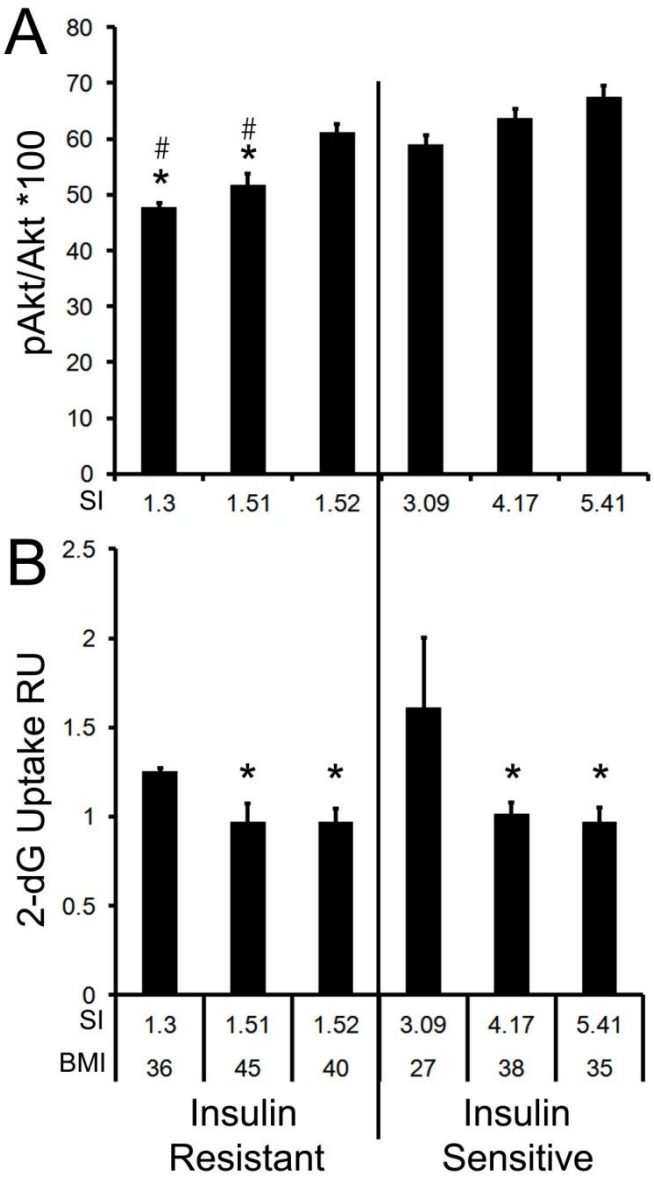

Figure 2.3. Insulin stimulated Akt phosphorylation is congruent with clinical insulin sensitivity, whereas insulin stimulated glucose transport is disconnected from both the insulin signaling and clinical insulin sensitivity. (A) pAkt/Akt ratios of human myotubes in response to 5nM insulin (from Figure 2.2 dose response) in ascending order of the insulin sensitivity of the donor. *significant differences from 3.09, 4.17, and 5.41 x 10^{-4} min^{-1}·(μU·ml)$^{-1}$ ($p<0.01$); #significant difference from 1.52 ($p<0.01$). (B) 2-deoxy-glucose uptake of human myotubes derived from the same donors and stimulation protocol as in (A), recorded as relative units by fold change over baseline. BMI of each subject is also indicated. Assays were performed at least twice and reported as means ± SEM. *significant difference from 1.3 ($p<0.05$).

DISCUSSION

Henry and colleagues reported that human primary myotubes retain stable intrinsic metabolic alterations consistent with the clinical profile of the host (30, 73), a result which has not been replicated since. We have observed differential growth characteristics that track with the insulin sensitivity of the host (unpublished data). Therefore, we posited that insulin response of the donor would be preserved in myotubes, consistent with the work of Henry et. al (30, 73). We measured the insulin stimulated Akt protein phosphorylation at serine 473 and glucose disposal in vitro on differentiated myotubes at late passage. The donor human subjects harbored a spectrum of clinical insulin responsiveness. This study revealed that insulin signaling through S473 pAkt/Akt percentage to be, for the most part, congruent with the clinical insulin sensitivity. However, glucose disposal, a further downstream result of insulin signaling, was disconnected from both the degree of Akt phosphorylation and clinical insulin sensitivity. Consequently, we conclude that skeletal muscle cells following several passages in vitro have lost the ability to respond to insulin at the level of glucose uptake.

The retention of insulin stimulated glucose uptake, glycogen synthesis, and active glycolysis enzymes that Henry and colleagues found with acutely differentiated myotubes from normal and T2DM subjects is striking (30, 73). Because of this, one of the most important inferences of that study was that there is a genetic basis for T2DM, which should be stable in muscle cells even at later

passages in vitro. The present work addresses that issue through the use of myotubes differentiated at passage 6 to 7 in culture (later passage), where we have found insulin signaling to be discontinuous from glucose disposal, and that partial retention exists only through S473 Akt phosphorylation. This partial retention of the insulin signaling cascade might suggest that perhaps there is a heritable epigenetic mechanism, but downstream glucose uptake seems not likely to be related to epigenetics. Further studies are required to confirm this hypothesis.

Our studies indicate that later passage myotubes in culture have become mostly insulin resistant at the level of glucose uptake, regardless of the clinical insulin responsiveness of the donor. One possible mechanism is that the distal events of glucose uptake may be inhibited by the removal of input from peripheral organs and tissues. There are experimental models to generate myotubes that are insulin resistant, besides simply harvesting them from insulin resistant donors. Treating mice with Streptozotocin (STZ) to destroy the beta cells in the pancreas, thereby eliminating insulin secretion, results in insulin resistance in muscle (186). Removal of the STZ-treated epitrochlear muscle followed by incubation in culture, resulted in loss of experimentally induced insulin resistance. The investigators utilizing this method cited another study that the lack of insulin over a long period of time, down regulates the glucose transport apparatus (88).

A second way to induce insulin resistance in vitro is to expose the myotubes to supra physiological concentrations of glucose (hyperglycemia) or

insulin (hyperinsulinemia), or both at the same time for a long duration (30). It has been proposed that this treatment down-regulates proteins associated with the insulin signaling machinery through negative feedback loops. One of these mechanisms could be playing a role in our study. To prevent differentiation, our laboratory maintains myoblasts at 20% FBS, which is likely to have a 10 fold higher endogenous bovine insulin than the 22 pM measured insulin in 2% FBS reported in Henry (30). The limiting factor in our study was producing enough cells for the glucose uptake assay, which required 2-3 weeks of propagation, and 2-3 passages. Endogenous insulin for humans between meals range from 57-79 pM (81), and during meals are reported to oscillate between 100 and 800 pM for a duration of 3-6 minutes (70). The primary organ responsible for removal of insulin from the blood is the liver. In culture we have removed the effects of other organs so there is the possibility that having a continuous dose of 200 pM of bovine insulin every 48-72 hours may set up an insulin resistant state in the myoblasts, prior to differentiation in 2% FBS. Henry and colleagues required a much higher 30 μM insulin for a period of 4-6 weeks to set up an experimentally induced insulin resistance in myotubes from normal subjects. In our hands, myotubes require a period of 10-12 days to differentiate into myotubes, where they are exposed to the lower 22 pM insulin found in 2% FBS, which in this case did not restore glucose uptake in response to exogenous insulin.

Lastly, much of the literature on insulin resistance focuses on the presence of a chronic low state of inflammation in the peripheral tissues mediated by tissue resident macrophages (68, 118). These reports suggest that

most of these inflammatory cytokine related mechanisms impinge on aberrant activation of Akt, through a multitude of mechanisms which either block recruitment of IRS1 to the insulin receptor or cause an inhibitory phosphorylation of IRS1 (5, 76, 94, 118), thereby inhibiting downstream processes. We have removed the peripheral affects of macrophages and other tissues in the in vitro study which resulted in insulin stimulated Akt phosphorylation largely tracking with the insulin sensitivity of the donor. Although 5 nM insulin was effective in eliciting a pAkt response, this dose did not elicit glucose uptake, which argues that while activation of Akt is functional, some component downstream in the signaling pathway leading to insulin stimulated glucose uptake is not responding properly.

While the data in this study indicate the distal glucose uptake response to be dysfunctional, insulin signaling seems to be preserved through Akt in the myotubes from donors with differing insulin sensitivities. Other investigators have suggested the mechanisms of insulin resistance most strongly impinge upon the molecular events leading up to the phosphorylation of Akt (78, 94, 118, 198). This suggests that there is utility in this in vitro model to study those events. The microplate format is especially convenient and economical for pharmacological studies of various molecular targets leading up to the phosphorylation of Akt.

Chapter 3: Adaptation to resistance or aerobic exercise with respect to age and obesity.

SUMMARY

The adaptation of skeletal muscle in response to exercise is not fully understood; evidence suggests macrophages are involved. Changes in muscle are important in the context of clinical obesity, insulin resistance, and aging, where exercise has been prescribed as an intervention. We have exercised human subjects harboring a wide range of clinical characteristics with eccentric (resistance) exercise, aerobic training or aerobic training followed by eccentric exercise. After each intervention we measured changes in abundance of distinct macrophage subtypes and gene transcripts in skeletal muscle biopsies. At baseline, inflammatory M1 macrophage density was correlated with obesity, but body mass index did not affect response to the exercise interventions. Age influenced response to exercise, most strongly associated with changes in macrophages of a mixed M1/M2 phenotype. These macrophages increased in the muscle of subjects >55 years of age when trained aerobically. Moreover, eccentric exercise following training increased these cells in subjects <55, but decreased cell abundance for subjects >55, a pattern appearing reciprocal. Overall, the relative abundance of M1 and M1/M2 macrophages was correlated to muscle gene expression related to specific functions. M1 and M1/M2

macrophage densities were associated with transcripts related to extracellular matrix (ECM) accumulation and fibrosis. Each type was associated with the expression of exclusive transcripts, with M1/M2 dominating this association, correlating most strongly with Secreted Protein Acidic and Rich in Cysteine (SPARC) mRNA expression. M1 and M1/M2 macrophages were also associated with messages related to angiogenesis, but there were some transcripts common to both, or exclusive to one type, with M1/M2 most highly correlated. Conversely, only M1 macrophage densities were associated with genes related to cellular homeostasis (protein turnover, autophagy, and apoptosis). Taken together these findings suggest that M1 and M1/M2 macrophages have distinct functions in ECM remodeling, angiogenesis, and homeostasis adaptations to exercise, that are altered with aging. Further studies are needed to show cause and effect.

INTRODUCTION

While there is a large body of evidence suggesting that macrophages are involved with muscle adaptation, the process is still not completely understood. Skeletal muscle is important in the context of clinical obesity, insulin resistance, and aging, where exercise is beneficial(133, 180, 185). In rodents, muscle injury and regeneration are well-studied processes, through manipulations such as genetic knock out and injection of caustic agents(36, 109, 117, 152, 171). But less is known in humans, where such interventions are not possible. Eccentric

contractions occur during the extension phase of weight training, a process of simultaneous elongation and contraction of the contractile filaments, causing damage to the muscle. Damage to the muscle is known to induce an influx of macrophages in humans(105) and in mice(177).

In the canonical view of macrophage biology(108), M1 inflammatory macrophages are phagocytic, secreting cytokines such as IL1β, TNFα, and pleotropic IL6, and express surface antigen CD11b. Inflammatory M1 macrophages populate skeletal muscle in response to damaging exercise(177), resulting in increased production of inflammatory cytokines within the muscle(56, 112, 126). Eccentric, damaging exercise is also known to cause a hypertrophic response. M2 alternatively activated macrophages are involved with remodeling processes in the tissues they inhabit, expressing the cell surface marker CD206, and secreting anti-inflammatory cytokines such as IL10. Certain phenotypes within the M2 class have distinct functions; M2A macrophages aid in allergic response, tissue remodeling and parasite containment via matrix deposition. M2C macrophages also serve in tissue remodeling and maintenance of the interstitium. There are a multitude of M1 and M2 phenotypes that cannot be described as either, but lie somewhere within a spectrum of function, mixing the M1 and M2 phenotypes(113). Less is known about M2 alternative macrophages and their involvement in muscle adaptation to exercise. This laboratory has reported in muscle the response to acute exercise for both M1 and M2 macrophages is defective in the context of aging(126) and that overall, macrophages are increased in muscle with obesity(184) . We have also reported

in adipose, in the context of obesity, that M2 macrophages are associated with fibrosis and decreased capillary density(162).

We have exercised adult human subjects harboring a wide range of clinical characteristics with eccentric (resistance) exercise, aerobic training or aerobic training followed by eccentric exercise; a regimen which we predict will reveal unique roles for macrophages in skeletal muscle adaptation within the context of obesity and aging. After each intervention we measured fluxes of distinct macrophage phenotypes, and gene transcripts in skeletal muscle biopsies. The beneficial effect of aerobic exercise is well accepted(55, 134). Our hypothesis is that the adverse health status of the subjects will be inhibitory to the beneficial adaptive process. One such beneficial adaptation may be the processing of free radicals, a result of an unpaired electron, also called reactive species, which are produced as a result of metabolism. These free radicals create chemical modifications to biomolecules, which are considered damage, known as adducts. Other investigators have reported that altered production of reactive species and stress buffers might be deficient due to aging(129). We posit that the different exercise interventions might yield different amounts of end point tissue damage as a result of differences in reactive species and their buffers, when comparing subjects of different ages. Additionally our hypothesis also includes modification to the flux of macrophages in response to these exercise interventions that varies by health status. As a result of beneficial muscle adaptation to aerobic training, we hypothesized that damage and the inflammatory macrophage response to a subsequent bout of eccentric exercise

would be reduced. We predict that the older, more obese or more insulin resistant subjects will not experience the decrease in inflammatory macrophages, compared to that observed in more healthy individuals.

MATERIALS AND METHODS

Subjects, Tissue Collection, and Clinical Measures.

Human non-diabetic subjects were recruited through local advertising. All subjects included in the study were recruited by informed consent under protocols that were approved by the institutional review board at the University of Kentucky. Muscle biopsies from 14 subjects were included in this study. Muscle biopsies via needle were collected from vastus lateralis muscle under local anesthesia in the Clinical Services Core of the UK Center for Clinical and Translational Sciences (CCTS). Standard fasting blood lipids were measured at the time of biopsy. The clinical insulin sensitivity (S_I) was measured by frequently sampled IV glucose tolerance test (FSIGT) with minimal model calculation (191), prior to and at the end of the study. See Table 3.1 for details. Metabolic measures were collected using a calibrated bicycle ergometer (Monarch 828E, Vansbro, Sweden) via indirect calorimetry and an integrated electrocardiogram

(12 lead ECG) using a SensorMedics Vmax29 metabolic cart (Carefusion, San Diego, CA) located in the Clinical Services Core of the CCTS.

Exercise Interventions

Knee extension exercise was performed on Keiser pneumatic weight lifting equipment. The eccentric exercise bout consisted of three sets of ten knee extensions at a load of 80% of 1-repetition max, followed by a fourth set to exhaustion. .

Aerobic exercise training employed cycling on a Monarch stationary ergometer. A graded exercise stress test was used to determine subject suitability for aerobic training, as well as to determine the VO_2 max for the aerobic exercise prescription. The 12 week training program was progressive with a stepwise increase in duration and intensity, for a maximum of 45 minutes, 3 times/week at 65% of their peak VO_2; 75-80% of maximum heart rate.

The study design, depicted in a timeline fashion is displayed in Figure 3.1. Biopsy 1, the baseline muscle biopsy, was taken before any intervention. Then the knee extension eccentric protocol was performed. Following 3 days of recovery, a second muscle biopsy was taken (post eccentric biopsy, PostECC). Following this, subjects underwent a 12 week training program of aerobic

Table 3.1 Clinical subject characteristics

	Sex	Age	Weight	SI Baseline	SI Post	BMI Baseline	BMI Post	VO2 Max Baseline	VO2 Max Post	Glucose Baseline	Glucose Post
	F	51	72.58	5.02	4.37	26.66	25.49	30.3	32.1	80	88
	F	64	71.22			26.16	26.09	28	27.5	85	86
	F	28	65.77	3.17	2.77	23.3	23.14	38	34.4	74	82
	M	62	85.28	2.49	4.01	25.41	25.63	32.7	36.1	88	90
	M	29	88.91	3.25	4.61	27.44	26.23	53.2	53.7	91	73
	M	26	79.83	3.89	7.05	23.33	23.59	46.9	56.6	89	79
	F	59	72.12	7.12	8.6	24.91	24.78	22.9	26.6	82	82
	M	39	99.34	6.55		32.73	31.55	37	39.2	92	86
	F	55	101.15	1.38	2.01	29.94	30.18	19.4	17.4	83	89
	F	45	80.74	1.55	2.12	31.43	33.43	23.8	21.5	83	78
	M	59	110.68	2.85	1.83	34.13	33.6	23.3	25.7	100	115
	F	43	91.63	1.73	2.54	36.07	34.08	24.4	22.1	83	86.5
	M	61	127.01	0.646	0.465	37.95	37.9	22.4	24.8	87	86
	F	42	107.05	1.61	1.6	41.82	40.4	29.3	33.5	87	88
Group	M/F										
BMI			*		*	*	*				
24-27	3/4	45.6±6.5	76.5±3.2	4.16±0.69	5.24±0.88	25.3±0.60	25.0±0.46	36.00±4.1	38.14±4.6	84.1±2.2	82.9±2.2
29-42	3/4	49.1±3.4	102.5±5.6	2.33±0.74	1.76±0.29	34.9±1.6	34.4±1.3	25.66±2.2	26.31±2.9	87.9±2.4	89.8±4.4
Age		*									
<55	2/4	41.5±3.0	90.0±5.1	3.29±0.85	3.05±0.61	32.7±2.3	31.9±2.3	33.00±4.5	33.68±4.9	86.0±2.0	83.3±2.6
>55	3/3	60.0±1.3	94.6±9.1	2.90±1.1	3.38±1.4	29.8±2.2	29.7±2.1	24.78±1.9	26.35±2.5	87.5±2.7	91.3±4.9
SI			*	*	*	*	*	*	*		
<3.0	3/4	52.4±3.3	100.5±6.1	1.75±0.27	2.08±0.40	33.8±2.1	33.6±1.8	25.04±1.7	25.87±2.5	87.3±2.3	90.4±4.4
>3.0	3/3	38.7±5.6	79.8±5.1	4.83±0.69	5.48±1.04	26.4±1.4	25.8±1.2	38.05±4.5	40.43±4.9	84.7±2.9	81.7±2.2
Entire Set	6/8	47.4±3.6	89.5±4.7	3.17±0.56	3.50±0.69	30.1±1.5	29.72±1.5	30.83±2.6	32.23±3.1	86.0±1.6	86.32±2.5

M=male, F=female, Measure (Units): Age (years), Weight (kg), Sensitivity to Insulin (S_I) (value x 10^{-4} $min^{-1}\cdot(\mu U\cdot ml)^{-1}$), Body Mass Index, BMI (kg/m^2), Maximum Oxygen Uptake, VO_2 max (ml/kg·min), Glucose(mg/dl), Glucose Post=2hr, for other measures Post=after the study was completed. Groupings by BMI, Age, and S_I, M/F= #of males/#females for the group. Means±SEM, *p<0.05

exercise, composed of stationary bicycle riding three times per week, followed by a three day recovery period, prior to biopsy 3, called Training. Lastly, the participants performed a second bout of eccentric exercise on the leg naive to the first bout of eccentric exercise, allowed to rest for three days, and the fourth and final biopsy was collected (post training post eccentric biopsy,PsTPsE). Each biopsy was assessed for macrophage content and copy number mRNA of selected genes.

Immunohistochemistry

For macrophage assessment, 8 um cryosections were mounted on Fisher PLUS slides, for each patient and biopsy; at least 5 sections/biopsy were assessed for macrophage density. Sections were fixed for 3 min with ice cold acetone, then blocked with 2.5% Normal Horse Serum (Vector Labs, cat#S-2012 Burlingame, CA) in PBS (NHS), for 1 hr at room temperature (RT). Primary antibodies were applied overnight in NHS; the next day the appropriate biotin-conjugated secondary antibody was applied at a dilution of 1:1000 in NHS for 1 hr at RT. Except for CD206, all assessments underwent Tyramide Signal Amplifcation TSA amplification using Alexa 594 or 488 fluorophore at 1:200 according to the manufactures instructions (Life Technologies, T20935, T20932, respectively, Grand Island, NY). Antibodies and dilutions used were as follows: as a marker of M1 inflammatory macrophages, Mouse α Human CD11b at 1:100 (Cell Sciences, MON1019-1, Canton, MA), M2 alternatively active macrophages

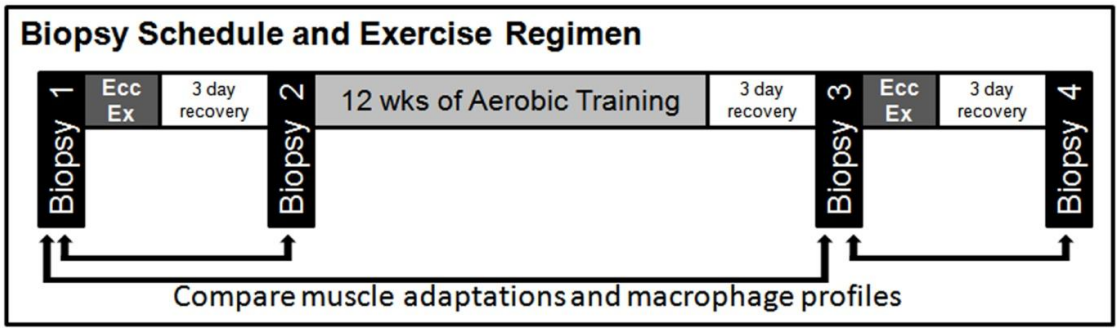

Figure 3.1 Vastus Lateralis Biopsy Schedule and Exercise Regimen. Biopsy 1 (Baseline) was taken before any intervention. Biopsy 2 (post-eccentric biopsy, PostECC) was taken 3 days after a bout of resistance exercise, emphasizing the eccentric component. Biopsy 3, (Training) was taken 3 days after the last aerobic training session. A second eccentric exercise bout was then performed and Biopsy 4 (post-training, post-eccentric, PsTPsE) was taken after 3 days of recovery. Each biopsy was assessed for macrophage content and mRNA copy number of selected genes. Bivariate analysis or pairwise comparisons were made using these measures or the groups described in Table 3.1, between Baseline and PostEcc, Baseline and Training, or Training and PsTPsE.

were determined via mannose receptor, CD206, and stained via Goat α Human CD206 at 1:200 (R&D Systems, AF2534, Minneapolis, MN), total macrophages were assessed via the pan-macrophage/monocyte marker, Mouse α Human CD68 at 1:100 (Dako, M0814, Carpinteria, CA). Secondary antibodies were Goat α Mouse biotin conjugate (Jackson Immunoresearch,115-065-205, West Grove, PA) and Rabbit α Goat biotin conjugate (Vector Labs, BA5000, Burlingame, CA). All sections were stained with DAPI to locate the nuclei (Life Technologies, D35471 Grand Island, NY) at 1:10,000 in PBS. Encoded slides were quantified by a blinded observer, where the total number of macrophage marker^{+}/DAPI^{+} nuclei were counted and divided by the total number of fibers assessed, for each patient, at each biopsy point. Experiment to experiment variability due to staining and counting was minimal because corresponding counts from CD68, CD68.206, CD11bhi206lo or CD11bhi206hi when plotted against one another showed very good correlations (R^2=0.24-0.68, $p<0.01$).

For reactive nitrogen species assessment via nitrotyrosine (NY) adducts, cryosections were rehydrated in PBS, then permeablized in 0.3% Triton (Sigma-Aldrich, T8787, St. Louis, MO) in PBS. The sections were then blocked in 10% normal goat serum in PBS for 1 hr at RT. Rabbit α NY antibody (Millipore, 06-284,) was applied at 1:100 in PBS for 2 hr at RT. Secondary antibody was Goat α Rabbit AlexFluor488 (Life Technologies, A11008 Grand Island, NY) at 1:500 in PBS for 1hr at RT. Sections were subsequently post-fixed in 4% paraformaldehide (Sigma-Aldrich, P6148, St. Louis, MO) in PBS for 10 min at RT. For each biopsy and patient, images were collected from at least 4 sections,

threshold was scaled considering sensitivity and saturation, then fixed prior to collection of measurements for all images for % area of NY stain using NIS-Elements software (Nikon, Melville, NY).

RNA isolation and nanoString Analysis

Muscle tissue samples were homogenized in Qiazol lysis reagent (Qiagen, 79306, Germantown, MD); then RNA was extracted with the RNeasy Mini Kit (Qiagen, 74104). cDNA was generated with the iScript cDNA Synthesis Kit (Bio-RAD 170-8890, Hercules, CA). One hundred fifty ng of cDNA sample was hybridized and ligated with probe sets and loaded onto cartridges according to the manufacturer's instructions for quantification with the nCounter instrument for each of 12 patients included in this analysis (NanoString Technologies Inc, Seattle, WA). Genes of interest were normalized to the geometric mean of ACTB (βActin), PP1A (cyclophilin A), PP1B (cyclophilin B), TBP (Tata binding protein), TUBB (βTubulin), UBC9 (Ubiquitin C) (See Table 3.2 for probe set accession numbers).

Figure 3.2 is a schematic diagram summarizing how nanoString (nS) technology works. Essentially nS technology combines affinity tagged, barcode

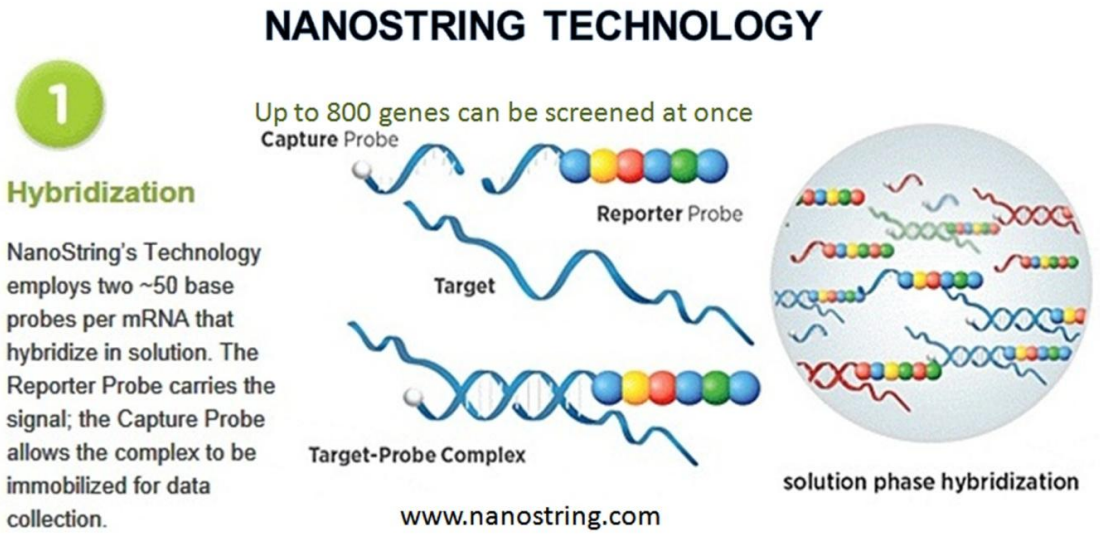

Figure 3.2 nanoString (nS) is a technology which combines affinity tagged capture probe, barcode tagged reporter probes that target a contiguous sequence in a transcript, hybridizes and ligates them in solution as a quantifiable northern blot. Only capture probes which have ligated with the reporter probe are detected by the detector, and counted for each probe set. In this way each count is analogous to one copy of mRNA.

tag probes and message templates and hybridizes them in solution as a quantifiable northern blot. In summary, cDNA message templates were

synthesized from RNA extracts derived from our biopsy samples. These templates were then combined with two probes in solution. One of the probes has a "capture" tag on it, which is an oligo which has an affinity tag on the 3' end. A second probe is an oligo which has a unique bar code tag (reporter) on the 5' end. Both of these probes form a contiguous sequence, which in the presence of template complimentary to these two distinct probes, juxtaposes them in close proximity to enable covalent linking with ligase. In this way, only probe sets which have been ligated were hybridized to their cognate message sequences. After hybridization in solution, the sample was run through a cartridge which captures the capture probe via the affinity tag, a cognate ligand coated on the surface of the cartridge, and then washed extensively to remove non-ligated capture and reporter probes. Only capture probes which have ligated with the reporter bar code probe are detected by the detector, and counted for each probe set. In this way each count is analogous to one copy of mRNA.

Statistical Analysis

JMP software (SAS Institute Inc. Cary, NC) was used for two-way ANOVA for comparisons of absolute macrophage numbers among biopsies, and all bivariate regression analysis. Pairwise comparisons for mathematical differences

related to change in macrophage densities were performed with Student's t-test. Due to the heterogeneity (or non-constant variance) in the data across biopsies and the small sample size, a linear mixed model (LMM) in SAS was also used to investigate the relationship of training and age on macrophage abundance(194). LMMs allowed for the comparison of mean outcome between age groups in the different biopsies; LMMs provide more flexibility in the assumptions associated with variability and independence than traditional ANOVA models. In our analyses, observations were correlated (not independent) because multiple biopsies were obtained from the same subject. Moreover, the variability increased as the experiment progressed. Hence, a LMM was used to investigate the main effects of age group (>55 or not), biopsy and the interaction of age group and biopsy. The variance-covariance structure for this model was selected using corrected Aiake Information Criteria (AICC); the Huynh-Feldt (HF) was selected and allowed for the heterogeneity across biopsies.

RESULTS

Table 3.1 summarizes the clinical characteristics of the 14 subjects included in this study. To identify the influence of these characteristics on study outcome, subjects were grouped in different ways for comparison; by Body Mass Index (BMI, kg/m^2), where 24-27 was considered healthy (mean = 25.3±0.60),

and 29-42 was considered obese (mean = 34.9±1.6); by age, which ranged from 26 to 64, grouped as <55 or >55 years of age, with mean group ages of 41.5±3.0 and 60.0±1.3, respectively; and in some cases, by insulin sensitivity. The insulin resistant cohort, had a sensitivity to insulin (S_I x 10^{-4} $min^{-1}\cdot(\mu U\cdot ml)^{-1}$) as measured by FSIGT of less than 3.0 (mean S_I = 1.75±0.27), whereas the insulin sensitive cohort had an S_I of greater than 3.0 (mean = 4.83±0.69).

Some measures of health status are also included in Table 3.1. Post measures, including S_I, BMI, maximal rate of oxygen consumption (VO_2 Max $ml\cdot kg^{-1}\cdot min^{-1}$), and fasting blood glucose, showed no statistically significant change following 12 weeks of aerobic training across all subjects. Grouping the subjects into categories did reveal some statistically significant differences in several clinical characteristics (Table 3.1, bottom). When grouped by healthy or obese BMI, as expected, the subjects had a statistical difference in mass (76.5±3.2 vs.102±5.6 kg, $p<0.05$). The BMI groupings did not yield a statistically significant difference in baseline S_I; however, after the training regimen, the mean S_I's diverged enough to yield a statistically significant difference between healthy and obese subjects (5.24±0.88 vs. 1.76±0.29, $p<0.05$). When grouped by S_I, characteristics such as weight, BMI, S_I, revealed significant differences as expected, since it is known that BMI and S_I have a good inverse correlation. The metabolic measure of VO_2 Max suggests a strong divergence in oxygen consumption related to the insulin sensitivity of the subjects. At baseline, insulin resistant subjects had a VO_2 Max of 25.04±1.7 $ml\cdot kg^{-1}\cdot min^{-1}$, whereas insulin sensitive subjects had a VO_2 Max of 38.05±4.5 $ml\cdot kg^{-1}\cdot min^{-1}$, a statistically

significant difference that suggests impaired metabolism in insulin resistant subjects; post measurement revealed no effect of exercise.

Our previous work showed that muscle macrophage content was higher in obese compared to lean individuals(184). In the current study, we wanted to determine the polarization state of muscle macrophages associated with specific muscle characteristics. Using immunohistochemistry (IHC) on muscle cross-sections, we identified all macrophages by the cell surface marker CD68, M1 macrophages via the marker CD11b, and alternative M2 macrophages by the M2 marker CD206. There was very good colocalization of CD68 with both CD11b and CD206 indicating that in muscle, the majority of cells expressing CD206 and CD11b are in fact macrophages. We illustrate our staining and counting methodology in Figure 3.3. In all cases, we identify markers only associated with nuclear DAPI staining, to ensure that our counts are cellular in nature. In Figure 3.3A, the two white arrows point out examples of cellular CD68 staining. In Figure 3.3B, the white arrow indicates a cell which has immunoreacted with the CD206 antibody. This cell also reacts with the CD68 antibody, illustrated in Figure 3.3C of the merged images (yellow arrow). The cells coexpressing the surface markers CD68 and CD206 appear a golden color, and are counted as M2 macrophages. Thus, the white arrow in panel C is a macrophage type other than an M2 macrophage. In this way, using various combinations of surface

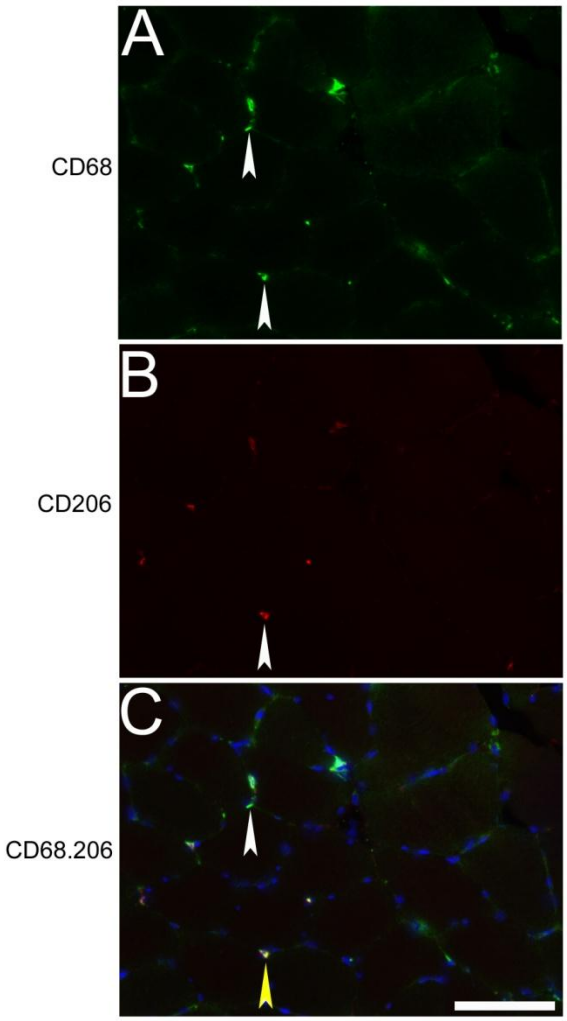

Figure 3.3 Immunohistochemical detection of macrophages in human muscle. (A) CD68, the arrows indicate pan macrophage, CD68 antigen detection (green). (B) CD206, the arrow indicates detection of the pan M2 marker, mannose receptor, CD206 antigen (red). (C) Merge. The detection indicated by the lower arrow in (A) and (B) reacts with both the CD68 and CD206 antibody, for double CD68.206 antigen detection (C, yellow arrow), when merged yields a golden color. The white arrow (C) points out only CD68 antigen. Antigens co-labeled with the nuclear stain DAPI (C, blue), are counted as cellular. Thus, DAPI stained CD68 (green) are counted as macrophages and CD68.206 double labeled (yellow) are counted as M2 macrophages. Macrophages counts are expressed by the number counted / number of muscle fibers in all sections counted for that patient's biopsy. Scale bar = 500μm.

markers we assessed the macrophage fluxes induced by each intervention in the context of obesity, aging or insulin resistance.

Figure 3.4 summarizes the baseline macrophage content from biopsy 1, within the context of BMI (Figures 3.4 A,C,E) or insulin resistance (Figure 3.4 B,D,F), by bivariate regression analysis. The Y axis is the total number of marker-expressing cells, divided by the total number of muscle fibers counted in all the sections for that subject at baseline. The X axis is the numerical value of either the BMI or the S_I of the subject counted at baseline. Figure 3.4A indicates a positive trend between CD68-expressing cells for each subject with available BMI, but was not significant (R^2=0.26 p=0.11 n=11). Figure 3.4B shows that when CD68+ cells were plotted against S_I, no relationship was noted between CD68 and S_I (R^2=0.02 p=0.72 n=10). Figures 3.4C and D assess CD68 and inflammatory M1 marker CD11b costaining, when plotted against BMI and S_I, respectively. CD68.CD11b coexpressing cells were positively correlated with BMI (Figure 3.4C, R^2=0.47 p=0.02 n=12). No relationship was noted between CD68.CD11b expressing cells and S_I (Figure 3.4D, R^2=0.01 p=0.79 n=12). Figures 3.4E and F assess the CD68.CD206 coexpressing cells, to quantify M2 macrophage densities in the baseline biopsies compared against BMI and S_I, respectively. Regression analysis revealed that CD68.CD206 coexpressing cells were positively trending with BMI, but was not significant (Figure 3.4E, R^2=0.22

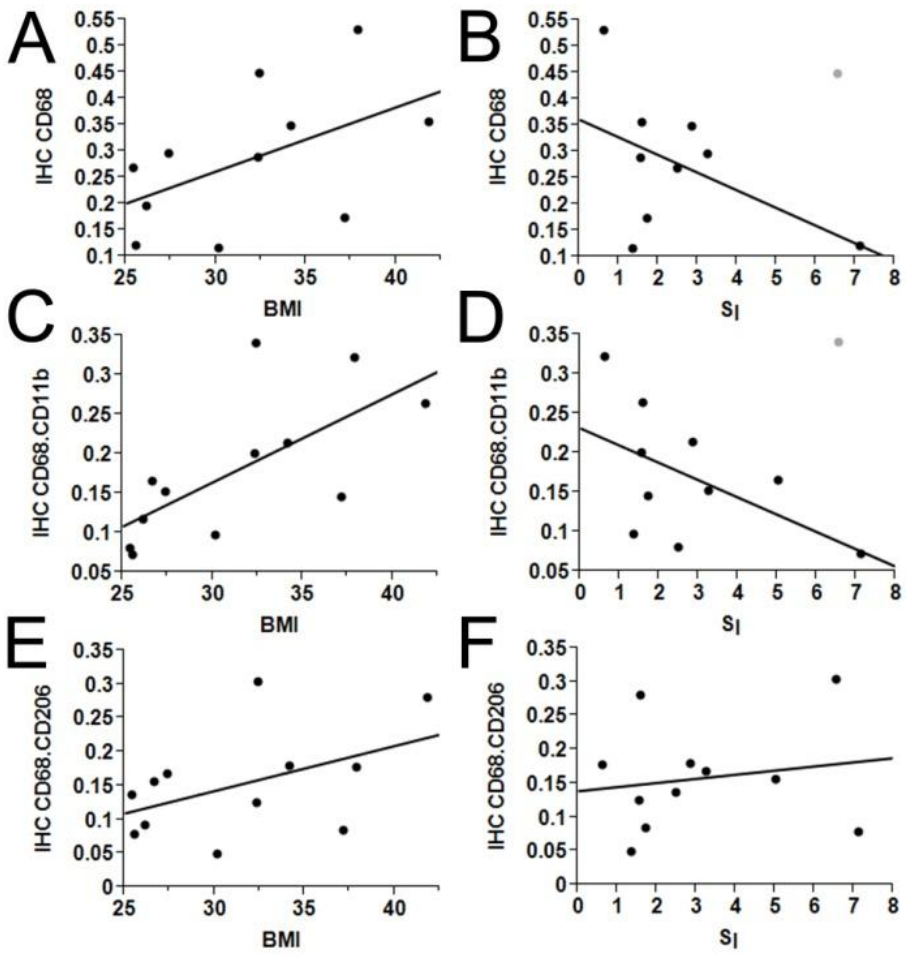

Figure 3.4 Characterization of muscle macrophages by subject BMI or S_I at baseline suggests that M1 macrophages are correlated to BMI. Macrophage counts vs. BMI (A,C,E) or insulin resistance (B,D,F), by bivariate regression analysis. (A) indicates a positive trend between the pan macrophage marker CD68 expressing cells for each subject with BMI, but was not significant (R^2=0.26 p=0.11 n=11). (B) No relationship was noted between $CD68^+$ cells and S_I (R^2=0.02 p=0.72 n=10). (C) CD68 and inflammatory M1 marker, CD11b costaining was correlated with BMI (R^2=0.47 p=0.02 n=12). (D) No relationship was noted between CD68 and CD11b costaining and S_I (R^2=0.01 p=0.79 n=12). (E) CD68 and alternative M2 marker, CD206 costaining was positively trending with BMI, but was not significant (R^2=0.22 p=0.12 n=12); (F) No relationship was found between CD68 and CD206 costaining and S_I (Figure 3.4F R^2=0.03 p=0.62 n=11). Gray dots are patients stastically excluded from regression.

p=0.12 n=12); no relationship was found between CD68 and CD206 costaining and S_I (Figure 3.4F R^2=0.03 p=0.62 n=11). These analyses suggest that muscle resident M1 macrophage abundance preferentially increases with obesity.

We assessed CD68 pan macrophage marker expression following each exercise intervention to quantify the macrophage fluxes related to clinical characteristics. The abundance of CD68+ cells following each exercise intervention was not correlated to either BMI or S_I (data not shown). However, when CD68 was assessed following each intervention with subjects grouped by age, some interesting fluxes were observed (Figure 3.5). Figure 3.5A is a representative image of CD68 (arrow) staining. Figure 3.5B is the DAPI stain which identifies nuclei (arrow) in the muscle section. Figure 3.5C is the overlay or merged image, that shows only CD68 staining (arrow) co-localized with a nucleus (Figure 3.5B, arrow), was counted as a cell. Figure 3.5D is the absolute quantification of CD68+ cells in subjects less than 55 years of age (<55, black bars), or greater than 55 years of age (>55, white bars) at baseline and following each exercise intervention. Surprisingly, the eccentric bout of exercise (biopsy 2, PostECC) had no effect on the overall number of CD68-expressing cells at any age. However, macrophage density increased following training preferentially in subjects >55 years of age (Figure 3.5E, 0.01±0.06 vs. 0.33±0.12, p=0.054, n= 8 vs.6). The training regimen influenced the subsequent macrophage response to the eccentric exercise bout in an age-dependent manner (Figures 3.5D and F). Following training, in younger subjects, macrophage number tended to increase, whereas it decreased in older subjects. This reciprocal relationship in the

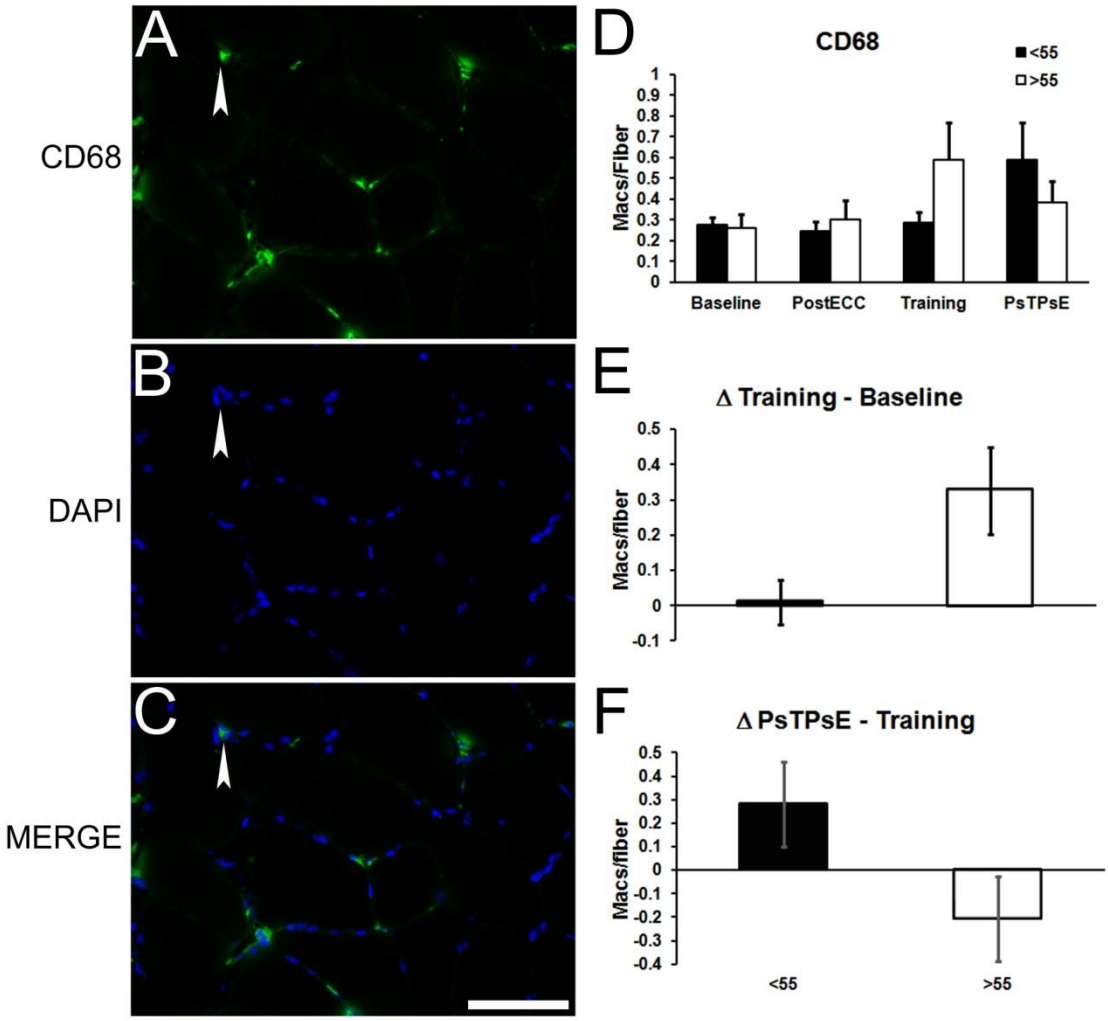

Figure 3.5 CD68 assessment of total macrophages. For older subjects, training increases macrophages, but eccentric exercise after training decreases them. For middle aged subjects, only eccentric exercise following training increases macrophages. (A) Representative image of CD68 (arrow) staining. (B) DAPI to visualize nuclei (arrow). (C) Merged image, CD68 stain (arrow) is counted when co-localized with a nucleus. (D) Absolute quantification of $CD68^{+}$ cells in subjects <55 years of age (black bars), or >55 years of age (white bars), at baseline and following each exercise intervention. (E) The difference between training and baseline in macrophage density increased preferentially in subjects >55 (0.01±0.06 vs. 0.33±0.12, p=0.054, n= 8 vs.6). (F) The difference between change in macrophage number between PsTPsE (biopsy 4) and following training (biopsy 3) in subjects <55 compared to >55 years of age approached statistical significance (Figure 3.5F, 0.28±0.18 vs -0.20±0.18, p=0.08, n= 7 vs.6). Scale bar = 500μm

PsTPsE and training in subjects <55 compared to >55 years of age approached statistical significance (0.28±0.18 vs -0.20±0.18, p=0.08, n= 7 vs.6).

Due to the heterogeneity in the data across biopsies, a linear mixed model was also used to investigate the relationship of training and age on macrophage abundance. There was a significant interaction effect (p=0.0353), which verifies that macrophage content in the different age groups changed differently following training. Taken together these findings indicate that the initial eccentric bout of exercise was not sufficient to elicit a macrophage response in muscle of sedentary subjects; however, training resulted in an increase in macrophages in subjects >55 years of age. Following training, eccentric exercise caused a decrease in macrophages in the older subjects, whereas they tended to increase in younger subjects. Thus, a reciprocal relationship is observed for the <55 and >55 age groups when comparing post training post eccentric exercise macrophage response.

We hypothesized that macrophages might be recruited to the muscle based upon differential damage or stress at different ages and in response to the exercise regimen. We tested this hypothesis by assessing free radical damage. Using IHC, we assessed nitro-tyrosine (NY) damage, a marker of NO stress (Figure 3.6). We show representative images of subjects ages 62 and 42, and the NY staining for each intervention (Figure 3.6A). Overall the staining appeared more intense for the subject age 62, when compared to the 42 year old for each intervention. Interestingly, the strongest staining for the subject age 62 was in the PostECC bout. However, the most intense staining for the subject age 42 appeared to be in the Training bout. Figure 3.6B is the absolute quantification for NY staining by % area for each intervention for 3 subjects in each age group.

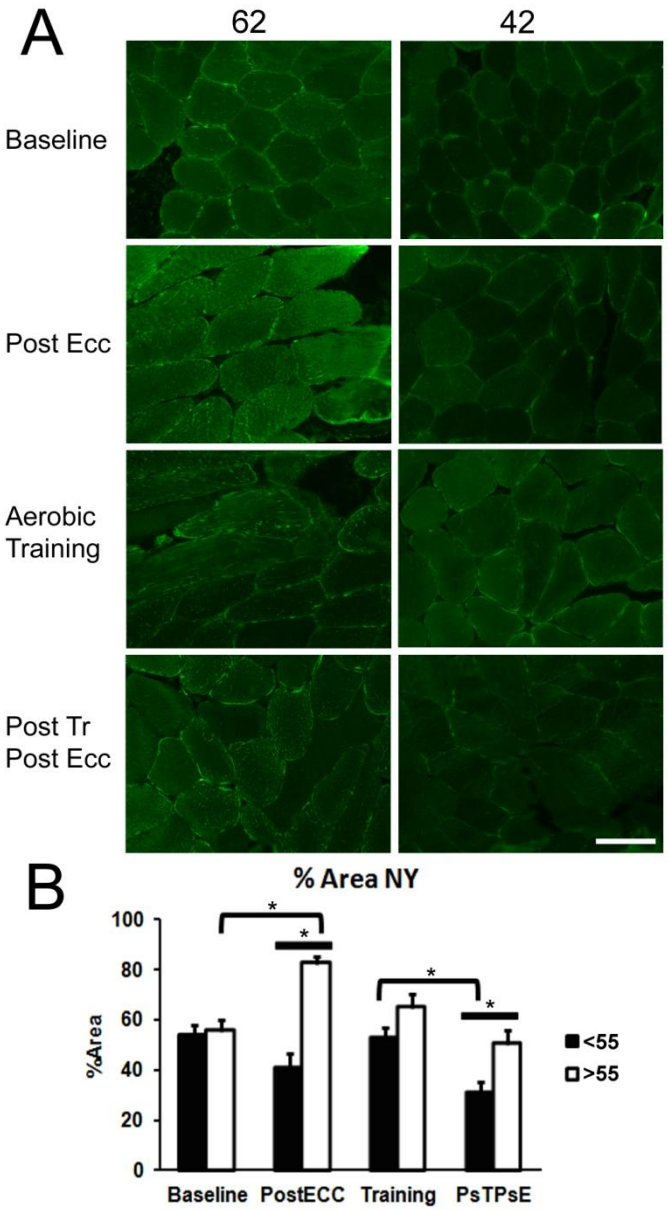

Figure 3.6 NO adducts, as assessed by nitro-tyrosine (NY) antibody immunohistochemistry, shows age-dependent differences in response to exercise. (A) Representative images of subjects ages 62 and 42, and the NY staining for each intervention. (B) Absolute quantification for NY staining by % area. NY damage is greater for the >55 group (white bars), when compared to the <55 group (black bars) at all interventions. There was an effect of age in the PostECC (40.5±6 vs. 81.9±3.5) and the PsTPsE (30.7±4.8 vs.50.2±5.5) biopsies. For the >55 group, there was a significant increase in NY damage when comparing the baseline and PostECC values (55±4.6 vs. 81.9±3.5). Conversely, subjects <55 showed an overall reduction in damage when comparing the Training to the PsTPsE interventions (52.5±4.5 vs. 30.7±4.8). *p<0.01, n=3. Scale bar = 500 μm.

Overall the assessment suggests that NY damage was greater for the >55 group in all biopsies. There was an effect of age in the PostECC (40.5±6 vs. 81.9±3.5, $p<0.01$) and the PsTPsE (30.7±4.8 vs.50.2±5.5, $p<0.01$) biopsies. Interestingly for the >55 group, there was a significant increase in NY damage when comparing the baseline and PostECC values (55±4.6 vs. 81.9±3.5, $p<0.01$). Conversely, subjects <55 showed an overall reduction in damage when comparing the Training to the PsTPsE interventions (52.5±4.5 vs. 30.7±4.8, $p<0.01$). Thus, although NO damage, as assessed by nitro-tyrosine, shows age-dependent differences in response to exercise, these differences did not correlate with total macrophage abundance.

We next characterized changes in macrophage types in muscle in response to each exercise intervention, starting with M2 macrophages, through CD68, CD206 double IHC (Figure 3.7). Figure 3.7A is the absolute quantification of CD68.CD206 double positive cells in subjects <55 (black bars) or >55 (white bars) years of age. As with CD68, the first bout of eccentric exercise (PostECC) had no effect on CD68.206 coexpressing cells. However, as with CD68, there was a trend for M2 macrophages to increase their density following training in subjects >55, but not for those <55 years of age, which approached statistical significance (Figure 3.7B, -0.01±0.04 vs. 0.16±0.08, $p=0.08$, $n= 8$ vs.6). We found again that following the increase in M2 macrophages with training in subjects >55, they tended to decrease in density in response to the PsTPsE exercise bout. Consistent with total macrophages identified with the CD68 antibody alone, there was no change with training for subjects <55 years of age,

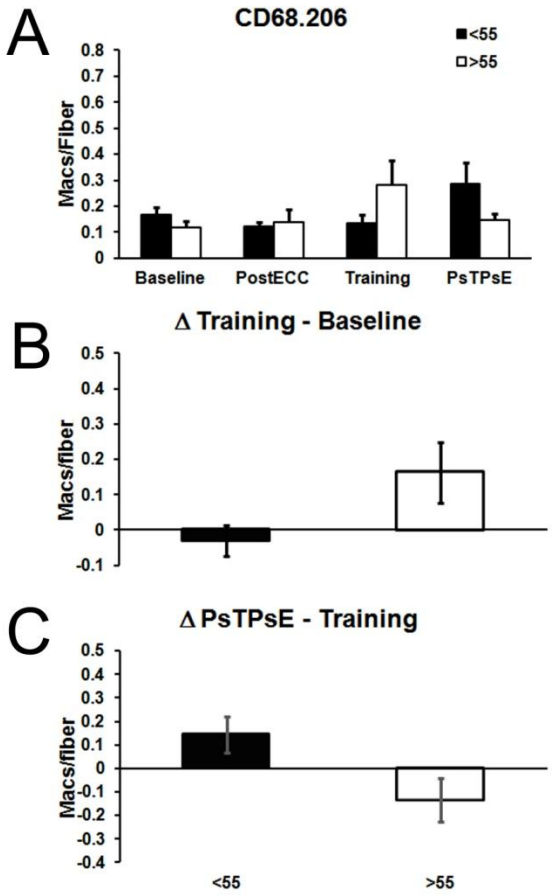

Figure 3.7 CD68.206 assessment for the detection of alternative M2 macrophages shows that training increases M2 abundance only in the older group. Eccentric exercise after training decreases the density of M2 macrophages in the older subjects, whereas it increases abundance in middle aged subjects. (A) Absolute quantification of CD68.CD206 double positive cells in subjects <55 (black bars) or >55 (white bars) years of age. As with CD68, the first bout of eccentric exercise (PostECC) had no effect on CD68.206 coexpressing cells. (B) M2 macrophages increase in abundance following training preferentially in subjects >55, which approached statistical significance (-0.01±0.04 vs. 0.16±0.08, p=0.08, n= 8 vs.6). (C) A significant reciprocal relationship was apparent when the difference between PsTPsE and training biopsies was compared between the age groups (0.14±0.08 vs -0.13±0.09, p=0.04, n= 7 vs.6). Refer to Figure 3.3 for a representative image.

but after the PsTPsE bout, CD68.CD206 macrophages tended to increase. A significant reciprocal relationship was apparent when the difference between PsTPsE and training biopsies was calculated and compared between the age groups (Figure 3.7C, 0.14±0.08 vs -0.13±0.09, p=0.04, n= 7 vs.6). Thus, following training, M2 macrophages increase in abundance in the muscle of younger subjects in response to eccentric exercise. By contrast, whereas M2 macrophages increase in older subjects in response to training, abundance decreases back to baseline levels following a subsequent eccentric bout of exercise.

IHC analysis of CD68.CD11b double positive cells showed similar trends as the CD68.CD206 double positive cells (data not shown); however, the counts were not additive suggesting there was considerable overlap between CD11b and CD206 expression. To explore this possibility, double IHC for CD11b, the M1 inflammatory macrophage marker, and CD206, the M2 alternatively activated marker, was performed. We classified the different levels of these markers as either high (^{hi}), low (^{lo}), or no expression ($^{-}$) . Figure 3.8A is a representative image of CD11b staining (green arrows) and CD206 staining (Figure 3.8B, red arrows) staining, the merged image (Figure 3.8C) shows examples of CD11b^{hi}206^{-} (green arrows) and CD11b^{hi}206^{hi} (yellow arrows) cells. This analysis yielded five distinct phenotypes: pure CD11b with no CD206 (CD11b^{hi}206^{-}); CD11b^{hi}206^{lo}; CD11b^{hi}206^{hi}; pure CD206 with no 11b (CD206^{hi}11b^{-}); and CD206^{hi}CD11b^{lo}. After quantification, we found the majority of the skeletal

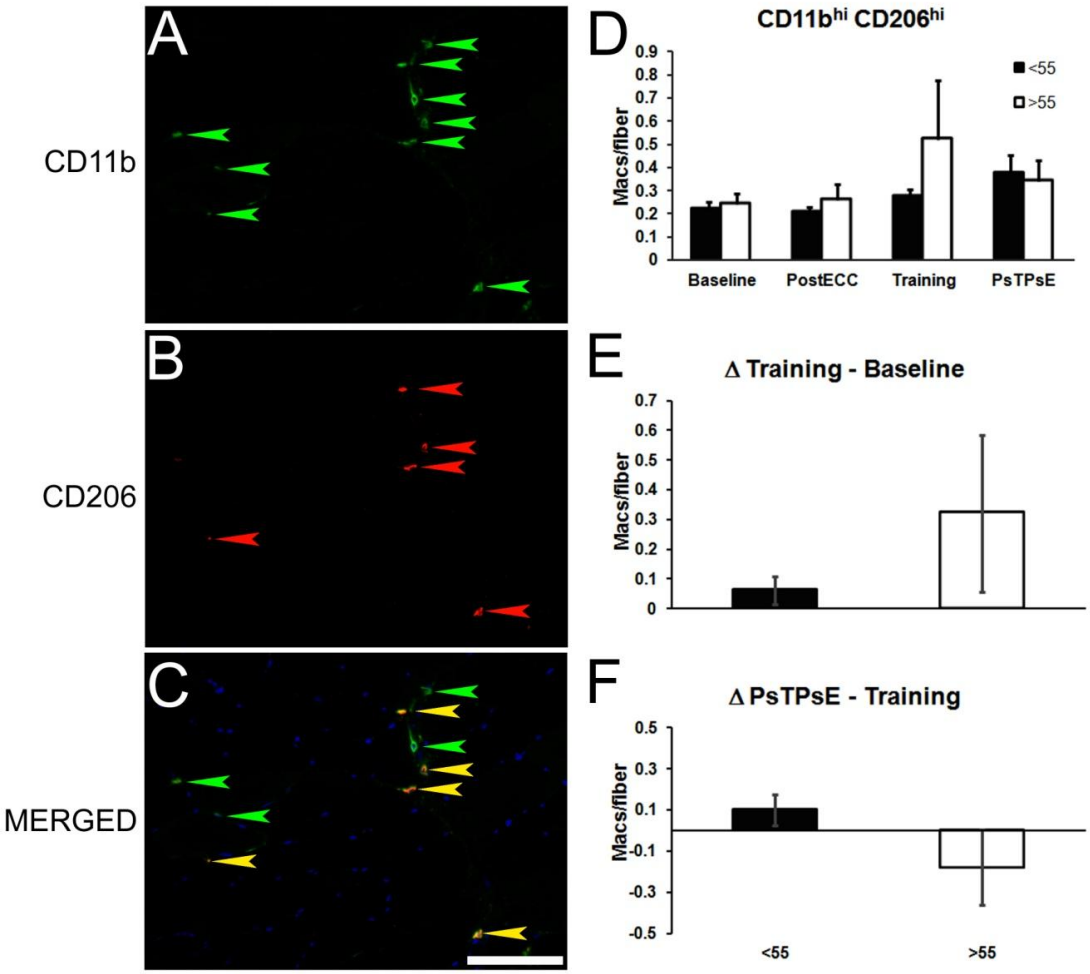

Figure 3.8 CD11b and CD206 double staining assessment for the detection of mixed M1/M2 CD11b^{hi}CD206^{hi} macrophages shows a reciprocal pattern of change in macrophage abundance in the different age groups. (A) Representative image of CD11b detection (green arrows) and (B) CD206 detection (red arrows). (C) Merged panel illustrates examples of CD11b^{hi}206^{-} (green arrows) and CD11b^{hi}206^{hi} (yellow arrows) macrophages, co-localized with nuclear DAPI staining (blue). (D) Absolute quantification of CD11b^{hi}206^{hi} macrophages of subjects <55 years of age (black bars), or >55 years of age (white bars), at baseline and following each exercise intervention. (E) The difference between training and baseline in subjects < or >55 years of age was not significant (0.06±0.05 vs. 0.32±0.26, p=0.27, n= 7 vs. 5). (F) Cells expressing CD11b^{hi}206^{hi} showed a reciprocal pattern of expression in response to an eccentric exercise bout following aerobic training in <55 compared to >55 subjects (0.09±0.08 vs -0.17±0.18, p=0.14, n= 8 vs. 6) but the changes were not significant. Scale bar = 500µm

muscle macrophages belonged to 3 phenotypes: $CD11b^{hi}206^{-}$, $CD11b^{hi}206^{lo}$, and mixed M1/M2 phenotype $CD11b^{hi}206^{hi}$. The pure CD206 and $CD206^{hi}CD11b^{lo}$ macrophages were very rare, present at a density of less than 1 per 100 muscle fibers, indicating that the majority of CD206 expressing macrophages also expressed M1 characteristics.

As we observed with CD68 and CD68.206 costaining, the same reciprocal trend existed in mixed M1/M2 ($CD11b^{hi}206^{hi}$) macrophage abundance following training and PsTPsE exercise (Figure 3.8). Figure 3.8D is the absolute quantification of $CD11b^{hi}206^{hi}$ macrophages of subjects <55 years of age (black bars), or >55 years of age (white bars) at baseline and following each exercise intervention. $CD11b^{hi}206^{hi}$ macrophages tended to increase in density with training in subjects >55, but not in subjects <55, but was not statistically significant. The difference between macrophage density following training compared to baseline between subjects < or >55 years of age also was not significant (Figure 3.8E, 0.06±0.05 vs. 0.32±0.26, p=0.27, n= 7 vs. 5). Similarly, the reciprocal pattern of change, increased density in younger subjects and decreased density in older subjects following PsTPsE exercise, was apparent but not significant (Figure 3.9F). Thus, overall, cells expressing CD206 showed a reciprocal pattern of expression in response to an eccentric exercise bout following aerobic training in younger compared to older subjects and a significant proportion of those cells have a mixed phenotype, also expressing an M1 cell surface marker. The same pattern of expression was observed for

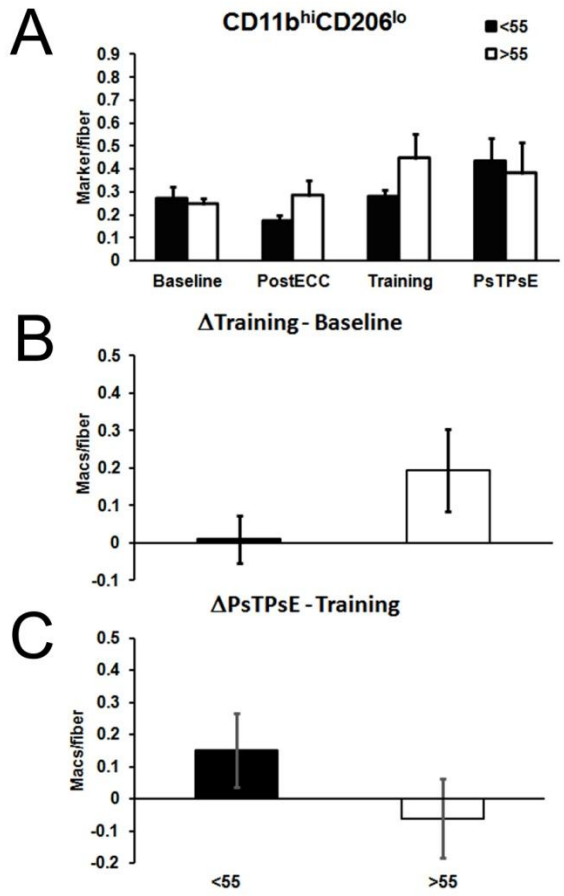

Figure 3.9 Inflammatory M1 ($CD11b^{hi}CD206^{lo}$) macrophages respond to exercise in a pattern similar to mixed M1/M2 macrophages (A) Absolute quantification of $CD11b^{hi}206^{lo}$ macrophages of subjects <55 years of age (black bars), or >55 years of age (white bars), at baseline and following each exercise intervention. (B) The difference between training and baseline between subjects < or >55 years of age was not significant (0.01±0.06 vs. 0.19±0.11, p=0.15, n= 7 vs. 5). (C) Cells expressing $CD11b^{hi}206^{lo}$ showed a reciprocal pattern of expression in response to an eccentric exercise bout following aerobic training in <55 compared to >55 subjects (0.15±0.11 vs -0.06±0.12, p=0.23, n= 8 vs. 6) but the changes were not significant. Refer to Figure 3A-C for representative images.

predominantly CD11b expressing macrophages ($CD11b^{hi}CD206^{lo/-}$), but the trends were not significant (Figures 3.9 A-C).

To assess changes in the muscle environment associated with the changes in macrophage density, gene expression was quantified using nanoString (nS) technology. One of the concerns with using message data is whether or not it translates faithfully to the end product protein. We have extensively quantified surface protein marker CD68 for macrophages. A bivariate analysis of CD68 mRNA expression via nS compared to IHC CD68 counts for all subjects and all biopsies showed a robust direct correlation (Figure 3.10, R^2=0.32,$p<0.001$, n=43), demonstrating consistency between the methods of analyses.

Probe sets for the nS analysis were designed to target specific genes and pathways of interest to our laboratory (Table 3.2). These include genes involved in inflammation, fibrosis, angiogenesis, insulin resistance and tissue homeostasis. nS analysis of the expression of 114 genes in the 4 biopsies from 12 individuals revealed few statistically significant changes. However, one gene, SPARC showed a pattern of expression consistent with the pattern of CD206+ macrophages. SPARC is involved in shuttling procollagen from the cytoplasm to the extracellular compartment and in collagen assembly in the extra cellular matrix (ECM). When SPARC malfunctions there is improper nucleation of collagen fibrils, resulting in fibrosis(20, 60).

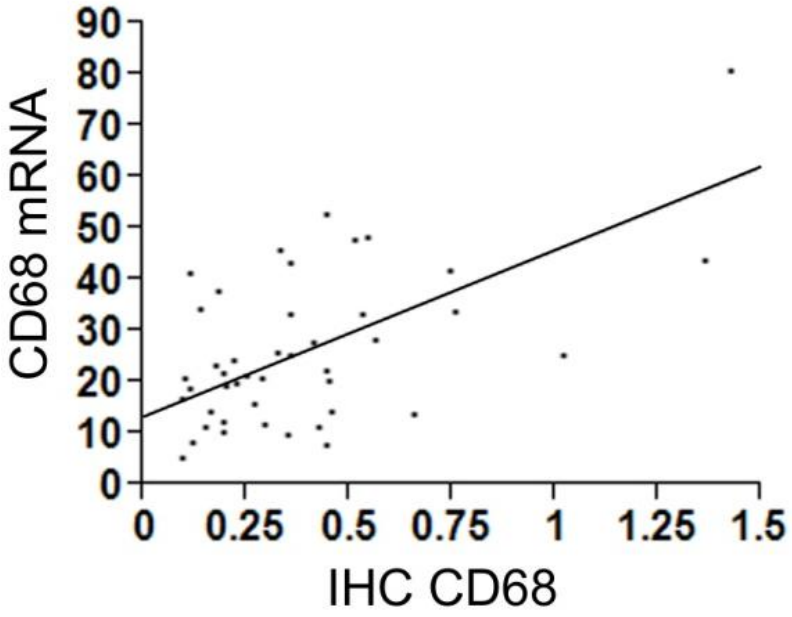

Figure 3.10 CD68 transcript levels correlate well with CD68 immunohistochemistry (IHC) demonstrating consistency between the methods of analyses. A bivariate analysis of CD68 mRNA expression via nS compared to IHC CD68 counts for all subjects and all biopsies showed a robust direct correlation (R^2=0.32, p<0.001, n=43).

Table 3.2 Genes analyzed by nanoString (nS) technology in muscle biopsies.

Cytokines/Inflammation/Chemotaxis	Accession	Angiogenesis	Accession	Fibrosis	Accession
IL-1 b	NM_000576.2	HIF 1 α	NM_001530.3	TGFβ	NM_000660.3
IL-4	NM_000589.2	VEGF A	NM_001025366.2	TSP1	NM_003246.2
IL-6	NM_000600.1	VEGF B (PlGF)	NM_002632.5	TSP2	NM_003247.2
IL-8	NM_000584.2	VEGF C	NM_005429.2	SPARC (Osteonectin)	NM_003118.2
IL-10	NM_000572.2	Angiopoeitin 1	NM_001146.3	CTGF	NM_001901.2
IL-12B	NM_002187.2	Angiopoeitin 2	NM_001147.2	PAI1	NM_000602.3
IL-13	NM_002188.2	Angiopoeitin 3	NM_004673.3	MMP-9	NM_004994.2
IL-15	NM_172174.1	Angiopoeitin 4	NM_015985.2	MMP-2	NM_004530.4
IL-18	NM_001562.2	FGF-2	NM_002006.4	MMP-3	NM_002422.3
TNF α	NM_000594.2	HGF	NM_000601.4	TIMP1	NM_003254.2
CCL2 (MCP-1)	NM_002982.3	IGF	NM_000618.3	TIMP2	NM_003255.4
CCL5	NM_002985.2	TF (Tissue Factor)	NM_001178096.1	Elastin	NM_001081754.1
CCL8 (MCP-2)	NM_005623.2	NPY	NM_000905.3	COL5A1	NM_000093.3
CX3CL1 (Fractalkine)	NM_002996.3	GM-CSF	NM_000758.2	COL6A1	NM_001848.2
CCL24	NM_002991.2	Heparin Binding EGF	NM_001945.2		
CCL 11	NM_002986.2	Cathepsin L	NM_001912.4		
CCL26	NM_006072.4	MMP12	NM_002426.4		
		Cd31	NM_000442.4		
		Tie1	NM_005424.2		
		Tie 2	NM_000459.3		
Immune Cell Markers		**Muscle**		**Metabolism/Homeostasis**	
HO-1	NM_002133.2	Cytochrome C Oxidase (MT-CO1)	YP_003024028.1	PPARγ	NM_005037.5
IL-1 Receptor α	NM_000577.4	Fbox040	NM_001094.4	PPARγ 2	NM_015869.4
CCL1	NM_002981.1	GDF8 (Myostatin)	NM_005259.2	LPL	NM_000237.2
CCL18	NM_002988.2	IGF1R	NM_000875.3	Lipase Maturation Factor	NM_022773.2
CCL 17	NM_002987.2	MAFbx (Atrogin-1)	NM_001242463.1	GPIHBP1	NM_178172.3
iNOS	NM_000625.4	Mrf4	NM_002469.2	FIAF	NM_001039667.1
MR	NM_006039.3	Myf5	NM_005593.2	PGC1α	NM_013261.3
CD163	NM_004244.4	MuRF1	NM_032588.2	PRDM 16	NM_022114.3
CD150 SLAM	NM_003037.2	MyoD	NM_002478.4	GPR120	NM_181745.3
CD 11c	NM_000887.3	Myogenin	NM_002479.4	CD36	NM_000072.3
CD 11b	NM_000632.3	NADH Dehydrogenase (MT-ND1)	YP_003024026.1	UCP-1	NM_021833.4
CD68	NM_001251.2	Wnt 10b	NM_003394.3	UCP-2	NM_003355.2
CD86	NM_175862.4	Pax7	NM_001135254.1	UCP-3	NM_003356.3
Siglec 8	NM_014442.2	SIRT1	NM_001142498.1	BcL2	NM_000633.2
Myeloperoxidase	NM_000250.1	Fn14	NM_016639.2	Bax	NM_004324.3
Human Mast Cell Tryptase β	NM_003294.3	TWEAK	NM_003809.2	Beclin 1	NM_003766.3
CD3	NM_000733.3				
House Keeping		**Adipose**			
ACTB (β Actin)	NM_001101.3	Adiponectin	NM_004797.3		
PP1A (Cyclophilin A)	NM_021130.3	CEBPα	NM_004364.3		
PP1B (Cyclophilin B)	NM_000942.4	CEBPβ	NM_005194.2		
UBC 9 (Ubiquitin c)	NM_021009.5	ATGL	NM_020376.3		
TBP (Tata Binding Protein)	NM_003194.4	CGI58	NM_016006.4		
TUBB (Tubulin β)	NM_178014.2	AdipoR2	NM_024551.2		
		AdipoR1	NM_015999.3		
		PKC α	NM_002737.2		

Functional classes of genes are within the black rows, genes are in the grey columns, and accession numbers are in the white columns. Each probe set consists of a capture probe and a reporter probe. See Figure 3.2 for details about nanoString.

Figure 3.11 is a graph showing nS absolute quantities for SPARC mRNA in each biopsy with subjects grouped by age. Although not statistically significant, we observed the age-dependent reciprocal pattern of expression following training and PsTPsE bouts. While both age groups tended to increase after training, this was most apparent for subjects >55 years of age. The level of SPARC mRNA was most elevated after PsTPsE exercise in younger subjects, whereas it decreased in older subjects in response to the PsTPsE exercise bout. The difference between SPARC mRNA following training compared to baseline in subjects < or >55 years of age did not reach statistical significance (265±197 vs. 849±276, p=0.11, n= 6 vs. 6), but trended to increase in subjects >55 following training. Similarly, the difference between PsTPsE and training showed a reciprocal trend between subjects < or >55 years of age (142±324 vs. -584±249, p=0.11, n= 6 vs.6). Taken together, these findings indicate that there is a mildly reciprocal behavior of SPARC mRNA in response to training and PsTPsE exercise based on age.

We next compared the expression of SPARC mRNA to the density of the two distinct populations of macrophages most abundant in skeletal muscle. Bivariate correlation analysis revealed several significant relationships between SPARC mRNA and mixed M1/M2 ($CD11b^{hi}206^{hi}$) macrophages; no correlation was apparent between SPARC mRNA and M1 ($CD11b^{hi}206^{lo/-}$) macrophages. Figure 3.12 depicts the bivariate plots of SPARC message measured by nS

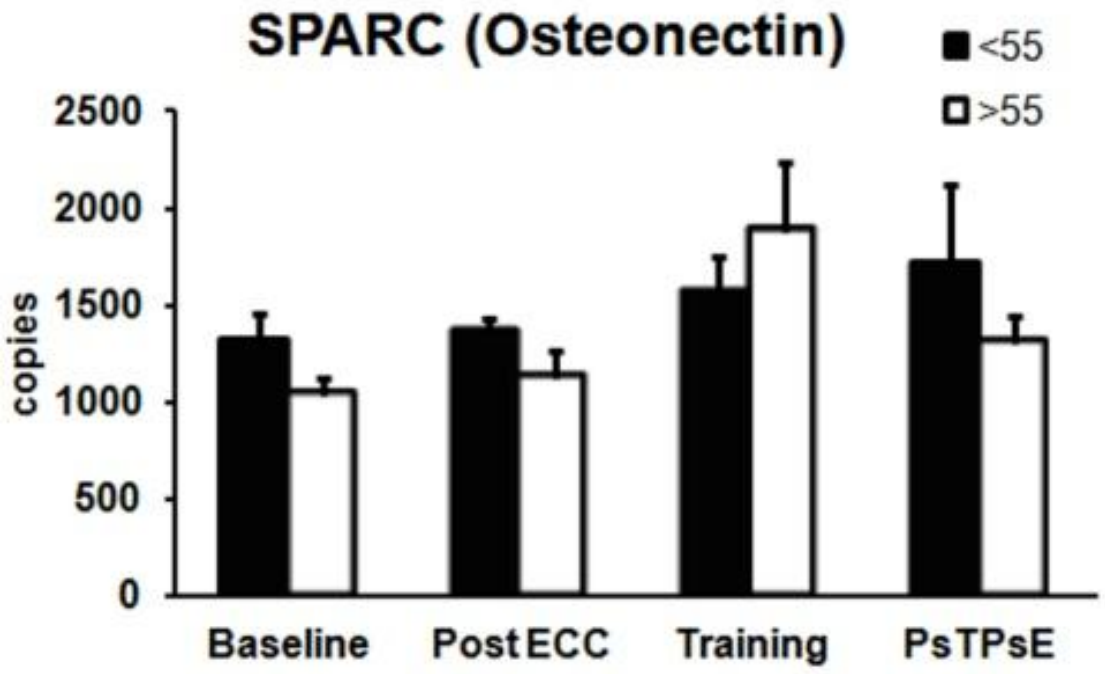

Figure 3.11 SPARC mRNA levels across interventions suggest a mildly reciprocal behavior in response to training and PsTPsE exercise based on age. SPARC mRNA is most abundant when comparing subjects <55 (black bars) to >55 at Baseline, PostECC and PsTPsE, but this trend reverses for training. SPARC mRNA was most elevated after PsTPsE exercise in subjects <55 years (black bars), whereas it decreased in subjects >55 (white bars) in response to the PsTPsE exercise bout. The trends described are not statistically significant.

versus the densities of CD11b^{hi}206^{hi} macrophages measured by IHC in muscle biopsies at baseline (Figure 3.12A), PostECC (Figure 3.12B), Training (Figure 3.12C), PsTPsE (Figure 12D) and in all 4 of the biopsy samples collapsed on the same axis (Figure 3.12E). The difference in the expression of SPARC message between PsTPsE and the training bout, plotted against age is also included (Figure 3.12F). At baseline, there was no relationship between SPARC and CD11b^{hi}206^{hi} macrophages (Figure 3.12A, R^2=0.001, p=0.93, n=10). After PostECC, the measurement of SPARC mRNA suggested a trend towards a direct association with hybrid CD11b^{hi}206^{hi} macrophages, although not significant (Figure 3.12B, R^2=0.10, p=0.31, n=12). As previous macrophage data suggested, we found a robust direct correlation between the levels of CD11b^{hi}206^{hi} macrophages and SPARC message after the training bout (Figure 3.12C, R^2=0.53, p=0.01, n=11), suggesting that their regulation may be linked in response to training. We also found a robust association between the levels of SPARC message and CD11b^{hi}206^{hi} macrophages in the PsTPsE biopsy (Figure 3.12D, R^2=0.48, p=0.02, n=11). Despite complex changes in both CD11b^{hi}206^{hi} macrophages and SPARC mRNA levels by exercise intervention in the context of aging, analysis of SPARC message compared to CD11b^{hi}206^{hi} macrophage density, when all biopsies are combined, still demonstrated a significant association (Figure 3.12E, R^2=0.30, p<0.001, n=44). One of the most striking observations we have made between the age groups is the *reciprocal* response of macrophages following PsTPsE exercise (Figure 5F, 7F, 8F, and 9C); SPARC mRNA showed a similar pattern of behavior (Figure 3.11). Comparing the

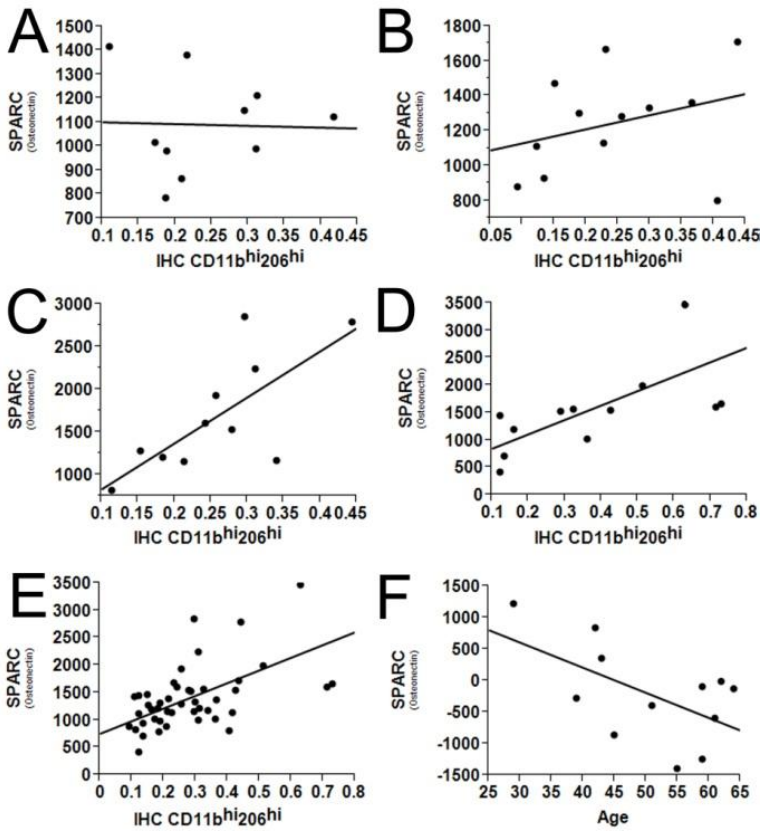

Figure 3.12 SPARC correlates with CD11b^{hi}206^{hi} macrophages after exercise and is inversely correlated with age. The graphs depict SPARC message measured by nS versus the densities of CD11b^{hi}206^{hi} macrophages measured by IHC in muscle biopsies at baseline (A), PostECC (B), Training (C), PsTPsE (D) and in all 4 of the biopsy samples collapsed on the same axis (E). (F) The difference in the expression of SPARC message between PsTPsE and the training bout, plotted against age. (A) Baseline indicated no relationship between SPARC and CD11b^{hi}206^{hi} macrophages (R^2=0.001, p=0.93, n=10). (B) PostECC, SPARC mRNA suggested a trend towards a direct association with hybrid CD11b^{hi}206^{hi} macrophages (R^2=0.10, p=0.31, n=12). (C) Training caused robust direct correlation between the levels of CD11b^{hi}206^{hi} macrophages and SPARC message (R^2=0.53, p=0.01, n=11). (D) PsTPsE induced a direct correlation between SPARC message and CD11b^{hi}206^{hi} macrophages (R^2=0.48, p=0.02, n=11). (E) The overall correlation of CD11b^{hi}206^{hi} macrophages and SPARC mRNA levels by all interventions, when all biopsies are combined demonstrated a significant association (R^2=0.30, p<0.001, n=44). (F) Comparing the difference between PsTPsE and Training for SPARC message measured by nS, plotted against age, showed an inverse correlation (Figure 3.12F, R^2=0.32, p=0.05, n=12).

difference between PsTPsE and Training for SPARC message measured by nS, plotted against age, showed a significant inverse correlation (Figure 3.12F, R^2=0.32, p=0.05, n=12), suggesting that there is a general drop in the level of SPARC message as a function of age.

The significant correlation observed between SPARC mRNA and $CD11b^{hi}206^{hi}$ macrophages across all biopsies from all subjects (Figure 3.12E) prompted us to perform correlation analyses across the entire gene set on all biopsies for both mixed M1/M2 and M1 macrophage abundance, the two most abundant macrophage subtypes in the biopsies. Although the expression of most genes was not correlated with macrophage abundance (data not shown), including those encoding cytokines and other inflammatory gene products, the expression of some genes related to distinct cellular functions were specifically correlated to abundance of the different macrophage populations (Tables 3.3-5). The nS output is in order of lowest to highest copy number; all R^2 values shown are significant. The correlations fell into three functional groups: fibrosis, angiogenesis and genes associated with tissue homeostasis, with the 2 types of macrophages differentially correlated to different processes, suggesting that M1/M2 mixed phenotype and M1 macrophages have discrete effects on muscle physiology.

Table 3.3 summarizes R^2 values for the association of mRNA copy numbers related to ECM and fibrosis and M1/M2 and M1 macrophages, where p<0.01 is in **bold**, and p<0.05 is in normal font, as the legend on the bottom of

Table 3.3 Transcripts involved with fibrosis are exclusively correlated to M1 or M1/M2 macrophage densities.

Fibrosis		
Messages	**M1**	**M1/M2**
TGFβ		**0.16**
TSP1	**0.14**	
SPARC		**0.3**
CTGF	0.1	
PAI1	**0.14**	
MMP2		0.13
MMP14		**0.21**
TIMP1	**0.26**	
TIMP2		0.14
Elastin		**0.14**
COL5A1		**0.14**
COL6A1		**0.17**
p value	**P<0.01**	P<0.05

R^2 values for the relationship of fibrosis related genes and M1/M2 or M1 macrophages, where p<0.01 is in **bold**, and p<0.05 is in normal font; blanks indicate no association.

the table indicates. M1/M2 and M1 macrophages were correlated with distinct sets of genes related to fibrosis, suggesting M1/M2 and M1 macrophages differentially contribute to that process. mRNAs which increased as M1 macrophage densities increased are TSP1, CTGF, PAI1, and TIMP1. Messages correlated with M1/M2 macrophage densities are TGFβ, SPARC (for absolute data at each biopsy point refer to Figure 3.12), MMP-1, MMP14, TIMP2, Elastin, COL5A1, and COL6A1.

Table 3.4 summarizes R^2 values for the relationship of angiogenic gene expression correlated to M1/M2 or M1 macrophages. In this angiogenesis gene set, VEGF A message decreased (R^2 values were multiplied by -1 if the slope of the regression line was negative) as M1 macrophages increased in density. For IGF1 and TF, both M1/M2 and M1 macrophage densities were associated and both increased with the activities of these genes; however, M1/M2 macrophages were associated with more robust increases. Lastly for Table 3.4, CD31, TIE1, and TIE2 mRNAs were specifically associated with M1/M2 macrophage densities. Table 3.5 lists the R^2 values for the correlation among mRNAs associated with cellular homeostasis, and M1/M2 or M1 macrophages. These genes are specifically related to protein turnover (MAFbx), autophagy (beclin), and apoptosis (Fn14, Bcl2, and Bax). The most striking observation was that only M1 macrophages were associated with expression of these genes; no correlations were apparent between these genes and M1/M2 macrophage

Table 3.4 Transcripts involved with angiogenesis are related to M1 and M1/M2 macrophage densities.

Angiogenesis		
Messages	**M1**	**M1/M2**
VEGF A	-0.09	
IGF	0.09	**0.44**
TF	0.11	**0.21**
CD31		0.1
TIE1		**0.17**
TIE2		0.09
p value	**P<0.01**	P<0.05

R^2 values for the correlation among mRNAs associated with cellular homeostasis and M1/M2 or M1 macrophages. p<0.01 is in **bold**, and p<0.05 is in normal font; blanks indicate no association

abundance. MAFbx, beclin, and Bcl2 were inversely correlated, whereas Fn14 and Bax were directly correlated with M1 macrophages. This inverse association suggests that as M1 macrophage densities increase in the muscle, the mRNA from MAFbx, beclin, and Bcl2 decrease from baseline copy numbers.

DISCUSSION

Figure 3.13 is a schematic diagram laying out the study design, in a timeline fashion of the biopsy schedule and exercise intervention regimen (white box). Using the clinical groupings we previously discussed, we attempted to analyze muscle adaptations induced by exercise in the context of aging, obesity, or insulin sensitivity. The remainder of the diagram summarizes our hypotheses regarding the muscle response (light gray) and macrophage response (dark gray) to exercise. We expected the eccentric exercise to damage the muscle (Chapter 1, Figure 1.4), causing an increase in macrophages. The beneficial effect of aerobic exercise is well accepted(55, 134). Aerobic exercise training increases oxidative capacity, by either increasing mitochondrial content, or augmenting the expression of genes involved with oxidative phosphorylation, or both. As oxidative capacity increases, the muscle naturally will increase the buffers to absorb the consequential free radical production from oxidative

Table 3.5 Transcripts involved with cellular and protein turnover are related exclusively to M1 macrophage density.

Cellular Homeostasis		
Messages	**M1**	**M1/M2**
MAFbx (Atrogin-1)	-0.12	
Beclin	-0.1	
Fn14	**0.17**	
BcL2	**-0.17**	
Bax	0.14	
p value	**P<0.01**	P<0.05

R^2 values for the correlation among mRNAs associated with cellular homeostasis and M1/M2 or M1 macrophages. p<0.01 is in **bold**, and p<0.05 is in normal font; blanks indicate no association.

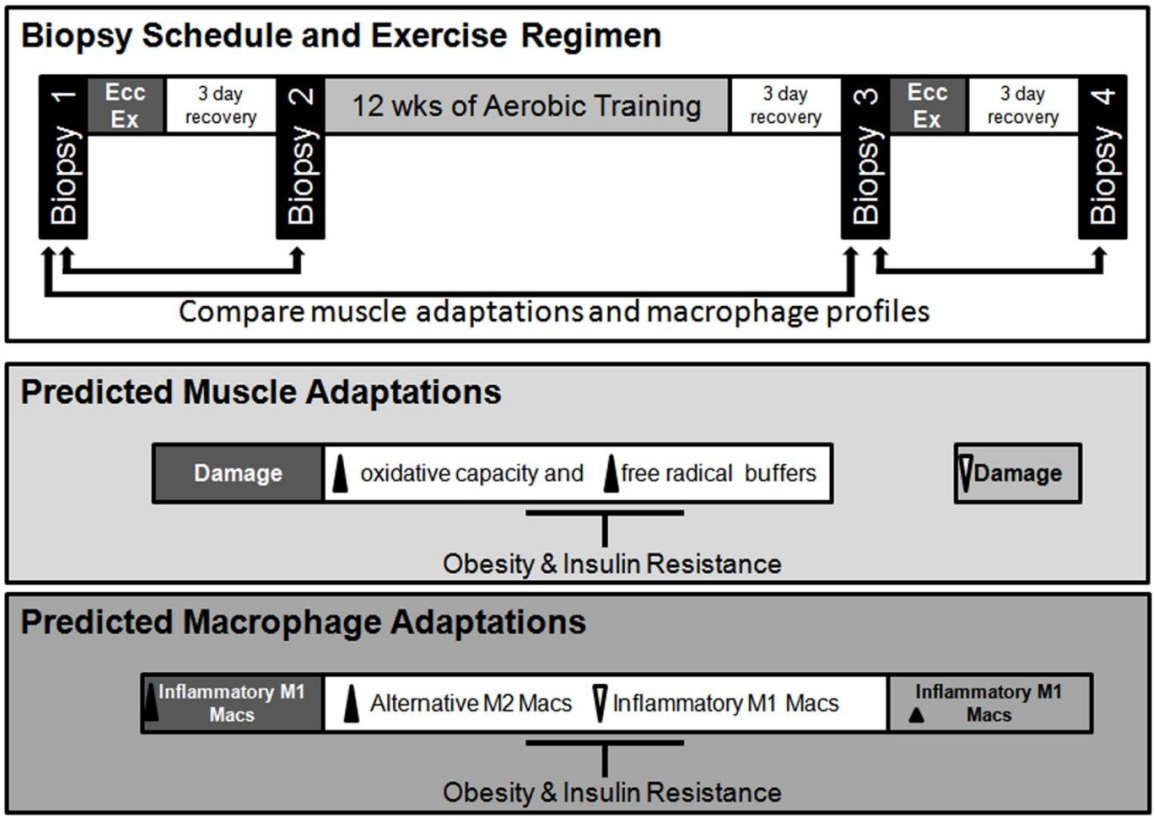

Figure 3.13 Timeline of the biopsy schedule, exercise intervention regimen and predicted adaptations by the muscle and the resident macrophages. Study design (white box). The predicted muscle response to exercise interventions (gray box). We predicted damage from eccentric exercise would induce inflammation, whereas beneficial aerobic exercise might change the muscle to have more efficient oxidative metabolism, and increase the free radical buffering capacity, thereby reducing radical stress, and that health factors such as aging might inhibit this process. Predicted macrophage response in muscle to the exercise interventions (dark gray box). We predicted the macrophages would infiltrate according to the adaptations incurred to the muscle by exercise, distinctly by macrophage phenotype. Sequentially, M1 macrophages infiltrate where there is more damage, M2 macrophages being recruited into the muscle during the aerobic training to modify the tissues in a beneficial way, and that after the training, additional eccentric damage would be reduced, which would subsequently recruit less M1 macrophages than in the initial bout of damage.

phosphorylation. Our original hypothesis was that the array of macrophages present in muscle would be altered with obesity and insulin resistance, influencing response to a bout of eccentric exercise. We further hypothesized that aerobic training would normalize the response to a subsequent bout of eccentric exercise. Of the clinical factors we explored, we found that age had the largest impact on the flux of macrophages in skeletal muscle in response to aerobic training, and aerobic training followed by eccentric exercise.

Our laboratory has reported a difference in human skeletal muscle between baseline and post eccentric exercise for $CD11b^+$ inflammatory M1, and $CD163^+$ alternative M2 macrophages for *17 male* subjects with a mean age of *31.9* years(126). Despite using a similar resistance exercise protocol and tissue processing, in this report, we detected no differences in any of the macrophages post eccentric exercise (PostECC) for our <55 age group, of *2 males and 4 females*, mean age of *41.5*. Additionally, we found the density of the M1 type macrophages to be roughly 10-fold higher at baseline compared to the Pryzbyla study. These discrepancies could be due to a roughly 10 year gap for the mean age for the younger groups, sex related differences in skeletal muscle adaptation to damaging exercise, sample size, and/or the different antibody for the detection of CD11b and the chemistry of detection between the two studies.

Studies suggest that positive muscle adaptation becomes much more difficult as we age (44, 56, 122, 126). The current study and the Pryzbyla study reported no change in the older age group in response to eccentric exercise (60±1.3 and 71.4±4.6 years, respectively). Subjects were younger in the present

study but functional mobility decline begins in the fifth decade of life(159). The increase in macrophages after aerobic training in the >55 group is interesting. The effects of aging, such as arthritis, overall energy reserves, and frailty, may promote a more sedentary lifestyle(84, 159), where subjects might be less *conditioned*, so that even the aerobic activity used in the exercise protocol may induce damage. The younger subject group is presumably more active at baseline. Indeed, subjects of the >55 age group had baseline VO_2 max values of 25±1.9 compared to that of the <55 age group at 33±4.5 ml/kg·min. Although this was only a trend, there is a variation of nearly 24%, between the two age groups. Macrophages enter muscle in response to damage(56, 112, 120, 123, 126, 176), but they can also inflitrate muscle due to the expression of chemokines and other similar chemotactic agents(142, 146, 147). Our age groups could have differential storage of glycogen(24) and production of ADP; glycogen depletion and elevated ADP readily activates AMPK, which can lead to the secretion of chemokines.

We detected very low levels of pure M2 macrophages in the skeletal muscle of subjects included in this study. To our knowledge, this is the first report describing mixed M1/M2 macrophages in skeletal muscle. Our group and others have also found a mixed phenotype in adipose(162, 192). A large amount of research activity in rodents suggests that there is phenotypic shifting from an M1 inflammatory to an M2 anti-inflammatory mode which promotes repair programs(6), protects against muscle atrophy(52), and supports muscle recovery *in vivo* and *in vitro*(23, 27, 52). Secretory products derived from M2 macrophages

directly aid in growth and repair by stimulating the activity of muscle stem cells, called satellite cells(135). Characterization of the mixed M1/M2 macrophages resident in muscle and those that respond to aerobic training in the older subjects and to eccentric exercise following training in younger subjects is required to determine their role in muscle adaptation.

Macrophages expressing only the M1 marker were significantly correlated to BMI in skeletal muscle. Obesity can be linked to high blood triglycerides, clinically termed hyperlipidemia, and can lead to ectopic deposition of fat in muscle(53). Presumably, macrophages scavenge this lipid, and are of the inflammatory M1 type(68, 192). Elevated M1 macrophages may contribute to low grade inflammation in muscle associated with obesity; however, M1 macrophages but do not appear elevated with age (45), even though aging is also associated with muscle inflammation(122). It is possible that with age, inflammatory cytokines are derived from muscle fibers themselves (see Chapter 4).

We hypothesized there would be differential effects on free radical damage dependent on age in skeletal muscle in response to exercise, and macrophage recruitment could be correlated to the damage. There is a significant body of evidence suggesting that free radical damage increases with age(33, 42, 59, 130, 140, 164, 174). Furthermore, free radical damage is an important adaptation to exercise(32, 82, 83). We measured free radical damage associated with NO production, assessed as % area of nitrotyrosine (NY) adducts in the skeletal muscle of our subjects grouped by age. Although we

found very robust age related differences in NY adducts in response to the exercise interventions, macrophage density based upon age, could not be attributed to the level of NY adducts.

Downhill running mice were shown to have increased hydrogen peroxide content, a marker of reactive oxygen species (ROS), and concomitant increase in transcripts for chemokines MCP1, CCLX14, and the macrophage marker F4/80 in the muscle(89). Mice pretreated with circumin, a radical scavenger, attenuated these changes, suggesting that ROS leads to the recruitment of macrophages. Perhaps if we had measured H_2O_2, or a different adduct, such as 4-hydroxy-2-nonenal (HNE) carbonyl or peroxynitrite, correlations to macrophage fluxes may have been observed in our study.

Another interesting possibility is that age-associated alterations in energy storage and utilization during exercise (24), may be differentially affecting macrophage recruitment via an AMPK/IL6 based mechanism. Aging decreases mitochondrial function in muscle in humans(3, 34, 35, 50, 96),in rats(12, 170), in mice(9, 154) and dogs (170), exacerbating glycogen depletion, activation of AMPK and subsequent IL6 secretion(51, 91). IL6 is induced by contracting muscle in humans(166). Aged men maintain IL6 secretion during 3 hours of dynamic knee extension exercise compared to young men(125). IL6 is also elevated in aged humans(188) and mice(41). IL6 may also act as a chemokine, attracting macrophages(31). In situations of IL6 resistance, such as that found in obesity and T2DM(141), more IL6 is secreted as well, which may lead to more

macrophage recruitment. Further experimentation is needed to support this hypothesis.

One of the most striking observations in this study is the reciprocal response of macrophages to eccentric exercise following training based on age. Following training, macrophages tended to decrease in response to a subsequent bout of eccentric exercise in the >55 age group, whereas in the <55 age group, macrophages increased. The decreasing trend in macrophage densities in the older age group suggests that the macrophages may be apoptosing(150, 163), but they may also be egressing. We observed that overall NY adducts decreased in <55 age group across exercise interventions, while in the >55 age group, these adducts were elevated throughout the exercise interventions, suggesting a beneficial effect of exercise in the younger individuals. The fact that following training, eccentric exercise elicited an increase primarily in M1/M2 macrophages in those <55 years of age implies a reparative role for the cells, which is blunted in the older individuals.

We characterized gene transcripts from human skeletal muscle in response to exercise and found that only a minority of transcripts correlated with age, or to the densities of macrophages of the M1 inflammatory and M1/M2 mixed phenotype. SPARC mRNA was robustly expressed, showing a change in expression pattern similar to macrophages. The significance of this observation remains to be determined. However, the function of SPARC is quite wide ranging(18). SPARC is involved in the shuttling of procollagen from the cytoplasm to the interstitium, and in collagen nucleation in the ECM(19). SPARC

has been proposed as a powerful anti-oxidant, and important in prescription of exercise in bladder cancer resolution. Furthermore, the loss of SPARC in a murine bladder cancer model was associated with an inflammatory phenotype of tumor-associated macrophages(136).

The correlation of M1 and M1/M2 macrophages to exclusive gene transcripts involved with fibrosis is striking, but also is congruent with what we know of M2 macrophage biology. Most notably, we found that SPARC transcripts were directly correlated to M1/M2 macrophage fluxes across our study. But the change in SPARC transcript in response to eccentric exercise post training was inversely correlated with age, suggesting that the normal SPARC response was inhibited in that bout in the older subjects. We have shown in adipose that M2 macrophages are associated with fibrosis and obesity(161, 162). M2 macrophages are described as wound healers and important in containing helminth parasites via matrix deposition(108). The fact that M1 and M1/M2 macrophage abundance showed similar trends in response to the different interventions and correlated with different fibrosis genes, suggest that there is some cooperation in ECM remodeling in response to exercise between these two macrophage types. Our research group has shown that strength outcomes were directly correlated with TIMP1 transcript at baseline and inversely correlated to the change in TIMP1 transcript in response to exercise(46). The current study correlated M1 but not M1/M2 density to TIMP1 transcript levels in response to exercise. This suggests that M1 inflammatory macrophages are important in modulating TIMP1 gene transcripts in ECM remodeling in response to exercise.

ECM must also be remodeled for adaptations to exercise in the vasculature, promoting angiogenesis to increase oxygen and nutrient delivery to the muscle(4). Our laboratory has reported that M2 macrophages in adipose have increased Collagen V deposition, which inhibits endothelial sprouting(161). In this study we found that macrophages and angiogenesis transcripts were also correlated in response to exercise, with the majority of transcripts within this functional group correlated with M1/M2 macrophages. Interestingly, we find that both M1 and M1/M2 macrophages correlate with expression of transcripts encoding insulin like growth factor 1 (IGF1), and tissue factor (TF) in response to exercise, suggesting an additive or potentiating effect. Studies in chemokine receptor null (CCR2$^{-/-}$) mice show decreased VEGF production, suggesting the importance for macrophages in the angiogenic program(117). We observe an inverse correlation for M1 macrophages and VEGF A mRNA fluxes in response to exercise. Studies in a rat model of exercise show that VEGF receptor antagonism blocked arteriogenesis but only partially blocked angiogenesis as a whole(100). Taken together these observations suggest that M1 macrophages may be inhibitory to portions of the angiogenic program.

Macrophages have been shown to be important in the preservation of myogenic cells by promoting cell survival pathways(157). The different macrophage phenotypes we have described have distinct effects on myoblasts. Work by the Chazaud group suggests that inflammatory M1 macrophages promote myogenic cell proliferation and that anti-inflammatory M2 macrophages promote differentiation(6). Further studies by Chazaud suggest that coinjected

bone marrow derived macrophages and myogenic precursor cells improve survival in myogenic precursor cells after implantation in mdx mouse skeletal muscle(98), but they did not identify the phenotype of the macrophages. The process of programmed cell death (apoptosis) is complex(54); we have measured genes transcripts related to the mitochondrial-mediated apoptosis. Functionally, Bcl2 and Bax are coupled, as they dimerize with one another; when present in an equal ratio, they suppress the formation of the permeability transition pore(97). When Bcl2 is suppressed, or if Bax levels increase, this promotes the formation of the permeability transition pore by Bax dimers in the mitochondrial envelope, releasing cytochrome C, promoting apoptosis. The fact that M1 macrophage densities were inversely correlated to Bcl2 mRNA copy numbers, while Bax mRNA copies were increased, supports the idea that M1 macrophages and apoptosis may be linked in muscle, but further experimentation is needed to confirm this hypothesis.

Studies on human subjects are limited on multiple levels. The major limitation of this study is in the ability to recruit and retain enough subjects. Additionally, human subjects have enormous genetic variation, which makes these types of studies statistically challenging. Although we have proposed many mechanisms for the correlations we have observed in this study, correlation does not prove cause and effect. Some of our observations may be coincidental, even though we have made efforts to validate our observations with the literature. Further studies are needed with physiological interventions which target

important components, such as macrophages, or molecular targets such as SPARC, to show cause and effect.

Chapter 4: Inflammatory and Alternatively Activated Macrophage Products Effect Myotube Glucose Uptake and Myokine Secretion Distinctly

SUMMARY

We have developed an *in vitro* model in which cultured myotubes from human muscle biopsies are exposed to activated macrophage products in conditioned media (CM), and compared for insulin induced glucose uptake and myokine profile. Untreated myotubes were extremely resistant to insulin stimulated glucose uptake. We unexpectedly observed that baseline myotube glucose uptake was approximately 2-fold higher following exposure to M1 or M2C macrophage CM. Insulin-stimulated glucose uptake trended inhibitory and enhancing for M1 and M2 CM, respectively, but did not reach statistical significance. The response may be influenced by the insulin sensitivity of the cell donor. Both M1 and M2C macrophage CM induced myotubes to secrete copious amounts of IL6 into the media when compared to untreated myotubes, which may be the primary factor affecting both baseline and insulin stimulated glucose uptake.

INTRODUCTION

The American Diabetes Association reports that mortality in persons with type 2 Diabetes Mellitus (T2DM) is due primarily to heart disease and stroke. Insulin resistance is a major determinant of T2DM that leads to two major symptoms, high serum fatty acids and high blood glucose. Skeletal muscle consumes the most glucose of any tissue in the body, yet there are no pharmacotherapies which specifically target muscle. In adipose tissue, macrophage mediated inflammation is a causal factor of insulin resistance(5, 118, 138, 198). Our lab reported total macrophage infiltration is also elevated in human muscle with obesity and insulin resistance(184). Depending on the stimulus, macrophages can differentiate into several subtypes, each having a distinctive cytokine signature. The current view suggests that M1 macrophages are classically pro-inflammatory and inhibitory to insulin signaling. Consistent with this idea, data presented in Chapter 3 showed that in muscle, M1 macrophage abundance is specifically associated with obesity. Conversely, M2 or alternatively activated macrophages are anti-inflammatory, and in muscle, play a crucial role within the context of muscle repair and exercise induced hypertrophy(177). The role of alternatively activated (M2) macrophages in insulin resistance is less clear. M2 macrophages have distinct functional variation, which are further classified into subtypes M2A and M2C(108). M2A macrophages function in allergic response, and isolation and killing of parasites, and secrete anti-inflammatory interleukin 10 (IL10) and pleiotropic IL6. M2C macrophages

serve similarly, and also serve in matrix deposition and tissue remodeling, secreting IL10. Contrary to reports in mice, our lab has shown that obesity and insulin resistance are associated with increased abundance of M2, particularly M2C, macrophages in human adipose, suggesting a negative role (162). Furthermore, our data presented in Chapter 3 suggest that M1/M2 "mixed" macrophages are present in muscle, but their contribution to peripheral insulin resistance is unknown.

This investigation utilizes a human cell culture model to dissect the role of M1 pro-inflammatory and M2 anti-inflammatory macrophages on insulin signaling in muscle cells derived from insulin sensitive and resistant subjects. We hypothesize that the insulin response in cultured human muscle cells will be modified distinctly as a result of activation of signaling pathways following exposure to secretory products from different macrophage subtypes. As presented in Chapter 2, myotubes were extremely resistant to glucose uptake. At baseline, myotube glucose uptake was approximately 2-fold higher following exposure to M1 or M2C macrophage conditioned media (CM); however, CM had only modest effects on insulin-stimulated glucose uptake, which differed based on the insulin sensitivity of the muscle cell donor. M1 and M2C CM induced myotubes to secrete copious amounts of IL6. The characterization of interactions between skeletal muscle cells and macrophages may lead to novel approaches for preventing and/or treating insulin impairment manifested by T2DM.

MATERIALS AND METHODS

Subjects and Tissue Collection

Human non-diabetic subjects were recruited through local advertising. All subjects included in the study were recruited by informed consent approved by the institutional review board at the University of Arkansas for Medical Sciences or the University of Kentucky. Myoblasts harvested from muscle biopsies taken from six subjects were included in this study. Muscle biopsies were collected from vastus lateralis muscle under local anesthesia. Standard fasting blood lipids were measured at the time of biopsy. The clinical insulin sensitivity (S_I) was measured by frequently sampled IV glucose tolerance test with minimal model calculation(191). Subjects were considered insulin sensitive at SI > 3.0 and resistant subjects at SI < 3.0 x 10^{-4} $min^{-1}\cdot(\mu U\cdot ml)^{-1}$. See Table 2.1 for details.

Muscle Cell Culture

Myoblasts were isolated as previously described (184) and in Chapter 2. Briefly, myoblasts were propagated in growth medium composed of Hams/F10 medium (Cellgro/Mediatech, 10-070-CV, Manassas, VA) supplemented with 20% fetal bovine serum (FBS, Atlanta Biologicals, S12450, Lawrenceville, GA), 5 mg/ml basic Fibroblast Growth Factor (bFGF Millipore, GF003) and 1% Pen/Strep, maintained with 5% CO_2 at 37°C. At passage 6 or 7, myoblasts were seeded onto 6-well Primaria plates at 72 cells/mm^2 in growth medium. The next morning the wells were washed once with PBS (Gibco/Life Technologies, 10010-023, Grand Island, NY) and the medium was changed to differentiation medium composed of αMEM, supplemented with 2% FBS and 1% Penicillin/Streptomycin (Gibco/Life Technologies, 15140). The cells were observed and the medium changed every 48-72 hours. When fully formed myotubes were present (approximately 12 days) the cells were treated as described below.

Macrophage Polarization

We have optimized protocols based upon the literature(25, 114, 179) to activate the human monocyte cell line, THP-1, into M1, M2A or M2C phenotypes. $2x10^6$ THP-1 cells were activated in macrophage serum free medium (MSFM) by treatment with 100 ng/ml lipopolysaccharide (LPS) and 20 ng/ml interferon gamma (INFγ) for M1. For M2A or M2C, $2x10^6$ cells were treated first with 5 nM phorbol ester 12-O-tetradecanoylphorbol-13-acetate (TPA) for 5 minutes, then with 20 ng/ml IL4 for M2A or IL10 for M2C. Undifferentiated THP-1 cells treated with vehicle served as control. Following 24 hours of treatment, differentiated cells were washed once with MSFM and allowed to grow in myotube differentiation medium for 48 hours, at which time, conditioned media (CM) were collected and stored at ˉ80˚C. Myotubes were pretreated (PreTx) with 1/2 strength CM (diluted with an equal volume of αMEM, supplemented with 2% FBS and 1% Pen/Strep) for 10-12 hours prior to insulin or vehicle treatment. The activation of the different macrophage types was confirmed by quantifying IL1β, IL10 and IL6 secreted into the medium prior to experimentation. Preliminary experiments confirmed that 1% Pen/Strep had no effect on the final results.

ELISA

ELISA kits for IL10 and IL6 were purchased from R&D Systems (Minneapolis, MN), and IL1β kit was from (Pearce/Thermo FIsher Scientific, EH2IL1B, Rockford, IL). Manufacturer's instructions were followed for the assays.

Glucose Transport Assay

As in Chapter 2, myotubes were washed once in 37°C Hank's balanced salt solution with phenol red (HBSS, Gibco/Life Technologies, 24020-117), then serum starved by another replacement of HBSS for 30 minutes. Subsequently, HBSS was replaced with either fresh warm HBSS or with 5 nM insulin in HBSS, and incubated at 37°C for 30 minutes. Cell plates were placed on a heated working surface composed of a top layer of 1 blue chuck, a fiber glass dinner tray as the middle layer, and a Sunbeam© heating pad as the bottom layer, prewarmed on the lowest setting. Cells were then washed three times in 37°C PBS supplemented with 100 μM Ca^{2+} and Mg^{2+} (PBSCaMg). Wells were carefully aspirated; 1ml of 0.33 μCi. 2-deoxy-d[1,2-^{3}H]glucose (NEN Life Science Products, NEC495250UC, Waltham, MA) in HBSS was applied/well, and incubated for 30 minutes. Cells were washed three times in 37°C HBSS. The cytoplasmic fraction was liberated with 550 μl of 1% Triton X-100 (Sigma-Aldrich,

X100-100ML St. Louis, MO) in PBS by incubating for at least 5 minutes. Four hundred µl was transferred to scintillation vials, then 4.5 ml of Scintiverse cocktail (ThermoFisher, SX18-4, Waltham, MA) was added and the vials counted for 10 minutes each in a Beckman Coulter liquid scintillation counter. Counts per minute of the insulin treated samples were normalized to the baseline samples, and reported as relative units.

Statistics

Differences between treatments were analyzed for statistical significance by two way ANOVA followed by two tailed Student's t-test for pairwise comparison. Cytokines were compared via one-way ANOVA, followed by two tailed Student's t-test. JMP software (SAS Institute Inc. Cary, NC) or Excel (Microsoft Corporation, Seattle, WA), was used for all analyses.

RESULTS

The human monocyte cell line, THP-1, was differentiated into M1, M2A and M2C polarized macrophage-like cells for preparation of conditioned medium (CM) to determine the effect of macrophage secretory products on myotube response to insulin. To confirm the macrophage phenotype following activation, selected inflammatory and anti-inflammatory cytokines secreted into the medium were measured by ELISA, including IL1β (Figure 4.1A, black bars), IL6 (Figure 4.1B, gray bars), and IL10 (Figure 4.1C, white bars). The amount of IL1β secreted into the medium differed significantly between the macrophages types (Figure 4.1A). As expected, M1 macrophages secreted the most IL1β (Figure4.1A, M1, 440±28 pg/ml); an intermediate IL1β level was characteristic of M2A CM, which contained approximately half the IL1β as M1 CM (Figure 4.1A, M2A, 214±23 pg/ml). M2C CM had an unexpectedly high level of IL1β (Figure 4.1A, M2C, 354±20 pg/ml), but also contained by far the largest amount of IL10 (Figure 4.1C, M2C, 5121±106 pg/ml). A high IL10:IL1β ratio is characteristic of M2C macrophages, whereas a high IL1β:IL10 ratio is characteristic of M1 macrophages, suggesting that these cells *in vitro* are mimicking the desired phenotypes. Since we used IL10 to activate THP1 cells into the M2C phenotype, we measured the IL10 content directly after the activation medium was removed and the cells were washed (data not shown); the residual IL10 detected did not

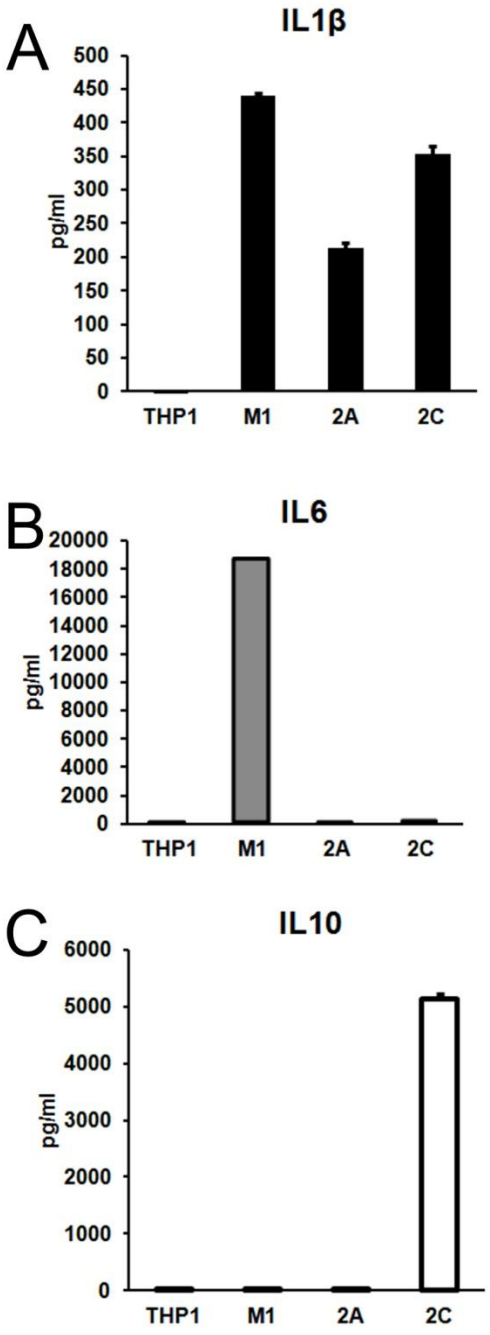

Figure 4.1 The human monocyte cell line, THP-1, was differentiated into M1, M2A and M2C polarized macrophage-like cells. Cytokines in conditioned media (CM) were measured by ELISA. (A) IL1β (black bars), (B) IL6 (gray bars), and (C) IL10 (white bars). A high IL10:IL1β ratio is characteristic of M2C macrophages, whereas a high IL1β:IL10 ratio is characteristic of M1 macrophages. Mean ± SEM

account for the IL10 measured in Figure 4.1C. Finally, M1 CM contained significantly higher levels of IL6 compared with the other cell types (Figure 4.1B, M1, $1.85x10^4$±300 pg/ml; M2A, none detected; M2C, 4.0±1.5 pg/ml). In summary, CM from THP1 cells activated as M1 inflammatory macrophages contained the highest levels of IL1β and IL6, and M2C CM had the highest level of IL10; however, the M2C macrophages may display a somewhat "mixed" M1/M2 hybrid macrophage type, with relatively high IL1β secretion. M2A CM was intermediate between M1 and M2C in terms of IL1β content, and distinct from M1 CM because it contained no IL6. In light of the findings of the "mixed" macrophage phenotype we found *in vivo* in Chapter 3, this result may suggest that we are mimicking the "mixed" M1/M2 macrophage *in vitro*.

Myotubes themselves are induced to express extremely high levels of cytokine mRNAs in response to coculture with inflammatory macrophages (184). We determined the effect of secretory products from the 3 different macrophage subtypes on myotube cytokine secretion using ELISA. Myotubes alone secrete very little IL-1β or IL10 after 10 hours of cell culture. When M1, 2A or 2C macrophage CM was applied to the myotubes, IL-1β and IL10 were not secreted at statistically different levels than were already present in the applied CM (data not shown). By contrast, M1, M2A and M2C CM induced myotubes to secrete IL6 (Figure 4.2, CM, black bars; post myotube CM, white bars). After 10 hours of cell culture, myotubes themselves, secreted IL6 (U.Tx 1727±46 pg/ml), which was suppressed following treatment with undifferentiated THP1 CM (THP1, 1000±20 pg/ml, $p<0.01$). Following culture of myotubes in M1 CM, IL6 content in the

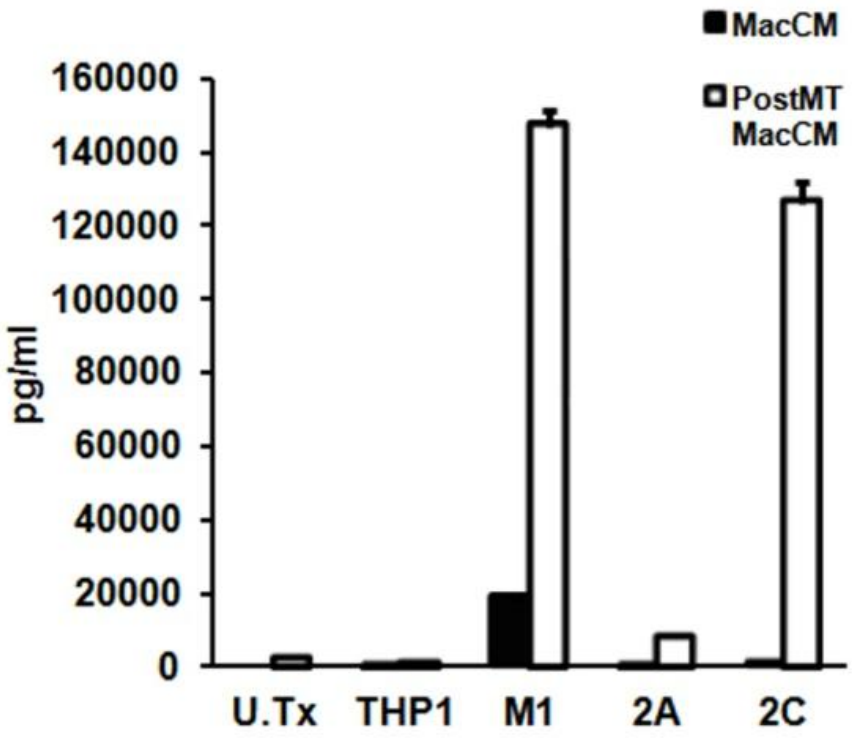

Figure 4.2 M1, 2A and 2C macrophage CM induce human myotubes to secrete IL6 after 10 hours of cell culture. Baseline CM (black bars); content of macrophage CM post myotube culture(white bars); untreated myotube media after 10 hours of culture without macrophage CM treatment (U.Tx).Mean ± SEM

medium increased nearly 6 fold (Figure 4.2, $1.85x10^4$±300 vs.$1.47x10^5$±4825 pg/ml, p<0.01). M2C CM contained very little IL6; however, when this medium was applied to myotubes, large quantities of IL6 were secreted (Figure 4.2, 4.0±1.5 vs. $1.26x10^5$±5564 pg/ml, p<0.01). No IL6 was detected in M2A CM; however, M2A CM also stimulated myotubes to secrete a modest but significant quantity of IL6 into the medium (8116±72 pg/ml). Thus, M1, 2A and M2C CM induce myotubes to secrete IL6, with M1 and M2C CM having the greatest effect.

We predicted that the different macrophage CMs would differentially affect myotube glucose uptake consistent with the cytokine content of the medium, quantified above. Results from myotubes from 4 different individuals, 2 insulin sensitive (S_I 3.09 and 4.17) and 2 insulin resistant (S_I 1.51 and 1.52), were pooled and the average glucose uptake following treatment, divided by glucose uptake of each untreated myotube culture, are shown in Figure 4.3. All donors were quite resistant to 5nM insulin (Figure 4.3, negative control undifferentiated THP1 CM 1.06±0.15 vs.1.29±0.20, p=0.12, n=4); higher doses of insulin were also ineffective (data not shown). Overall, M1 macrophage CM enhanced baseline glucose uptake (Figure 4.3, 1.06±0.15 vs. 2.02 ±0.25, p<0.05, n=4); in the presence of insulin, glucose uptake trended down, but was not significant (2.02±0.25 vs. 1.60±0.31, p=0.23, n=4). M2C macrophage CM also enhanced baseline glucose uptake (Figure 4.3, 1.06±0.15 vs. 2.10 ±0.30, p<0.05, n=4). In the presence of insulin, glucose uptake trended up, but this change was not statistically significant (2.10±0.30 vs. 2.30 ±0.31, p=0.43, n=4). M2A

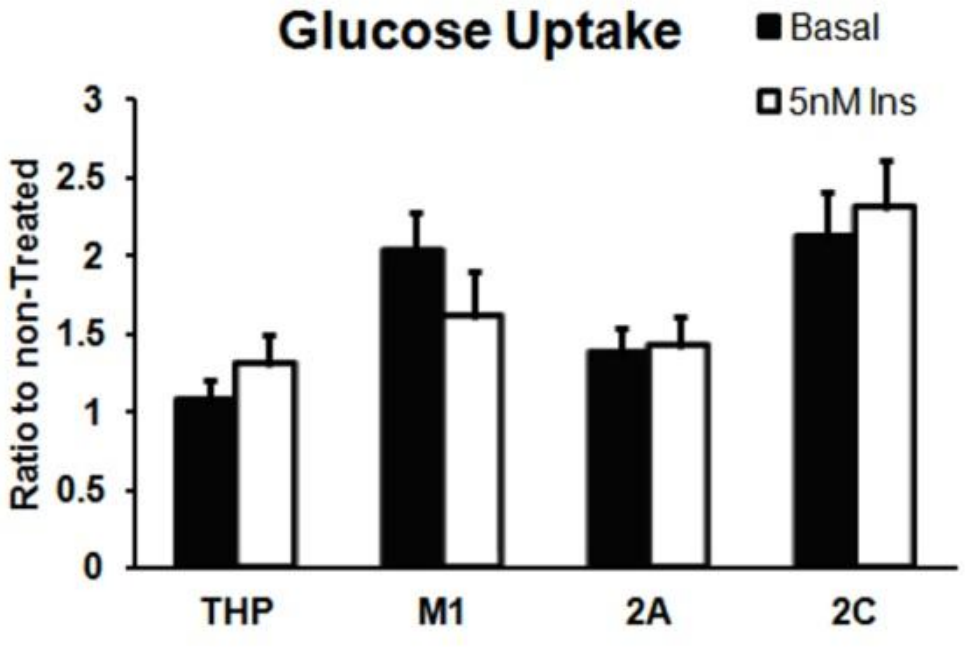

Figure 4.3 Macrophage CM after 10-12 hours of culture stimulates baseline glucose uptake (black bars). Glucose uptake with 5 nM insulin treatment (white bars) trended down for M1 CM and trended up for M2C CM. Units are the ratio of glucose uptake of the treatment over the glucose uptake of the non-treated myotube culture. Mean ± SEM, n=4

macrophage CM had no effect on basal or insulin stimulated glucose uptake (Figure 4.3).

Data for each individual are shown in Figure 4.4, to explore the possibility that the insulin sensitivity of the muscle cell donor influenced insulin-stimulated glucose uptake in response to macrophage secretory products. Insulin resistant myotubes followed our initial hypothesis; M1 CM inhibited (Figure 4.4B, dashed and dotted lines) and M2C CM enhanced (Figure 4.4D, dashed and dotted lines) insulin stimulated glucose uptake. M2A CM had a very slight positive effect (Figure 4.4C, dashed and dotted lines). By contrast, insulin sensitive myotubes either responded oppositely or did not respond to macrophage CM (Figures 4.4B-D, thin or bold solid lines). Thus, differences in sensitivity to macrophage secretory products between myotubes from different individuals may be stable *in vitro,* but appear counter to the clinical features of the cell donor.

DISCUSSION

This study examined how both classically (M1) and alternatively activated (M2A and M2C) macrophages modulate glucose uptake in human skeletal muscle-derived myotubes. *In vivo*, nearly all tissues contain resident macrophages. The results presented show that *in vitro* there is cross talk between muscle and specific macrophage subtypes, suggesting that *in vivo*,

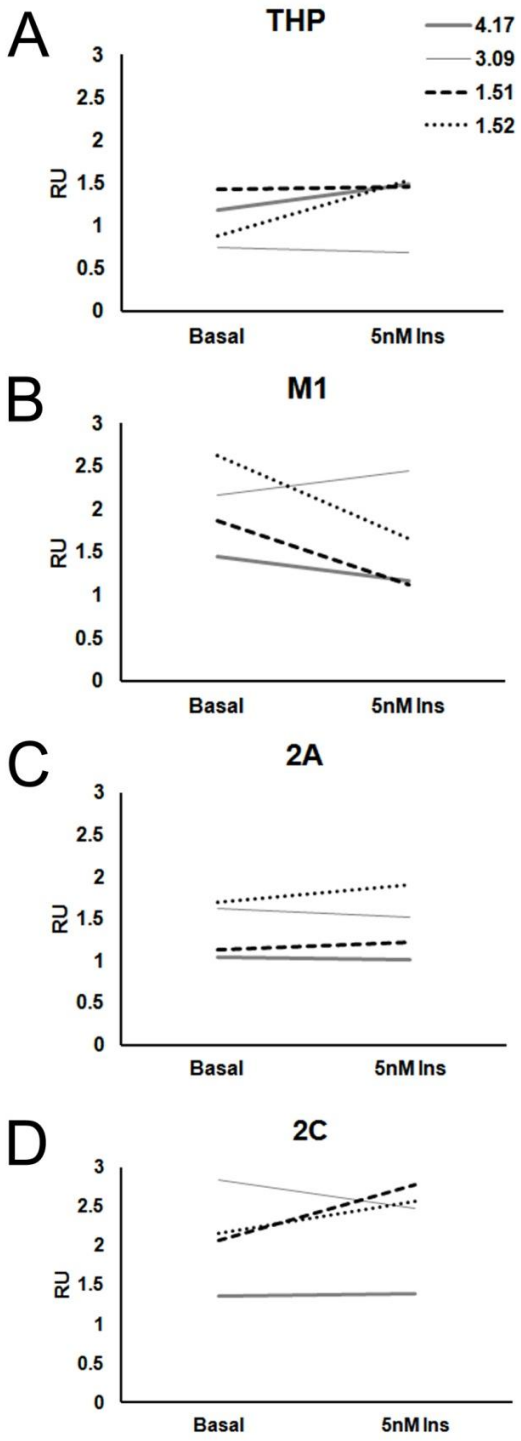

Figure 4.4 Myotubes respond differentially to macrophage CM based upon clinical features of the donor. We have designated donors by their sensitivity to insulin (S_I) value. Insulin sensitive (solid gray lines) 4.17 (bold), 3.09 (fine). Insulin resistant (broken black lines), 1.51 (dashed), 1.52 (dotted). Donor 3.09 had a BMI of 27, the other donors were clinically obese

macrophages and skeletal muscle integrate as an organ, contributing to whole body homeostasis.

Macrophages are functionally heterogeneous, with a continuum of phenotypes(108, 113). Some harbor both M1 and M2 "mixed" characteristics, similar to what we observe in our activated "M2C" macrophages *in vitro*; both inflammatory IL1β and anti-inflammatory IL10 were secreted. We found that our activation to M1 resulted in secretion of both IL1β and pleiotropic IL6. Studies have shown that IL6 secretion is induced by IL1β in epithelial cells(110, 116), and mast cells(87), or by autocrine response(92). We found IL1β to be a significant constituent in all of our activated macrophage conditioned media, so may be responsible for the induction of the IL6 secreted from the myotube cultures. Although IL10 is inhibitory to IL6 secretion(40), M2C macrophage CM contained a large amount of IL10, yet still activated IL6 production by myotubes.

Due to the overwhelming secretion of IL6 and IL10, we argue that the majority of our observations are mediated via these two cytokines.

IL6 is important in glucose homeostasis, but is pleiotropic, likely due to distinct effects of IL6 on glucose uptake in different tissues *in vivo*, which are sometimes opposite to the actions of insulin. IL6 is elevated in the blood of insulin resistant compared to healthy subjects(173, 183), suggesting a compensation for IL6 resistance in adults(167) and in type 1 diabetic children(101). Studies of recombinant human IL6 infusion in healthy humans show robust whole body glucose disposal(22) and glucose uptake by muscle

tissue(69), which were blunted in diabetic subjects. IL6 is secreted from muscle with exercise(69, 158, 165, 181) and overall appears to shunt energy stores and production throughout the body to the muscle in times of activity(90). IL6 mediated glucose uptake *in vivo* relies on intact components of the IL6 signaling cascade, including STAT3 and SOCS3, leading to robust AMPK activation and glucose uptake in skeletal muscle(93, 124). These activities are distinct from insulin; IL6 induces glucose uptake via an AMPK mediated mechanism, whereas insulin relies on the PI3K pathway to stimulate glucose transport (Chapter 1, Figure 1.1). High IL6 secreted from myotubes in response to CM may be responsible for the increase in baseline glucose uptake.

Although IL6 is normally stimulatory to glucose uptake in muscle, in adipose, it is inhibitory to glucose uptake(10) and stimulatory to lipolysis(103). Opposite to the activity of IL6 in adipose, insulin inhibits lipolysis via hormone sensitive lipase(7) and stimulates glucose uptake in adipose. Insulin's integrated activity in terms of overall homeostasis, is primarily storage of energy such as lipid and glucose and growth. Insulin secretion occurs when nutrients such as glucose rise in concentration in the blood, which induces glucose uptake in both muscle and adipose by a PI3K mediated mechanism (Chapter 1, Figure 1.1). These processes may differ in rodents compared to humans, complicating interpretation of *in vivo* studies. For instance, IL6 infusion in rodents, induces a robust hepatic insulin resistance, which does not occur in humans(148, 149, 189). Furthermore, studies from primary cells taken out of the organism are further complicated because of the absence of inputs from other organs and

peripheral tissues, which we suggest alters outcomes that were demonstrated *in vivo,* as discuss below(85).

IL6 resistance, with attenuated AMPK activation, results in inhibition of insulin stimulated glucose uptake in muscle(85). There is some evidence that IL6 dysfunction may be influenced by the activation p38 MAPK via cellular stress(26, 72, 99). Not only is IL6 sensitivity a requirement for robust induction of AMPK, promoting overall glucose uptake, but resistance to IL6 leads to aberrant downstream signaling of STAT3 and SOCS3(141). SOCS3 suppresses expression of inflammatory genes; SOCS3 deficiency or suppression promotes an M1 phenotype in human monocytes(127). There is some evidence that NO stress can damage anti-inflammatory cytokines(61), thereby de-repressing inflammatory genes. The expression of inflammatory genes is directly inhibitory to the insulin signal cascade and insulin stimulated glucose uptake. IL1β, preferentially secreted by M1 macrophages, has insulin desensitizing activity, eliciting STAT1/SOCS2-dependent ubiquitinylation of the insulin receptor substrate 1 (IRS1) and subsequent IRS1 degradation (Figure 1.3, red pathway), and concomitant activation of NF-κB and JNK inflammatory pathways(189).

There are few studies in human myotubes *in vitro* which address the role of pleotropic IL6 in insulin resistance and obesity. The IL6 gene is induced in muscle cells in response to macrophage coculture(184). Like insulin, IL6 can induce both glucose uptake and glycogen synthesis(85). The Zierath group at Karolinska, found that myotubes secreted more IL6 from T2DM donors, and had blunted glycogen synthesis and glucose uptake when stimulated with either

insulin or IL6, or both. Glycogen synthesis and glucose uptake in healthy myotubes was specifically induced two fold over baseline by the synergistic effect of both insulin and IL6, which had no effect on myotubes from T2DM donors. They went on to suggest that these observations were mechanistically due to resistance of IL6 signaling in T2DM myotubes; however, the components of insulin or IL6 signaling were only modestly stimulated, and could not explain the glucose uptake and glycogen synthesis measured in response to insulin or IL6(85). A second study by the same group showed that STAT3, a component downstream of IL6, was constitutively active in the skeletal muscle of T2DM patients(111). The Pedersen group found that distinct portions of the IL6 cascade were modified in myocytes of obese donors, and obese donors with T2DM when compared to healthy controls. The authors concluded that obese donors were IL6 receptor deficient, but in T2DM donors, the IL6 cascade was dysfunctional at downstream components STAT3 and SOCS3(141). In our myotube cultures, those from clinically insulin resistant donors appeared more sensitive to the insulin stimulated effects of CM than those from insulin sensitive subjects, arguing against IL6 mediated insulin resistance consistent with clinical features of the cell donor. We attempted to measure activation of IL6 signaling molecules in our studies of myotubes exposed to macrophage CM, but were not successful (data not shown). Clearly, this pathway must be studied in more detail in a larger number of samples to enable conclusions regarding sensitivity to IL6.

IL10 (present at significant levels only in M2C CM) induces glucose uptake in cultured rat myotubes(139). The classical view of IL10, however, is that

it is an anti-inflammatory cytokine that reverses the effects of inflammatory cytokines. IL10 inhibits TNFα gene activity(156) and IL1β secretion in human primary macrophages(61). Data on the interaction of IL6 and IL10 are sparse. In human monocyte-derived macrophages, IL6 and IL10 activate STAT3(115, 132) via a gp130 mediated mechanism(182). In classical IL6 signaling, STAT3 activates SOCS3, which is a feedback inhibitor of IL6 signaling. SOCS3 inhibits IL6 signaling by docking at a cognate pY motif on the IL6R. Constitutive SOCS3 activation results in insulin resistance(151). However, IL10 is not susceptible to SOCS3 inhibition, because SOCS3 does not interact with pY residues on the IL10R(1). It has been reported that pretreatment of macrophages with IL10 inhibited IL6 mediated STAT3 activation, but preincubation of IL6 had no effect on IL10 activation of STAT3(139). Although myotube secretion of IL6 after exposure to M2C CM was significant, we speculate that IL6-mediated STAT3 signaling should be suppressed by the SOCS3 activation afforded through IL10. The mechanism by which IL6-mediated SOCS3 is suppressed in the context of insulin resistance is not known, nor if IL10-mediated activation of SOCS3 is preserved. IL6R is down regulated in the context of obesity which may be via feedback inhibition due to greater pSTAT3 activity(141). However, if IL10- and IL6-mediated glucose uptake share the same mechanism, then IL10 mediated STAT3/SOCS signaling and subsequent glucose uptake should be preserved even in IL6 resistant myotubes. This may be the case in myotubes from insulin resistant donors that showed a trend to increase insulin stimulated glucose uptake in response to M2C macrophage CM. Myotubes from the insulin sensitive

donors in terms of insulin stimulated glucose uptake, did not respond appreciably to any CM, suggesting an overall impairment of IL6, IL10 and insulin signaling *in vitro.*

Elevated circulating free fatty acids associated with obesity may alter muscle macrophage function, which has been modeled *in vitro*. Our lab showed previously that inflammatory macrophages cocultured with myotubes inhibited myotube activation of Akt (pAkt), an important molecule in the insulin signaling cascade. Cocultures with macrophages and palmitate, a nonesterified fatty acid, potentiated the inhibition of pAkt, suggesting that macrophages and free fatty acids in combination exacerbate insulin resistance(184). A different study by the Klip lab at The Hospital for Sick Children in Toronto, also found interesting effects of lipids and macrophages on rat muscle cells(139). The model utilized L6-GLUT4myc myoblasts exposed to CM from RAW 264.7 macrophages pretreated with palmitate (CM-P) or LPS (CM-LPS). CM-P inhibited Akt phosphorylation, GLUT4 translocation, insulin-stimulated glucose uptake, and elevated inflammation markers. Conversely, CM-LPS potentiated Akt phosphorylation, GLUT4 translocation, insulin-stimulated glucose uptake, but showed no markers of inflammation. The CM-LPS had elevated IL10 levels, and IL10, potentiated insulin action in myoblasts; IL10 neutralizing antibodies partially blunted the positive influence of CM-LPS. LPS is used in our work as part of the activation regimen for inducing the M1 phenotype (see Methods), but does not result in IL10 activation and instead generates an inflammatory macrophage phenotype. The fact that Samokhvalov et al. detected IL10 from LPS treated RAW 264.7

macrophages suggests a mixed phenotype, similar to the "M2C" phenotype in our study. In conclusion, we posit that macrophage-derived cytokines in muscle, such as IL6, IL1β and IL10, interact to alter signaling in muscle fibers in different ways dependent on health status of the individual, to uniquely influence baseline or insulin stimulated glucose uptake. Future studies will be designed to dissect the signaling pathways in human myotubes leading to inflammation and insulin resistance, potentially identifying new targets for early intervention and prevention of progression to T2DM.

Chapter 5: Conclusions and possible future directions

Macrophages are important in skeletal muscle physiology and we attempted to study the human muscle cell-macrophage interaction both *in vivo* and in *vitro*. *In vivo*, we focused on the macrophage response to both aerobic and resistance exercise. We found that changes in M1 and M1/M2 macrophages abundance in response to exercise is altered by age, and that macrophage densities are uniquely correlated to expression of specific genes involved in ECM remodeling, angiogenesis, and homeostasis adaptations to exercise.

In vitro, we show that late passage myotubes activate insulin signaling pathways consistent with the clinical insulin sensitivity of the donor, but that did not extend to insulin stimulated glucose disposal. We applied different macrophage conditioned media (CM) to myotubes from donors of varied insulin sensitivity and found that myotube glucose uptake was approximately 2-fold higher following exposure to M1 or M2C macrophage CM. The M2C-activated macrophages secreted significant quantities of IL1β and IL10, suggesting a mixed M1/M2 phenotype, consistent with *in vivo* results. Insulin-stimulated glucose uptake trended inhibitory and enhancing for M1 and M2C macrophage CM, respectively, which also appeared to be influenced by the insulin sensitivity of the cell donor. Both M1 and M2C macrophage CM induced myotubes to secrete copious amounts of IL6 into the media, which may be the primary factor affecting both baseline and insulin-stimulated glucose uptake. Taken together these results suggest a functional distinction between inflammatory (M1) and

alternative macrophages (M2) in insulin resistance and exercise that is altered with age. Aging may be the primary factor in skeletal muscle health.

To our knowledge this is the first report describing a mixed phenotype of M1/M2 macrophages in human skeletal muscle. Furthermore we found an association of macrophage phenotype with expression of genes in muscle involved in ECM remodeling and angiogenesis in the context of aging, that may impact overall health status. Over the years, the view on the physiology of ECM has evolved. The old view was ECM was solely structural; however, relatively recent discoveries have uncovered that ECM is also a powerful signaling arena, that communicates with surrounding cells and to other peripheral organs and tissues. Moreover, the interactions with healthy or aged ECM may influence the phenotype of tissue resident macrophages, and affect the insulin signaling or exercise response of the muscle. These discoveries suggest ECM is a novel target for pharmacotherapeutics that may influence aging and insulin resistance in muscle. Lastly, exercise effects on the older subjects were blunted; perhaps some kind of cotherapy, such as massage, with exercise may allow older subjects to better gain the beneficial effect of exercise.

Our laboratory specifically studies muscle aging and insulin resistance. Although inflammatory macrophages were elevated with obesity in muscle, the macrophage response to exercise was not correlated to BMI or insulin sensitivity. On the other hand, when grouped by age, exercise response differed, suggesting that aging has more impact on muscle-macrophage interplay than obesity. There is some evidence that macrophages themselves age. Additionally the substrates

macrophages process in the aged environment may be damaged, due to reactive species elevation and decrease in buffering capacity that has been reported in the aged(122). This theory may explain the elevation in macrophages we reported for the older age group in response to aerobic exercise training. In this theory, a greater number of macrophages infiltrate the muscle in older individuals in response to exercise, because they are less effective and increase their population as a compensatory mechanism. To address these ideas experiments could be designed to collect human monocytes from aged or young people, and apply these monocytes in equal densities across experiments to control collagen, and collagen which has been exposed to H_20_2 which will cause adducts by superoxide radicals. The cells can be collected, lysed and enzyme assays for matrix metalloproteinase and westerns for collagen cleavage products, normalized to total proteins, can be performed. Additionally, the phenotype of adhering monocytes can be assessed at the mRNA level and cytokine secretion into the media quantified, normalized to total protein from the plate. Careful attention should be given to genes such as SPARC. Chemotaxis on adducted collagen could be measured for old and young macrophages. In this way we can test the efficacy of old and young macrophages on control and adducted substrates, verifying the aged macrophage and/or damaged substrate hypothesis.

In myotubes *in vitro*, loss of input from other organs and tissues (liver, adipose, nerves, pancreas, bone marrow), limits the cues that contribute to normal muscle glucose uptake *in vivo*. Possibly epigenetic silencing of muscle

genes occurs progressively over time, which is derepressed by those inputs. Among those missing inputs is the vasculature, specifically endothelial cells. Our analysis of gene expression suggested that angiogenesis and macrophage function are linked. Further, endothelial cells are a robust source of NO in muscle. NO is an important acute signaling molecule which modifies the dilatation of smooth muscle, an important adaptation to exercise, but has also been suggested to affect glucose uptake. It has been reported that sodium nitroprusside (an NO agonist) administration in skeletal muscle cell cultures *in vitro* (74) and *in vivo* (75) induces glucose uptake. Taken together these findings suggest that NO may be an important signaling molecule that induces exercise stimulated glucose uptake. Additionally we have shown in this report that nitrotyrosine (NY), an adduct resulting from the production of NO radicals, differs in subjects by age in response to exercise. It is not known how NO radicals affect exercise-stimulated glucose uptake during muscle aging and should be explored. Lastly, macrophages are important mediators of muscle adaptation in the response to exercise. It is not known what role NO or NY adducts have on the macrophage and myofiber/satellite cell interactions. Impaired signaling or NY adducts themselves may be inhibitory to macrophages or muscle cells when trying to mount the hypertrophic response. Future studies should explore the possibility that addition of sodium nitroprusside may restore normal glucose uptake response in myotubes.

REFERENCES

1. **Ahmed ST and Ivashkiv LB.** Inhibition of IL-6 and IL-10 signaling and Stat activation by inflammatory and stress pathways. *J Immunol* 165: 5227-5237, 2000.
2. **Alkhateeb H, Chabowski A, Glatz JF, Luiken JF, and Bonen A.** Two phases of palmitate-induced insulin resistance in skeletal muscle: impaired GLUT4 translocation is followed by a reduced GLUT4 intrinsic activity. *Am J Physiol Endocrinol Metab* 293: E783-793, 2007.
3. **Amara CE, Shankland EG, Jubrias SA, Marcinek DJ, Kushmerick MJ, and Conley KE.** Mild mitochondrial uncoupling impacts cellular aging in human muscles in vivo. *Proc Natl Acad Sci U S A* 104: 1057-1062, 2007.
4. **Amaral SL, Papanek PE, and Greene AS.** Angiotensin II and VEGF are involved in angiogenesis induced by short-term exercise training. *Am J Physiol Heart Circ Physiol* 281: H1163-1169, 2001.
5. **Arkan MC, Hevener AL, Greten FR, Maeda S, Li ZW, Long JM, Wynshaw-Boris A, Poli G, Olefsky J, and Karin M.** IKK-beta links inflammation to obesity-induced insulin resistance. *Nat Med* 11: 191-198, 2005.
6. **Arnold L, Henry A, Poron F, Baba-Amer Y, van Rooijen N, Plonquet A, Gherardi RK, and Chazaud B.** Inflammatory monocytes recruited after skeletal muscle injury switch into antiinflammatory macrophages to support myogenesis. *J Exp Med* 204: 1057-1069, 2007.
7. **Badin PM, Vila IK, Louche K, Mairal A, Marques MA, Bourlier V, Tavernier G, Langin D, and Moro C.** High-fat diet-mediated lipotoxicity and insulin resistance is related to impaired lipase expression in mouse skeletal muscle. *Endocrinology* 154: 1444-1453, 2013.
8. **Banerjee P, Caulfield B, Crowe L, and Clark A.** Prolonged electrical muscle stimulation exercise improves strength and aerobic capacity in healthy sedentary adults. *J Appl Physiol (1985)* 99: 2307-2311, 2005.
9. **Bartke A and Westbrook R.** Metabolic characteristics of long-lived mice. *Front Genet* 3: 288, 2012.
10. **Bastard JP, Maachi M, Van Nhieu JT, Jardel C, Bruckert E, Grimaldi A, Robert JJ, Capeau J, and Hainque B.** Adipose tissue IL-6 content correlates with resistance to insulin activation of glucose uptake both in vivo and in vitro. *J Clin Endocrinol Metab* 87: 2084-2089, 2002.
11. **Berkes CA and Tapscott SJ.** MyoD and the transcriptional control of myogenesis. *SeminCell Dev Biol* 16: 585-595, 2005.
12. **Betik AC, Thomas MM, Wright KJ, Riel CD, and Hepple RT.** Exercise training from late middle age until senescence does not attenuate the declines in skeletal muscle aerobic function. *Am J Physiol Regul Integr Comp Physiol* 297: R744-755, 2009.

13. **Biddinger SB and Kahn CR.** From mice to men: insights into the insulin resistance syndromes. *Annu Rev Physiol* 68: 123-158, 2006.

14. **Bilan PJ, Samokhvalov V, Koshkina A, Schertzer JD, Samaan MC, and Klip A.** Direct and macrophage-mediated actions of fatty acids causing insulin resistance in muscle cells. *Arch Physiol Biochem* 115: 176-190, 2009.
15. **Bluestone JA and Abbas AK.** Natural versus adaptive regulatory T cells. *Nat Rev Immunol* 3: 253-257, 2003.
16. **Bodles AM, Varma V, Yao-Borengasser A, Phanavanh B, Peterson CA, McGehee RE, Jr., Rasouli N, Wabitsch M, and Kern PA.** Pioglitazone induces apoptosis of macrophages in human adipose tissue. *J Lipid Res* 47: 2080-2088, 2006.
17. **Bouzakri K, Koistinen HA, and Zierath JR.** Molecular mechanisms of skeletal muscle insulin resistance in type 2 diabetes. *Curr Diabetes Rev* 1: 167-174, 2005.
18. **Bradshaw AD.** Diverse biological functions of the SPARC family of proteins. *Int J Biochem Cell Biol* 44: 480-488, 2012.
19. **Bradshaw AD.** The role of SPARC in extracellular matrix assembly. *J Cell Commun Signal* 3: 239-246, 2009.
20. **Bradshaw AD and Sage EH.** SPARC, a matricellular protein that functions in cellular differentiation and tissue response to injury. *J Clin Invest* 107: 1049-1054, 2001.
21. **Brooks SV, Vasilaki A, Larkin LM, McArdle A, and Jackson MJ.** Repeated bouts of aerobic exercise lead to reductions in skeletal muscle free radical generation and nuclear factor kappaB activation. *J Physiol* 586: 3979-3990, 2008.
22. **Carey AL, Steinberg GR, Macaulay SL, Thomas WG, Holmes AG, Ramm G, Prelovsek O, Hohnen-Behrens C, Watt MJ, James DE, Kemp BE, Pedersen BK, and Febbraio MA.** Interleukin-6 increases insulin-stimulated glucose disposal in humans and glucose uptake and fatty acid oxidation in vitro via AMP-activated protein kinase. *Diabetes* 55: 2688-2697, 2006.
23. **Carmichael MD, Davis JM, Murphy EA, Carson JA, Van Rooijen N, Mayer E, and Ghaffar A.** Role of brain macrophages on IL-1beta and fatigue following eccentric exercise-induced muscle damage. *Brain Behav Immun* 24: 564-568, 2010.
24. **Cartee GD.** Influence of age on skeletal muscle glucose transport and glycogen metabolism. *Med Sci Sports Exerc* 26: 577-585, 1994.
25. **Chan WK, Cheung CC, Law HK, Lau YL, and Chan GC.** Ganoderma lucidum polysaccharides can induce human monocytic leukemia cells into dendritic cells with immuno-stimulatory function. *J Hematol Oncol* 1: 9, 2008.
26. **Chaves de Souza JA, Nogueira AV, Chaves de Souza PP, Kim YJ, Silva Lobo C, Pimentel Lopes de Oliveira GJ, Cirelli JA, Garlet GP, and Rossa C, Jr.** SOCS3 expression correlates with severity of inflammation, expression of proinflammatory cytokines, and activation of STAT3 and p38 MAPK in LPS-induced inflammation in vivo. *Mediators Inflamm* 2013: 650812, 2013.
27. **Chazaud B.** Macrophages: Supportive cells for tissue repair and regeneration. *Immunobiology*, 2013.

28. **Chazaud B, Brigitte M, Yacoub-Youssef H, Arnold L, Gherardi R, Sonnet C, Lafuste P, and Chretien F.** Dual and beneficial roles of macrophages during skeletal muscle regeneration. *Exerc Sport Sci Rev* 37: 18-22, 2009.
29. **Chazaud B, Chretien F, and Gherardi RK.** [Macrophages regulate skeletal muscle regeneration]. *Med Sci (Paris)* 23: 794-795, 2007.
30. **Ciaraldi TP, Abrams L, Nikoulina S, Mudaliar S, and Henry RR.** Glucose transport in cultured human skeletal muscle cells. Regulation by insulin and glucose in nondiabetic and non-insulin-dependent diabetes mellitus subjects. *J Clin Invest* 96: 2820-2827, 1995.
31. **Clahsen T and Schaper F.** Interleukin-6 acts in the fashion of a classical chemokine on monocytic cells by inducing integrin activation, cell adhesion, actin polymerization, chemotaxis, and transmigration. *J Leukoc Biol* 84: 1521-1529, 2008.
32. **Close GL, Ashton T, Cable T, Doran D, and MacLaren DP.** Eccentric exercise, isokinetic muscle torque and delayed onset muscle soreness: the role of reactive oxygen species. *Eur J Appl Physiol* 91: 615-621, 2004.
33. **Coelho Horta B, Steinberg Perilo C, Caldeira Costa D, Nogueira-Machado JA, and Martins Chaves M.** Aging: functional metabolic balance among cAMP, cGMP and reactive oxygen intermediate generation by human granulocytes. *Gerontology* 51: 363-368, 2005.
34. **Conley KE, Amara CE, Jubrias SA, and Marcinek DJ.** Mitochondrial function, fibre types and ageing: new insights from human muscle in vivo. *Exp Physiol* 92: 333-339, 2007.
35. **Conley KE, Marcinek DJ, and Villarin J.** Mitochondrial dysfunction and age. *Curr Opin Clin Nutr Metab Care* 10: 688-692, 2007.
36. **Contreras-Shannon V, Ochoa O, Reyes-Reyna SM, Sun D, Michalek JE, Kuziel WA, McManus LM, and Shireman PK.** Fat accumulation with altered inflammation and regeneration in skeletal muscle of CCR2-/- mice following ischemic injury. *Am J Physiol Cell Physiol* 292: C953-967, 2007.
37. **Cossu G and Biressi S.** Satellite cells, myoblasts and other occasional myogenic progenitors: possible origin, phenotypic features and role in muscle regeneration. *Semin Cell Dev Biol* 16: 623-631, 2005.
38. **Cousins JC, Woodward KJ, Gross JG, Partridge TA, and Morgan JE.** Regeneration of skeletal muscle from transplanted immortalised myoblasts is oligoclonal. *J Cell Sci* 117: 3259-3269, 2004.
39. **Cozzone D, Frojdo S, Disse E, Debard C, Laville M, Pirola L, and Vidal H.** Isoform-specific defects of insulin stimulation of Akt/protein kinase B (PKB) in skeletal muscle cells from type 2 diabetic patients. *Diabetologia* 51: 512-521, 2008.
40. **Dagvadorj J, Naiki Y, Tumurkhuu G, Noman AS, Iftekar EKI, Koide N, Komatsu T, Yoshida T, and Yokochi T.** Interleukin (IL)-10 attenuates lipopolysaccharide-induced IL-6 production via inhibition of IkappaB-zeta activity by Bcl-3. *Innate Immun* 15: 217-224, 2009.
41. **Daynes RA, Araneo BA, Ershler WB, Maloney C, Li GZ, and Ryu SY.** Altered regulation of IL-6 production with normal aging. Possible linkage to the

age-associated decline in dehydroepiandrosterone and its sulfated derivative. *J Immunol* 150: 5219-5230, 1993.
42. **Dean RT, Gebicki J, Gieseg S, Grant AJ, and Simpson JA.** Hypothesis: a damaging role in aging for reactive protein oxidation products? *Mutat Res* 275: 387-393, 1992.
43. **Delaporte C, Dautreaux B, and Fardeau M.** Human myotube differentiation in vitro in different culture conditions. *Biol Cell* 57: 17-22, 1986.
44. **Dennis RA, Przybyla B, Gurley C, Kortebein PM, Simpson P, Sullivan DH, and Peterson CA.** Aging alters gene expression of growth and remodeling factors in human skeletal muscle both at rest and in response to acute resistance exercise. *Physiol Genomics* 32: 393-400, 2008.
45. **Dennis RA, Trappe TA, Simpson P, Carroll C, Huang BE, Nagarajan R, Bearden E, Gurley C, Duff GW, Evans WJ, Kornman K, and Peterson CA.** Interleukin-1 polymorphisms are associated with the inflammatory response in human muscle to acute resistance exercise. *J Physiol* 560: 617-626, 2004.
46. **Dennis RA, Zhu H, Kortebein PM, Bush HM, Harvey JF, Sullivan DH, and Peterson CA.** Muscle expression of genes associated with inflammation, growth, and remodeling is strongly correlated in older adults with resistance training outcomes. *Physiol Genomics* 38: 169-175, 2009.
47. **Dhawan J and Rando TA.** Stem cells in postnatal myogenesis: molecular mechanisms of satellite cell quiescence, activation and replenishment. *Trends Cell Biol* 15: 666-673, 2005.
48. **Di Gregorio GB, Yao-Borengasser A, Rasouli N, Varma V, Lu T, Miles LM, Ranganathan G, Peterson CA, McGehee RE, and Kern PA.** Expression of CD68 and macrophage chemoattractant protein-1 genes in human adipose and muscle tissues: association with cytokine expression, insulin resistance, and reduction by pioglitazone. *Diabetes* 54: 2305-2313, 2005.
49. **DiPasquale DM, Cheng M, Billich W, Huang SA, van Rooijen N, Hornberger TA, and Koh TJ.** Urokinase-type plasminogen activator and macrophages are required for skeletal muscle hypertrophy in mice. *Am J Physiol Cell Physiol* 293: C1278-1285, 2007.
50. **Donges CE, Burd NA, Duffield R, Smith GC, West DW, Short MJ, Mackenzie R, Plank LD, Shepherd PR, Phillips SM, and Edge JA.** Concurrent resistance and aerobic exercise stimulates both myofibrillar and mitochondrial protein synthesis in sedentary middle-aged men. *J Appl Physiol (1985)* 112: 1992-2001, 2012.
51. **Du JH, Xu N, Song Y, Xu M, Lu ZZ, Han C, and Zhang YY.** AICAR stimulates IL-6 production via p38 MAPK in cardiac fibroblasts in adult mice: a possible role for AMPK. *Biochem Biophys Res Commun* 337: 1139-1144, 2005.
52. **Dumont N and Frenette J.** Macrophages protect against muscle atrophy and promote muscle recovery in vivo and in vitro: a mechanism partly dependent on the insulin-like growth factor-1 signaling molecule. *Am J Pathol* 176: 2228-2235, 2010.
53. **Eckardt K, Taube A, and Eckel J.** Obesity-associated insulin resistance in skeletal muscle: role of lipid accumulation and physical inactivity. *Rev Endocr Metab Disord* 12: 163-172, 2011.

54. **Elmore S.** Apoptosis: a review of programmed cell death. *Toxicol Pathol* 35: 495-516, 2007.
55. **Ferreira JC, Bacurau AV, Bueno CR, Jr., Cunha TC, Tanaka LY, Jardim MA, Ramires PR, and Brum PC.** Aerobic exercise training improves Ca2+ handling and redox status of skeletal muscle in mice. *Exp Biol Med (Maywood)* 235: 497-505, 2010.
56. **Fielding RA and Evans WJ.** Aging and the acute phase response to exercise: implications for the role of systemic factors on skeletal muscle protein turnover. *Int J Sports Med* 18 Suppl 1: S22-27, 1997.
57. **Fink LN, Costford SR, Lee YS, Jensen TE, Bilan PJ, Oberbach A, Bluher M, Olefsky JM, Sams A, and Klip A.** Pro-Inflammatory macrophages increase in skeletal muscle of high fat-Fed mice and correlate with metabolic risk markers in humans. *Obesity (Silver Spring)*, 2013.
58. **Fink LN, Oberbach A, Costford SR, Chan KL, Sams A, Bluher M, and Klip A.** Expression of anti-inflammatory macrophage genes within skeletal muscle correlates with insulin sensitivity in human obesity and type 2 diabetes. *Diabetologia* 56: 1623-1628, 2013.
59. **Fleming TH, Humpert PM, Nawroth PP, and Bierhaus A.** Reactive metabolites and AGE/RAGE-mediated cellular dysfunction affect the aging process: a mini-review. *Gerontology* 57: 435-443, 2011.
60. **Frangogiannis NG.** Matricellular proteins in cardiac adaptation and disease. *Physiol Rev* 92: 635-688, 2012.
61. **Freels JL, Nelson DK, Hoyt JC, Habib M, Numanami H, Lantz RC, and Robbins RA.** Enhanced activity of human IL-10 after nitration in reducing human IL-1 production by stimulated peripheral blood mononuclear cells. *J Immunol* 169: 4568-4571, 2002.
62. **Fujisaka S, Usui I, Bukhari A, Ikutani M, Oya T, Kanatani Y, Tsuneyama K, Nagai Y, Takatsu K, Urakaze M, Kobayashi M, and Tobe K.** Regulatory mechanisms for adipose tissue M1 and M2 macrophages in diet-induced obese mice. *Diabetes* 58: 2574-2582, 2009.
63. **Geng T, Li P, Okutsu M, Yin X, Kwek J, Zhang M, and Yan Z.** PGC-1alpha plays a functional role in exercise-induced mitochondrial biogenesis and angiogenesis but not fiber-type transformation in mouse skeletal muscle. *Am J Physiol Cell Physiol* 298: C572-579, 2010.
64. **Green CJ, Bunprajun T, Pedersen BK, and Scheele C.** Physical activity is associated with retained muscle metabolism in human myotubes challenged with palmitate. *J Physiol* 591: 4621-4635, 2013.
65. **Gustafsson T and Kraus WE.** Exercise-induced angiogenesis-related growth and transcription factors in skeletal muscle, and their modification in muscle pathology. *Front Biosci* 6: D75-89, 2001.
66. **Gustafsson T, Puntschart A, Kaijser L, Jansson E, and Sundberg CJ.** Exercise-induced expression of angiogenesis-related transcription and growth factors in human skeletal muscle. *Am J Physiol* 276: H679-685, 1999.
67. **Hawrylowicz CM and O'Garra A.** Potential role of interleukin-10-secreting regulatory T cells in allergy and asthma. *Nat Rev Immunol* 5: 271-283, 2005.

68. **Heilbronn LK and Campbell LV.** Adipose tissue macrophages, low grade inflammation and insulin resistance in human obesity. *Curr Pharm Des* 14: 1225-1230, 2008.
69. **Helge JW, Stallknecht B, Pedersen BK, Galbo H, Kiens B, and Richter EA.** The effect of graded exercise on IL-6 release and glucose uptake in human skeletal muscle. *J Physiol* 546: 299-305, 2003.
70. **Hellman B.** [Insulin biosynthesis, storage and secretion. 13. The possibility of local regulation of the insulin secretion by factors in the immediate environment of the beta-cells]. *Lakartidningen* 65: 3618-3621, 1968.
71. **Hellman B and Westman S.** Palmitate Utilization in Obese-Hyperglycemic Mice. In Vitro Studies of Epididymal Adipose Tissue and Liver. *Acta Physiol Scand* 61: 65-72, 1964.
72. **Henriksen EJ, Diamond-Stanic MK, and Marchionne EM.** Oxidative stress and the etiology of insulin resistance and type 2 diabetes. *Free Radic Biol Med* 51: 993-999, 2011.
73. **Henry RR, Abrams L, Nikoulina S, and Ciaraldi TP.** Insulin action and glucose metabolism in nondiabetic control and NIDDM subjects. Comparison using human skeletal muscle cell cultures. *Diabetes* 44: 936-946, 1995.
74. **Henstridge DC, Drew BG, Formosa MF, Natoli AK, Cameron-Smith D, Duffy SJ, and Kingwell BA.** The effect of the nitric oxide donor sodium nitroprusside on glucose uptake in human primary skeletal muscle cells. *Nitric Oxide* 21: 126-131, 2009.
75. **Henstridge DC, Kingwell BA, Formosa MF, Drew BG, McConell GK, and Duffy SJ.** Effects of the nitric oxide donor, sodium nitroprusside, on resting leg glucose uptake in patients with type 2 diabetes. *Diabetologia* 48: 2602-2608, 2005.
76. **Hevener AL, Olefsky JM, Reichart D, Nguyen MT, Bandyopadyhay G, Leung HY, Watt MJ, Benner C, Febbraio MA, Nguyen AK, Folian B, Subramaniam S, Gonzalez FJ, Glass CK, and Ricote M.** Macrophage PPAR gamma is required for normal skeletal muscle and hepatic insulin sensitivity and full antidiabetic effects of thiazolidinediones. *J Clin Invest* 117: 1658-1669, 2007.
77. **Holloway GP, Bezaire V, Heigenhauser GJ, Tandon NN, Glatz JF, Luiken JJ, Bonen A, and Spriet LL.** Mitochondrial long chain fatty acid oxidation, fatty acid translocase/CD36 content and carnitine palmitoyltransferase I activity in human skeletal muscle during aerobic exercise. *J Physiol* 571: 201-210, 2006.
78. **Hong EG, Ko HJ, Cho YR, Kim HJ, Ma Z, Yu TY, Friedline RH, Kurt-Jones E, Finberg R, Fischer MA, Granger EL, Norbury CC, Hauschka SD, Philbrick WM, Lee CG, Elias JA, and Kim JK.** Interleukin-10 prevents diet-induced insulin resistance by attenuating macrophage and cytokine response in skeletal muscle. *Diabetes* 58: 2525-2535, 2009.
79. **Huang ES, Basu A, O'Grady M, and Capretta JC.** Projecting the future diabetes population size and related costs for the U.S. *Diabetes Care* 32: 2225-2229, 2009.
80. **Ikeda SI, Tamura Y, Kakehi S, Takeno K, Kawaguchi M, Watanabe T, Sato F, Ogihara T, Kanazawa A, Fujitani Y, Kawamori R, and Watada H.**

Exercise-induced enhancement of insulin sensitivity is associated with accumulation of M2-polarized macrophages in mouse skeletal muscle. *Biochem Biophys Res Commun*, 2013.
81. **Iwase H, Kobayashi M, Nakajima M, and Takatori T.** The ratio of insulin to C-peptide can be used to make a forensic diagnosis of exogenous insulin overdosage. *Forensic Sci Int* 115: 123-127, 2001.
82. **Jackson MJ.** Microdialysis as a window on interstitial reactive oxygen species in human tissues? A commentary on "Antioxidant supplementation enhances the exercise-induced increase in mitochondrial uncoupling protein 3 and endothelial nitric oxide synthase mRNA content in human skeletal muscle," by Hellsten et al. *Free Radic Biol Med* 43: 351-352, 2007.
83. **Jackson MJ.** Reactive oxygen species and redox-regulation of skeletal muscle adaptations to exercise. *Philos Trans R Soc Lond B Biol Sci* 360: 2285-2291, 2005.
84. **Jeejeebhoy KN.** Malnutrition, fatigue, frailty, vulnerability, sarcopenia and cachexia: overlap of clinical features. *Curr Opin Clin Nutr Metab Care* 15: 213-219, 2012.
85. **Jiang LQ, Duque-Guimaraes DE, Machado UF, Zierath JR, and Krook A.** Altered response of skeletal muscle to IL-6 in type 2 diabetic patients. *Diabetes* 62: 355-361, 2013.
86. **Kahn SE, Hull RL, and Utzschneider KM.** Mechanisms linking obesity to insulin resistance and type 2 diabetes. *Nature* 444: 840-846, 2006.
87. **Kandere-Grzybowska K, Letourneau R, Kempuraj D, Donelan J, Poplawski S, Boucher W, Athanassiou A, and Theoharides TC.** IL-1 induces vesicular secretion of IL-6 without degranulation from human mast cells. *J Immunol* 171: 4830-4836, 2003.
88. **Karnieli E, Hissin PJ, Simpson IA, Salans LB, and Cushman SW.** A possible mechanism of insulin resistance in the rat adipose cell in streptozotocin-induced diabetes mellitus. Depletion of intracellular glucose transport systems. *J Clin Invest* 68: 811-814, 1981.
89. **Kawanishi N, Kato K, Takahashi M, Mizokami T, Otsuka Y, Imaizumi A, Shiva D, Yano H, and Suzuki K.** Curcumin attenuates oxidative stress following downhill running-induced muscle damage. *Biochem Biophys Res Commun*, 2013.
90. **Keller C, Keller P, Marshal S, and Pedersen BK.** IL-6 gene expression in human adipose tissue in response to exercise--effect of carbohydrate ingestion. *J Physiol* 550: 927-931, 2003.
91. **Keller C, Steensberg A, Pilegaard H, Osada T, Saltin B, Pedersen BK, and Neufer PD.** Transcriptional activation of the IL-6 gene in human contracting skeletal muscle: influence of muscle glycogen content. *FASEB J* 15: 2748-2750, 2001.
92. **Keller P, Keller C, Carey AL, Jauffred S, Fischer CP, Steensberg A, and Pedersen BK.** Interleukin-6 production by contracting human skeletal muscle: autocrine regulation by IL-6. *Biochem Biophys Res Commun* 310: 550-554, 2003.

93. **Kelly M, Keller C, Avilucea PR, Keller P, Luo Z, Xiang X, Giralt M, Hidalgo J, Saha AK, Pedersen BK, and Ruderman NB.** AMPK activity is diminished in tissues of IL-6 knockout mice: the effect of exercise. *Biochem Biophys Res Commun* 320: 449-454, 2004.
94. **Kim JH, Kim JE, Liu HY, Cao W, and Chen J.** Regulation of interleukin-6-induced hepatic insulin resistance by mammalian target of rapamycin through the STAT3-SOCS3 pathway. *J Biol Chem* 283: 708-715, 2008.
95. **Kimball SR, Farrell PA, and Jefferson LS.** Invited Review: Role of insulin in translational control of protein synthesis in skeletal muscle by amino acids or exercise. *J Appl Physiol (1985)* 93: 1168-1180, 2002.
96. **Konopka AR, Suer MK, Wolff CA, and Harber MP.** Markers of Human Skeletal Muscle Mitochondrial Biogenesis and Quality Control: Effects of Age and Aerobic Exercise Training. *J Gerontol A Biol Sci Med Sci*, 2013.
97. **Lea RG, Riley SC, Antipatis C, Hannah L, Ashworth CJ, Clark DA, and Critchley HO.** Cytokines and the regulation of apoptosis in reproductive tissues: a review. *Am J Reprod Immunol* 42: 100-109, 1999.
98. **Lesault PF, Theret M, Magnan M, Cuvellier S, Niu Y, Gherardi RK, Tremblay JP, Hittinger L, and Chazaud B.** Macrophages improve survival, proliferation and migration of engrafted myogenic precursor cells into MDX skeletal muscle. *PLoS One* 7: e46698, 2012.
99. **Liu Z and Cao W.** p38 mitogen-activated protein kinase: a critical node linking insulin resistance and cardiovascular diseases in type 2 diabetes mellitus. *Endocr Metab Immune Disord Drug Targets* 9: 38-46, 2009.
100. **Lloyd PG, Prior BM, Li H, Yang HT, and Terjung RL.** VEGF receptor antagonism blocks arteriogenesis, but only partially inhibits angiogenesis, in skeletal muscle of exercise-trained rats. *Am J Physiol Heart Circ Physiol* 288: H759-768, 2005.
101. **Lo HC, Lin SC, and Wang YM.** The relationship among serum cytokines, chemokine, nitric oxide, and leptin in children with type 1 diabetes mellitus. *Clin Biochem* 37: 666-672, 2004.
102. **Lumeng CN, Bodzin JL, and Saltiel AR.** Obesity induces a phenotypic switch in adipose tissue macrophage polarization. *J Clin Invest* 117: 175-184, 2007.
103. **Lyngso D, Simonsen L, and Bulow J.** Interleukin-6 production in human subcutaneous abdominal adipose tissue: the effect of exercise. *J Physiol* 543: 373-378, 2002.
104. **Mackey AL, Bojsen-Moller J, Qvortrup K, Langberg H, Suetta C, Kalliokoski KK, Kjaer M, and Magnusson SP.** Evidence of skeletal muscle damage following electrically stimulated isometric muscle contractions in humans. *J Appl Physiol (1985)* 105: 1620-1627, 2008.
105. **Malm C, Nyberg P, Engstrom M, Sjodin B, Lenkei R, Ekblom B, and Lundberg I.** Immunological changes in human skeletal muscle and blood after eccentric exercise and multiple biopsies. *J Physiol* 529 Pt 1: 243-262, 2000.
106. **Malm C, Sjodin TL, Sjoberg B, Lenkei R, Renstrom P, Lundberg IE, and Ekblom B.** Leukocytes, cytokines, growth factors and hormones in human

skeletal muscle and blood after uphill or downhill running. *J Physiol* 556: 983-1000, 2004.
107. **Manning BD and Cantley LC.** AKT/PKB signaling: navigating downstream. *Cell* 129: 1261-1274, 2007.
108. **Mantovani A, Sica A, Sozzani S, Allavena P, Vecchi A, and Locati M.** The chemokine system in diverse forms of macrophage activation and polarization. *Trends Immunol* 25: 677-686, 2004.
109. **Martinez CO, McHale MJ, Wells JT, Ochoa O, Michalek JE, McManus LM, and Shireman PK.** Regulation of skeletal muscle regeneration by CCR2-activating chemokines is directly related to macrophage recruitment. *Am J Physiol Regul Integr Comp Physiol* 299: R832-842, 2010.
110. **Mascarenhas JO, Goodrich ME, Eichelberger H, and McGee DW.** Polarized secretion of IL-6 by IEC-6 intestinal epithelial cells: differential effects of IL-1 beta and TNF-alpha. *Immunol Invest* 25: 333-340, 1996.
111. **Mashili F, Chibalin AV, Krook A, and Zierath JR.** Constitutive STAT3 phosphorylation contributes to skeletal muscle insulin resistance in type 2 diabetes. *Diabetes* 62: 457-465, 2013.
112. **McLennan IS.** Degenerating and regenerating skeletal muscles contain several subpopulations of macrophages with distinct spatial and temporal distributions. *J Anat* 188 (Pt 1): 17-28, 1996.
113. **Mosser DM and Edwards JP.** Exploring the full spectrum of macrophage activation. *Nat Rev Immunol* 8: 958-969, 2008.
114. **Netea MG, Lewis EC, Azam T, Joosten LA, Jaekal J, Bae SY, Dinarello CA, and Kim SH.** Interleukin-32 induces the differentiation of monocytes into macrophage-like cells. *Proc Natl Acad Sci U S A* 105: 3515-3520, 2008.
115. **Niemand C, Nimmesgern A, Haan S, Fischer P, Schaper F, Rossaint R, Heinrich PC, and Muller-Newen G.** Activation of STAT3 by IL-6 and IL-10 in primary human macrophages is differentially modulated by suppressor of cytokine signaling 3. *J Immunol* 170: 3263-3272, 2003.
116. **O'Shaughnessy C, Prosser E, Keane T, and O'Neill L.** Differential stimulation of IL-6 secretion following apical and basolateral presentation of IL-1 on epithelial cell lines. *Biochem Soc Trans* 24: 83S, 1996.
117. **Ochoa O, Sun D, Reyes-Reyna SM, Waite LL, Michalek JE, McManus LM, and Shireman PK.** Delayed angiogenesis and VEGF production in CCR2-/- mice during impaired skeletal muscle regeneration. *Am J Physiol Regul Integr Comp Physiol* 293: R651-661, 2007.
118. **Olefsky JM and Glass CK.** Macrophages, inflammation, and insulin resistance. *Annu Rev Physiol* 72: 219-246, 2010.
119. **Park JY, Wang PY, Matsumoto T, Sung HJ, Ma W, Choi JW, Anderson SA, Leary SC, Balaban RS, Kang JG, and Hwang PM.** p53 improves aerobic exercise capacity and augments skeletal muscle mitochondrial DNA content. *Circ Res* 105: 705-712, 711 p following 712, 2009.
120. **Paulsen G, Egner I, Raastad T, Reinholt F, Owe S, Lauritzen F, Brorson SH, and Koskinen S.** Inflammatory markers CD11b, CD16, CD66b,

CD68, myeloperoxidase and neutrophil elastase in eccentric exercised human skeletal muscles. *Histochem Cell Biol* 139: 691-715, 2013.
121. **Peake J, Della Gatta P, and Cameron-Smith D.** Aging and its effects on inflammation in skeletal muscle at rest and following exercise-induced muscle injury. *Am J Physiol Regul Integr Comp Physiol* 298: R1485-1495.
122. **Peake J, Della Gatta P, and Cameron-Smith D.** Aging and its effects on inflammation in skeletal muscle at rest and following exercise-induced muscle injury. *Am J Physiol Regul Integr Comp Physiol* 298: R1485-1495, 2010.
123. **Peake J, Nosaka K, and Suzuki K.** Characterization of inflammatory responses to eccentric exercise in humans. *Exerc Immunol Rev* 11: 64-85, 2005.
124. **Pedersen BK.** IL-6 signalling in exercise and disease. *Biochem Soc Trans* 35: 1295-1297, 2007.
125. **Pedersen M, Steensberg A, Keller C, Osada T, Zacho M, Saltin B, Febbraio MA, and Pedersen BK.** Does the aging skeletal muscle maintain its endocrine function? *Exerc Immunol Rev* 10: 42-55, 2004.
126. **Przybyla B, Gurley C, Harvey JF, Bearden E, Kortebein P, Evans WJ, Sullivan DH, Peterson CA, and Dennis RA.** Aging alters macrophage properties in human skeletal muscle both at rest and in response to acute resistance exercise. *Exp Gerontol* 41: 320-327, 2006.
127. **Qin H, Holdbrooks AT, Liu Y, Reynolds SL, Yanagisawa LL, and Benveniste EN.** SOCS3 deficiency promotes M1 macrophage polarization and inflammation. *J Immunol* 189: 3439-3448, 2012.
128. **Rasouli N, Yao-Borengasser A, Varma V, Spencer HJ, McGehee RE, Jr., Peterson CA, Mehta JL, and Kern PA.** Association of scavenger receptors in adipose tissue with insulin resistance in nondiabetic humans. *Arterioscler Thromb Vasc Biol* 29: 1328-1335, 2009.
129. **Reid MB and Durham WJ.** Generation of reactive oxygen and nitrogen species in contracting skeletal muscle: potential impact on aging. *Ann N Y Acad Sci* 959: 108-116, 2002.
130. **Reiter RJ, Guerrero JM, Garcia JJ, and Acuna-Castroviejo D.** Reactive oxygen intermediates, molecular damage, and aging. Relation to melatonin. *Ann N Y Acad Sci* 854: 410-424, 1998.
131. **Reznik M.** Origin of myoblasts during skeletal muscle regeneration. Electron microscopic observations. *Lab Invest* 20: 353-363, 1969.
132. **Riley JK, Takeda K, Akira S, and Schreiber RD.** Interleukin-10 receptor signaling through the JAK-STAT pathway. Requirement for two distinct receptor-derived signals for anti-inflammatory action. *J Biol Chem* 274: 16513-16521, 1999.
133. **Ryan AS.** Exercise in aging: its important role in mortality, obesity and insulin resistance. *Aging health* 6: 551-563, 2010.
134. **Ryan AS, Li G, Blumenthal JB, and Ortmeyer HK.** Aerobic exercise + weight loss decreases skeletal muscle myostatin expression and improves insulin sensitivity in older adults. *Obesity (Silver Spring)* 21: 1350-1356, 2013.
135. **Saclier M, Cuvellier S, Magnan M, Mounier R, and Chazaud B.** Monocyte/macrophage interactions with myogenic precursor cells during skeletal muscle regeneration. *FEBS J* 280: 4118-4130, 2013.

136. **Said N, Frierson HF, Sanchez-Carbayo M, Brekken RA, and Theodorescu D.** Loss of SPARC in bladder cancer enhances carcinogenesis and progression. *J Clin Invest* 123: 751-766, 2013.
137. **Sakamoto K and Holman GD.** Emerging role for AS160/TBC1D4 and TBC1D1 in the regulation of GLUT4 traffic. *Am J Physiol Endocrinol Metab* 295: E29-37, 2008.
138. **Saltiel AR and Kahn CR.** Insulin signalling and the regulation of glucose and lipid metabolism. *Nature* 414: 799-806, 2001.
139. **Samokhvalov V, Bilan PJ, Schertzer JD, Antonescu CN, and Klip A.** Palmitate- and lipopolysaccharide-activated macrophages evoke contrasting insulin responses in muscle cells. *Am J Physiol Endocrinol Metab* 296: E37-46, 2009.
140. **Sasaki T, Unno K, Tahara S, and Kaneko T.** Age-related increase of reactive oxygen generation in the brains of mammals and birds: is reactive oxygen a signaling molecule to determine the aging process and life span? *Geriatr Gerontol Int* 10 Suppl 1: S10-24, 2010.
141. **Scheele C, Nielsen S, Kelly M, Broholm C, Nielsen AR, Taudorf S, Pedersen M, Fischer CP, and Pedersen BK.** Satellite cells derived from obese humans with type 2 diabetes and differentiated into myocytes in vitro exhibit abnormal response to IL-6. *PLoS One* 7: e39657, 2012.
142. **Sell H, Dietze-Schroeder D, Kaiser U, and Eckel J.** Monocyte chemotactic protein-1 is a potential player in the negative cross-talk between adipose tissue and skeletal muscle. *Endocrinology* 147: 2458-2467, 2006.
143. **Sell H and Eckel J.** Monocyte chemotactic protein-1 and its role in insulin resistance. *Curr Opin Lipidol* 18: 258-262, 2007.
144. **Sell H, Eckel J, and Dietze-Schroeder D.** Pathways leading to muscle insulin resistance--the muscle--fat connection. *Arch Physiol Biochem* 112: 105-113, 2006.
145. **Sell H, Habich C, and Eckel J.** Adaptive immunity in obesity and insulin resistance. *Nat Rev Endocrinol* 8: 709-716, 2012.
146. **Sell H, Kaiser U, and Eckel J.** Expression of chemokine receptors in insulin-resistant human skeletal muscle cells. *Horm Metab Res* 39: 244-249, 2007.
147. **Sell H, Laurencikiene J, Taube A, Eckardt K, Cramer A, Horrighs A, Arner P, and Eckel J.** Chemerin is a novel adipocyte-derived factor inducing insulin resistance in primary human skeletal muscle cells. *Diabetes* 58: 2731-2740, 2009.
148. **Senn JJ, Klover PJ, Nowak IA, and Mooney RA.** Interleukin-6 induces cellular insulin resistance in hepatocytes. *Diabetes* 51: 3391-3399, 2002.
149. **Senn JJ, Klover PJ, Nowak IA, Zimmers TA, Koniaris LG, Furlanetto RW, and Mooney RA.** Suppressor of cytokine signaling-3 (SOCS-3), a potential mediator of interleukin-6-dependent insulin resistance in hepatocytes. *J Biol Chem* 278: 13740-13746, 2003.
150. **Shi FD, Bai XF, Li HL, and Link H.** Macrophage apoptosis in muscle tissue in experimental autoimmune myasthenia gravis. *Muscle Nerve* 21: 1071-1074, 1998.

151. **Shi H, Tzameli I, Bjorbaek C, and Flier JS.** Suppressor of cytokine signaling 3 is a physiological regulator of adipocyte insulin signaling. *J Biol Chem* 279: 34733-34740, 2004.
152. **Shireman PK, Contreras-Shannon V, Ochoa O, Karia BP, Michalek JE, and McManus LM.** MCP-1 deficiency causes altered inflammation with impaired skeletal muscle regeneration. *J Leukoc Biol* 81: 775-785, 2007.
153. **Shireman PK, Contreras-Shannon V, Reyes-Reyna SM, Robinson SC, and McManus LM.** MCP-1 parallels inflammatory and regenerative responses in ischemic muscle. *J Surg Res* 134: 145-157, 2006.
154. **Siegel MP, Kruse SE, Percival JM, Goh J, White CC, Hopkins HC, Kavanagh TJ, Szeto HH, Rabinovitch PS, and Marcinek DJ.** Mitochondrial-targeted peptide rapidly improves mitochondrial energetics and skeletal muscle performance in aged mice. *Aging Cell* 12: 763-771, 2013.
155. **Simpson E.** Special regulatory T-cell review: Regulation of immune responses--examining the role of T cells. *Immunology* 123: 13-16, 2008.
156. **Smallie T, Ricchetti G, Horwood NJ, Feldmann M, Clark AR, and Williams LM.** IL-10 inhibits transcription elongation of the human TNF gene in primary macrophages. *J Exp Med* 207: 2081-2088, 2010.
157. **Sonnet C, Lafuste P, Arnold L, Brigitte M, Poron F, Authier FJ, Chretien F, Gherardi RK, and Chazaud B.** Human macrophages rescue myoblasts and myotubes from apoptosis through a set of adhesion molecular systems. *J Cell Sci* 119: 2497-2507, 2006.
158. **Spangenburg EE, Brown DA, Johnson MS, and Moore RL.** Exercise increases SOCS-3 expression in rat skeletal muscle: potential relationship to IL-6 expression. *J Physiol* 572: 839-848, 2006.
159. **Speakman JR and Westerterp KR.** Associations between energy demands, physical activity, and body composition in adult humans between 18 and 96 y of age. *Am J Clin Nutr* 92: 826-834, 2010.
160. **Spencer M, Finlin BS, Unal R, Zhu B, Morris AJ, Shipp LR, Lee J, Walton RG, Adu A, Erfani R, Campbell M, McGehee RE, Jr., Peterson CA, and Kern PA.** Omega-3 fatty acids reduce adipose tissue macrophages in human subjects with insulin resistance. *Diabetes* 62: 1709-1717, 2013.
161. **Spencer M, Unal R, Zhu B, Rasouli N, McGehee RE, Jr., Peterson CA, and Kern PA.** Adipose tissue extracellular matrix and vascular abnormalities in obesity and insulin resistance. *J Clin Endocrinol Metab* 96: E1990-1998, 2011.
162. **Spencer M, Yao-Borengasser A, Unal R, Rasouli N, Gurley CM, Zhu B, Peterson CA, and Kern PA.** Adipose tissue macrophages in insulin-resistant subjects are associated with collagen VI and fibrosis and demonstrate alternative activation. *Am J Physiol Endocrinol Metab* 299: E1016-1027, 2010.
163. **Spencer MJ, Walsh CM, Dorshkind KA, Rodriguez EM, and Tidball JG.** Myonuclear apoptosis in dystrophic mdx muscle occurs by perforin-mediated cytotoxicity. *J Clin Invest* 99: 2745-2751, 1997.
164. **Stadtman ER and Berlett BS.** Reactive oxygen-mediated protein oxidation in aging and disease. *Drug Metab Rev* 30: 225-243, 1998.
165. **Steensberg A, Febbraio MA, Osada T, Schjerling P, van Hall G, Saltin B, and Pedersen BK.** Interleukin-6 production in contracting human skeletal

muscle is influenced by pre-exercise muscle glycogen content. *J Physiol* 537: 633-639, 2001.
166. **Steensberg A, Keller C, Starkie RL, Osada T, Febbraio MA, and Pedersen BK.** IL-6 and TNF-alpha expression in, and release from, contracting human skeletal muscle. *Am J Physiol Endocrinol Metab* 283: E1272-1278, 2002.
167. **Stephens JW, Hurel SJ, Lowe GD, Rumley A, and Humphries SE.** Association between plasma IL-6, the IL6 -174G>C gene variant and the metabolic syndrome in type 2 diabetes mellitus. *Mol Genet Metab* 90: 422-428, 2007.
168. **Stitt TN, Drujan D, Clarke BA, Panaro F, Timofeyva Y, Kline WO, Gonzalez M, Yancopoulos GD, and Glass DJ.** The IGF-1/PI3K/Akt pathway prevents expression of muscle atrophy-induced ubiquitin ligases by inhibiting FOXO transcription factors. *Mol Cell* 14: 395-403, 2004.
169. **Stupka N, Tarnopolsky MA, Yardley NJ, and Phillips SM.** Cellular adaptation to repeated eccentric exercise-induced muscle damage. *J Appl Physiol (1985)* 91: 1669-1678, 2001.
170. **Sugiyama S, Takasawa M, Hayakawa M, and Ozawa T.** Changes in skeletal muscle, heart and liver mitochondrial electron transport activities in rats and dogs of various ages. *Biochem Mol Biol Int* 30: 937-944, 1993.
171. **Sun D, Martinez CO, Ochoa O, Ruiz-Willhite L, Bonilla JR, Centonze VE, Waite LL, Michalek JE, McManus LM, and Shireman PK.** Bone marrow-derived cell regulation of skeletal muscle regeneration. *FASEB J* 23: 382-395, 2009.
172. **Tapscott SJ and Weintraub H.** MyoD and the regulation of myogenesis by helix-loop-helix proteins. *J Clin Invest* 87: 1133-1138, 1991.
173. **Testa R, Olivieri F, Bonfigli AR, Sirolla C, Boemi M, Marchegiani F, Marra M, Cenerelli S, Antonicelli R, Dolci A, Paolisso G, and Franceschi C.** Interleukin-6-174 G > C polymorphism affects the association between IL-6 plasma levels and insulin resistance in type 2 diabetic patients. *Diabetes Res Clin Pract* 71: 299-305, 2006.
174. **Thomas JA and Mallis RJ.** Aging and oxidation of reactive protein sulfhydryls. *Exp Gerontol* 36: 1519-1526, 2001.
175. **Thong FS, Bilan PJ, and Klip A.** The Rab GTPase-activating protein AS160 integrates Akt, protein kinase C, and AMP-activated protein kinase signals regulating GLUT4 traffic. *Diabetes* 56: 414-423, 2007.
176. **Tidball JG.** Inflammatory cell response to acute muscle injury. *Med Sci Sports Exerc* 27: 1022-1032, 1995.
177. **Tidball JG and Villalta SA.** Regulatory interactions between muscle and the immune system during muscle regeneration. *Am J Physiol Regul Integr Comp Physiol* 298, 2010.
178. **Tilg H and Moschen AR.** Inflammatory mechanisms in the regulation of insulin resistance. *Mol Med* 14: 222-231, 2008.
179. **Tjiu JW, Chen JS, Shun CT, Lin SJ, Liao YH, Chu CY, Tsai TF, Chiu HC, Dai YS, Inoue H, Yang PC, Kuo ML, and Jee SH.** Tumor-associated macrophage-induced invasion and angiogenesis of human basal cell carcinoma cells by cyclooxygenase-2 induction. *J Invest Dermatol* 129: 1016-1025, 2009.

180. **Toledo FG and Goodpaster BH.** The role of weight loss and exercise in correcting skeletal muscle mitochondrial abnormalities in obesity, diabetes and aging. *Mol Cell Endocrinol* 379: 30-34, 2013.
181. **Tomiya A, Aizawa T, Nagatomi R, Sensui H, and Kokubun S.** Myofibers express IL-6 after eccentric exercise. *Am J Sports Med* 32: 503-508, 2004.
182. **Traum D, Timothee P, Silver J, Rose-John S, Ernst M, and LaRosa DF.** IL-10-induced gp130 expression in mouse mast cells permits IL-6 trans-signaling. *J Leukoc Biol* 91: 427-435, 2012.
183. **Tuttolomondo A, La Placa S, Di Raimondo D, Bellia C, Caruso A, Lo Sasso B, Guercio G, Diana G, Ciaccio M, Licata G, and Pinto A.** Adiponectin, resistin and IL-6 plasma levels in subjects with diabetic foot and possible correlations with clinical variables and cardiovascular co-morbidity. *Cardiovasc Diabetol* 9: 50, 2010.
184. **Varma V, Yao-Borengasser A, Rasouli N, Nolen GT, Phanavanh B, Starks T, Gurley C, Simpson P, McGehee RE, Jr., Kern PA, and Peterson CA.** Muscle inflammatory response and insulin resistance: synergistic interaction between macrophages and fatty acids leads to impaired insulin action. *Am J Physiol Endocrinol Metab* 296: E1300-1310, 2009.
185. **Vincent HK, Raiser SN, and Vincent KR.** The aging musculoskeletal system and obesity-related considerations with exercise. *Ageing Res Rev* 11: 361-373, 2012.
186. **Wallberg-Henriksson H, Zetan N, and Henriksson J.** Reversibility of decreased insulin-stimulated glucose transport capacity in diabetic muscle with in vitro incubation. Insulin is not required. *J Biol Chem* 262: 7665-7671, 1987.
187. **Wang X, Hu Z, Hu J, Du J, and Mitch WE.** Insulin resistance accelerates muscle protein degradation: Activation of the ubiquitin-proteasome pathway by defects in muscle cell signaling. *Endocrinology* 147: 4160-4168, 2006.
188. **Wei J, Xu H, Davies JL, and Hemmings GP.** Increase of plasma IL-6 concentration with age in healthy subjects. *Life Sci* 51: 1953-1956, 1992.
189. **Weigert C, Hennige AM, Lehmann R, Brodbeck K, Baumgartner F, Schauble M, Haring HU, and Schleicher ED.** Direct cross-talk of interleukin-6 and insulin signal transduction via insulin receptor substrate-1 in skeletal muscle cells. *J Biol Chem* 281: 7060-7067, 2006.
190. **Weisberg SP, McCann D, Desai M, Rosenbaum M, Leibel RL, and Ferrante AW, Jr.** Obesity is associated with macrophage accumulation in adipose tissue. *J Clin Invest* 112: 1796-1808, 2003.
191. **Welch S, Gebhart SS, Bergman RN, and Phillips LS.** Minimal model analysis of intravenous glucose tolerance test-derived insulin sensitivity in diabetic subjects. *J Clin Endocrinol Metab* 71: 1508-1518, 1990.
192. **Wentworth JM, Naselli G, Brown WA, Doyle L, Phipson B, Smyth GK, Wabitsch M, O'Brien PE, and Harrison LC.** Pro-inflammatory CD11c+CD206+ adipose tissue macrophages are associated with insulin resistance in human obesity. *Diabetes* 59: 1648-1656, 2010.

193. **Westman S and Hellman B.** Influence of palmitate on the in vitro metabolism of glucose in epididymal adipose tissue from mice. *Med Exp Int J Exp Med* 7: 324-328, 1962.
194. **Wolfinger RD.** Heterogeneous Variance: Covariance Structures for Repeated Measures. *Journal of Agricultural, Biological, and Environmental Statistics* 1: 205-230, 1996.
195. **Yan Z, Okutsu M, Akhtar YN, and Lira VA.** Regulation of exercise-induced fiber type transformation, mitochondrial biogenesis, and angiogenesis in skeletal muscle. *J Appl Physiol (1985)* 110: 264-274, 2011.
196. **Yeaman SJ, Armstrong JL, Bonavaud SM, Poinasamy D, Pickersgill L, and Halse R.** Regulation of glycogen synthesis in human muscle cells. *Biochem Soc Trans* 29: 537-541, 2001.
197. **Yuasa T, Uchiyama K, Ogura Y, Kimura M, Teshigawara K, Hosaka T, Tanaka Y, Obata T, Sano H, Kishi K, and Ebina Y.** The Rab GTPase-activating protein AS160 as a common regulator of insulin- and Galphaq-mediated intracellular GLUT4 vesicle distribution. *Endocr J* 56: 345-359, 2009.
198. **Zeyda M and Stulnig TM.** Obesity, inflammation, and insulin resistance--a mini-review. *Gerontology* 55: 379-386, 2009.
199. **Zierath JR, He L, Guma A, Odegoard Wahlstrom E, Klip A, and Wallberg-Henriksson H.** Insulin action on glucose transport and plasma membrane GLUT4 content in skeletal muscle from patients with NIDDM. *Diabetologia* 39: 1180-1189, 1996.

VITA

JASON S. GROSHONG BS

CITEZENSHIP **USA**

EDUCATION

Doctor of Philosophy, Physiology, in Progress

University of Kentucky, Lexington, KY.

PhD candidate October 2010. *Expected by Dec 2013* Dissertation: The role of macrophages in exercise and insulin resistance in human skeletal muscle. Committee Members: Philip A. Kern, Michael Reid, Karyn Esser, and Charlotte A. Peterson. Outside examiner: Daniel Noonan, University of Kentucky 2013.

Integrated Biomedical Sciences,2008-2009 University of Kentucky, Lexington, KY

Molecular Biology, University of Minnesota, Minneapolis, MN. 2002 (non degree status)

Bachelor of Sciences in Biotechnology, Biology and Chemistry (3 different programs) from Saint Cloud State University, Saint Cloud, Minnesota, 56301. 1995.

EXPERIENCE

October 2010 – Current. Ph. D candidate, Physiology, University of Kentucky, Lexington, KY.

September 2009 – October 2010. Graduate Research Associate, Physiology, University of Kentucky, Lexington, KY.

September 2008 – August 2009 Graduate Research Associate, IBS Rotations, University of Kentucky, Lexington KY.

Sept 2006 – June 2008. Research Specialist IV, University of Pittsburgh Cancer Institute, Pittsburgh, PA.

July 2000-June 2006. Assistant Scientist, Department of Neurology, University of Minnesota. Minneapolis, MN.

July 1999-June 2000. Junior Scientist, Department of Neurology, University of Minnesota. Minneapolis, MN.

April 1998- July 1999. Liquid Chromatography Technologist, Medtox Laboratories, St. Paul, MN.

September 1994-May 1995. Laboratory Technician, Department of Biological Sciences, Saint Cloud State University, Saint Cloud, MN.

September 1992-May 1994. Laboratory Volunteer, Department of Biological Sciences, Saint Cloud State University. Saint Cloud, MN.

September 1991-May1992. Laboratory Technician, Department of Biological Sciences, Saint Cloud State University. Saint Cloud, MN.

September 1990-May 1991. Laboratory Volunteer, Department of Biological Sciences, Saint Cloud State University. Saint Cloud, MN.

September 1989-May 1990. Laboratory Assistant, Department of Biological Sciences, Saint Cloud State University. Saint Cloud, MN.

PROFESSIONAL MEMBERSHIPS

Sigma Xi (Full Member)
AAAS
American Chemical Society

JOURNAL REVIEW (Ad Hoc)

Neurobiology of Disease

AWARDS AND HONORS:

03/01/2010- 06/30/2011 NIH T32 Scholar: “Research Training in Muscle Biology of Cardiopulmonary disease.” $29840/yr 5 T32 HL 86341-2

05/17/2011 Barnstable Brown Obesity and Diabetes Research Day Award Certificate for an Outstanding Research Presentation **“**Polarized macrophages alter insulin response distinctly in human skeletal myotubes”. $200

07/01/2011-06/30/2012 American Heart Association Predoctoral Fellowship: “Studies on insulin resistance in human skeletal muscle” $23000. 11PRE7690028

2011 Graduate Student Incentive Program: extramural funding award. University of Kentucky. $1150

MENTORSHIP

Shivang Patel, 2004-2006. Neuroscience Student. University of Minnesota, Minneapolis, MN. Current position: Surgeon, Monmouth Medical Center, Long Branch, NJ

William Grubb, 2006-2008. Biology Student, Pre-Med, University of Pittsburg, Pittsburgh, PA. Currently a medical student at Miami University Medical School, Oxford, OH.

PUBLICATIONS

Yang Y, **Groshong JS**, Matta H, Gopalakrishnan R, Yi H, Chaudhary PM. Constitutive NF-kappaB activation confers interleukin 6 (IL6) independence and resistance to dexamethasone and Janus kinase inhibitor INCB018424 in murine plasmacytoma cells. J Biol Chem. 2011 Aug 12;286(32):27988-97. doi: 10.1074/jbc.M110.213363. Epub 2011 Jun 24 PMID:21705340

Ahmad A*, **Groshong JS***, Matta H, Schamus S, Punj V, Robinson LJ, Gill PS, Chaudhary PM Kaposi's sarcoma associated herpesvirus-encoded viral FLICE inhibitory protein (vFLIP) K13 cooperates with Myc to promote lymphoma in mice. Cancer Biol Ther. 2010 Nov 9;10(10). ***equally contributing authors**

Jason S. Groshong, Melissa J. Spencer, Bula S. Bhattacharyya, Bhupinder P.S. Vohra, Roberto Zayas, Robert L. Wollmann, Richard J. Miller, Christopher M. Gomez. Calpain activation impairs neuromuscular transmission in a mouse model of the slow-channel myasthenic syndrome.. Jour of Clin Invest. 2007 Oct;117(10):2903-12

Zayas R, **Groshong JS**, Gomez CM. Inositol-1,4,5-triphosphate receptors mediate activity-induced synaptic Ca2+ signals in muscle fibers and Ca2+ overload in slow-channel syndrome. Cell Calcium. 2007 Apr;41(4):343-52

Bhupinder P.S. Vohra*, Jason S. Groshong*, Roberto Zayas, Robert L. Wollmann and Christopher M. Gomez. Activation of apoptotic pathways at muscle fiber synapses is circumscribed and reversible in a slow-channel syndrome model. Neurobiol. of Disease, 2006. Aug;23(2):462-70 ***equally contributing authors, cover image.**

Vohra BP, **Groshong JS**, Maselli RA, Verity MA, Wollmann RL, Gomez CM. Focal caspase activation underlies the endplate myopathy in slow-channel syndrome. Ann Neurol. 2004 Mar;55(3):347-52

Gomez CM, Maselli RA, **Groshong J**, Zayas R, Wollmann RL, Cens T, Charnet P. Active calcium accumulation underlies severe weakness in a panel of mice with slow-channel syndrome. J Neurosci 2002 Aug 1;22(15):6447-57

PRESENTATIONS

Adaptation to damaging or aerobic exercise with respect to age and obesity. Center for Muscle Biology, University of Kentucky, Lexington, KY October 2013

Inflammation and insulin resistance in skeletal muscle myotubes. Physiology department seminar series. Department of Physiology, University of Kentucky, Lexington, KY, May 2011

Calpastatin overexpression improves neuromuscular transmission in slow-channel syndrome Program No. 523.4. *2002 Abstract Viewer/Itinerary Planner.* Washington, DC: Society for Neuroscience, 2002. Online.

POSTERS

Polarized macrophages alter insulin response distinctly in human skeletal myotubes. Jason S. Groshong BS, BeiBei Zhu PhD,Philip A. Kern MD, Mike B. Reid PhD, Charlotte A. Peterson PhD. Barnstable Brown Obesity and Diabetes Research Day, 2011, Poster presentation award.

Different macrophage phenotypes M1, M2a, and M2c alter insulin induced Akt activation distinctly in human skeletal myotubes. Jason S Groshong, BeiBei Zhu PhD, Filomena Dimayuga PhD, Phillip A Kern MD, Mike B Reid PhD, Charlotte A Peterson PhD. Center for Muscle Biology retreat, University of Kentucky 2010

Polarized macrophages alter myokine secretion and glucose uptake distinctly in human skeletal myotubes dependent on obesity and IL6 induced insulin resistance. Jason S. Groshong, BeiBei Zhu, Jonah D. Lee, Margo F. Ubele, Philip A. Kern, and Charlotte A. Peterson. Center for Muscle Biology retreat, University of Kentucky, 2012